1

Niantic River Estuary Ecosystem Model (NREEM) Report

3
4   v. 2020.11.11
5

6   Jamie Vaudrey, Ph.D.; Jason Krumholz, Ph.D.; Christopher Calabretta, Ph.D.
7   Department of Marine Sciences
8   University of Connecticut
9   1080 Shennecossett Road
10   Groton, CT 06340
11   jamie.vaudrey@uconn.edu
12   860-405-9149

13
14
15   Second Interim report for the TAC
16   Project: Data Synthesis and Modeling of Nitrogen Effects on Niantic River Estuary
17
18
19
20
21

Contents

64

65
66 *This report is provided as a Microsoft Word document to allow for easy commenting and editing. This*
67 *interim report will eventually become part of the final technical report. Feedback is appreciated; please*
68 *forward comments to jamie.vaudrey@uconn.edu.*

69
70 *Suggested citation*: Vaudrey, J.M.P., Krumholz, J., Calabretta, C. (2020) DRAFT Model Report, v. 2020-11-
71 11. University of Connecticut, Department of Marine Sciences, Groton, CT. prepared for the Niantic
72 Nitrogen Work Group. 127 p.

73
74 This report is a review of the modeling portion of the project. This report addresses *Task 2: Model*
75 *Development: Utilize existing data to develop an ecosystem model (biogeochemical model coupled to a*
76 *physical mixing model). Two models will be evaluated, including Vaudrey's work modeling Narragansett*
77 *Bay (Brush 2002; Brush and Nixon 2010; Kremer et al. 2010; Vaudrey 2014) and the Massachusetts*
78 *Estuary Project model (Howes et al. 2001).*

79

1 Executive Summary

80

81
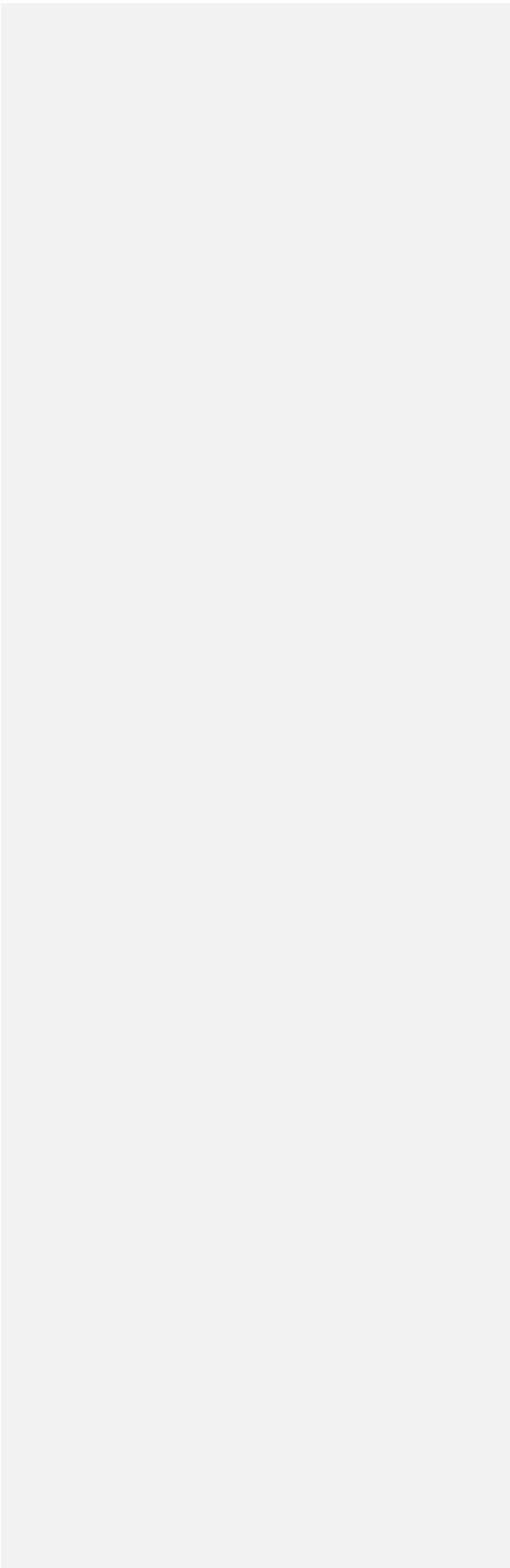
2 General Approach to Model Development

82

83 The development of any model incorporates a series of steps moving from defining the purpose through
84 the final stages of model testing. In recognition of the broad audience with interests in this model, a
85 brief summary of these steps are provided below with reference to sections of the report where these
86 steps are discussed in detail. Most readers will be familiar with the steps involved with hypothesis driven
87 experimental science. Modeling also follows a series of steps, though some readers may be less familiar
88 with the process. Jakeman and colleagues (2006) provide a review of model development, detailing the
89 ten major steps in the modeling process. The steps employed in model development are presented in a
90 diagram (Figure 1) and followed by a brief description of the steps as they apply to the development of
91 the Niantic River Estuary Ecosystem Model (NREEM). The goal of this section is to introduce the general
92 approach to model development and testing employed in this project. The details of each step are
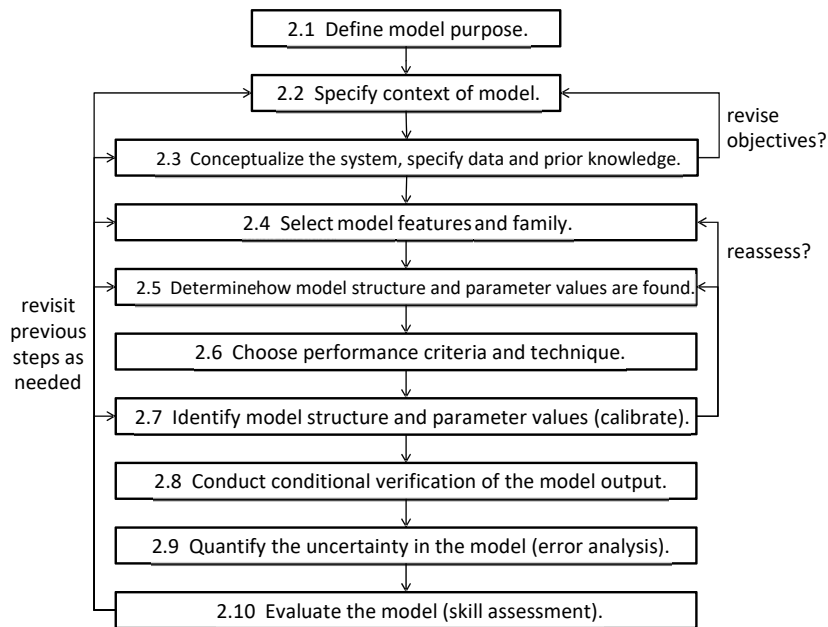93 provided later in this report.

94

95 *Figure 1: Overview of Basic Modeling – 10 Steps*
96 *The numbers in the boxes refer to the Section in the text where the step as it pertains to this model is covered. Based on process*
97 *described by Jakeman et al. (2006).*

98

2.1 Define Model Purpose

99

100 → The primary objective of this model is to inform management decisions supportive of good water
101   quality in NRE.

102 The synthesis of existing data will be used to understand the dynamics of the system in relation to
103 climate and nutrient loads. An analysis of the potential impact of nutrient mitigation strategies will guide
104 prioritization of activities in the watershed, with the Niantic River Watershed Commission evaluating our
105 suggestions and assessment of feasibility.

106 A number of secondary objectives have been identified.

107 • The model will be used to predict the level of nutrient loads supportive of eelgrass and shellfish
108   (as indicators of good water quality) under a warming climatic regime.
109 • Identify gaps in the data which, if filled, will improve our understanding of shallow water habitat
110   characteristics and improve the ability of the model to predict ecosystem state variables as
111   indicators of response to nutrient loads and temperature increases.
112 • Determine if the ecosystem model is robust for cross-system comparison, i.e. it does not require
113   locally specific modification of parameters when moving to a new site.

2.2 Specification of the Modeling Context: scope and resources

114

115 The Niantic River Estuary Ecosystem Model is specifically developed for the Long Island Sound
116 embayment, Niantic River. While the model framework and formulations are transferrable to other
117 locations, the ranges of parameters may vary if estuarine conditions are considerably different from
118 Niantic River. The model may also be reconfigured to include the contribution and predict conditions for
119 other species (e.g. oysters), provided that the other species are most influenced by the same forcing
120 factors as are included in the model (light availability, temperature, nutrient load).

121 The model output consists of daily estimates of state variables and rates associated with these changes.
122 The state variables are: salinity, dissolved oxygen, phytoplankton biomass, seagrass biomass,
123 macroalgae biomass, water column nitrogen, water column phosphorus, and benthic carbon. The model
124 domain includes three boxes within the Niantic River and a large box representing Niantic Bay. The
125 boxes are assumed to be vertically well-mixed, though predictions of surface-bottom differences in
126 some parameters are estimated (e.g. oxygen, chlorophyll) using a mass-balance approach and an
127 estimate of vertical dispersion through a well-mixed water column. Freshwater inflow is determined
128 from the USGS gaging station of Latimer Brook and extrapolated to the other freshwater inputs (other
129 tributaries, groundwater).

> **Commented [VJ1]:** Need to develop & write this up in methods section
>
> **Commented [VJ2]:** will need to address how the model can include multiple layers in stratified systems

130 Temporally, the model is representative of daily averaged conditions. The diel changes in parameters
131 (oxygen, chlorophyll, atc.) are not assessed by the model.

2.3 Conceptualization of the system, specification of data and prior knowledge

The success of eelgrass within the system is known to be linked to a number of forcing factors. Light, temperature, water quality, and the amount of other primary producers have all been identified as affecting eelgrass. Criteria for eelgrass success in Long Island Sound have been identified for these parameters (Table 2-1, page 7).

Development of the model proceeded under certain assumptions:

➢ The physical mixing in the estuary is adequately represented by a simple dilution model approach to estimating hydrodynamic exchange.
➢ The NYHOPS model salinity output accurately represents the salinity structure of Niantic River and Niantic Bay.
➢ Extrapolation of the river flow from Latimer Brook's USGS gage data to other streams and groundwater inflow is reasonable.
➢ River flow data are available for Latimer Brook from 9/17/08 to 9/30/2015. Model output from NYHOPS is available for 1/1/1981 to 12/31/16. River flow data for the missing period can be extrapolated from other gaged streams in Connecticut.
➢ The primary producers compete for resources (light, nutrients) and this competition is well-represented by Michaelis-Menten-type dynamics.

Table 2-1: Recommended habitat requirements for established eelgrass beds in Long Island Sound.
Copied from Vaudrey (2008a), based on work discussed in Vaudrey (2008a, 2008b) and Yarish et al. (2006).

	Suggested Guidelines for LIS	Guideline Type	Analysis Status
Minimum Light Requirement at the leaf surface (%)	> 15 (CB)	primary requirement (must estimate epiphyte biomass)	no data available
Water Column Light Requirement (%)	< 22 (CB)	substitute for Min. Light Requirement at the Leaf Surface	no data available
Kd (1/m)	< 0.7	provided for reference, use minimum light as the standard	3 case study sites
Chlorophyll-*a* (µg / L)	< 5.5	secondary requirement (diagnostic tool)	3 case study sites
Dissolved Inorganic Nitrogen (mg/L)	< 0.03	secondary requirement (diagnostic tool)	3 case study sites
Dissolved Inorganic Phosphorus (mg/L)	< 0.02 (CB and LIS)	secondary requirement (diagnostic tool)	data not analyzed
Total Suspended Solids (mg/L)	< 15 (CB) < 30 (LIS)	secondary requirement (diagnostic tool)	no data available
Sediment Organics (%)	< 10	habitat constraint	3 case study sites
Vertical Distribution (m)	Zmax = 1m + Zmin	habitat constraint	3 case study sites
Sediment Grain Size	< 20% silt and clay	habitat constraint	no data available
Sediment Sulfide Concentration (µM)	< 400	habitat constraint	no data available
Current Velocity (cm/s)	5 < X < 100	habitat constraint	data not analyzed, case study sites within this range

2.4 Model Features and Family

153 The physical mixing in the estuary is driven by a simple dilution model approach to estimating
154 hydrodynamic exchange (Section 4, page 16).

155 The ecological model family (Section 5, page 22) is best characterized as a "black box" model, meaning
156 that empirical data are used to define relationships of forcing factors (light, temperature, freshwater
157 input, wind) to model output (state variable) without specifying the exact biological processes involved
158 (e.g. consumption of phytoplankton classes by zooplankton). Instead of focusing on the mechanistic
159 processes, a statistical relationship between the forcing factors and model output is employed. The
160 model is deterministic; in other words, the same inputs will always yield the same outputs.

161 The model consists of relatively few processes and coefficients, and is thus termed a mid-level or
162 intermediate complexity model. Formulations are based on empirically derived relationships from the
163 literature. A general overview of the model is provided in Figure 2. Eight state variables are modeled:
164 salt, phytoplankton biomass, macroalgae biomass, eelgrass biomass, nitrogen, phosphorus, benthic
165 carbon, and oxygen. Differential equations define the rate of change in each state variable. The change
166 due to mixing is not included in the differential equations of the ecological portion of the model, the
167 mixing is handled in a separate part of the model. A full description of the processes included and
168 justifications for constants and coefficients forms the bulk of this report.

169
170 *Figure 2: Overview of Model Processes*
171 *Processes within the model are indicated by the blue arrows with the basis for the formulation shown in black italicized text. The*
172 *state variables are nitrogen, phosphorus, sediment organic carbon, phytoplankton, macroalgae, seagrass, and oxygen. Black*
173 *arrows indicate transport of state variables across the boundary of the model domain. For example, N enters via river and*
174 *groundwater input from the watershed and from atmospheric deposition to the surface of the embayment. N is exchanged with*
175 *Niantic Bay / Long Island Sound via hydrodynamics and is lost to the atmosphere via denitrification. Note, the black arrows do*
176 *not always point to the symbol for the state variable to which they are contributing in order to keep the graphical display*
177 *uncluttered, but their contribution is assigned to those pools. C is carbon, N is nitrogen, P is phosphorus, O_2 is oxygen, T is*
178 *temperature, OM is organic matter or biomass. The "≡" symbol indicates equivalency, that the N and P are calculated*
179 *stoichiometrically from C.*

2.5 Choice of How Model Structure and Parameter Values are to be Found

The Occam's Razor principle of parsimony was employed when deciding upon the parameters to include (Jakeman et al. 2006). This refers to choosing the lowest number of parameters that yield accurate results. In modeling, the inclusion of additional parameters past a certain point increases uncertainty without a substantial increase in accuracy. This is due to estimation of parameters or processes, each having an error associated with the estimate which reflects temporal and spatial variability, sparseness of data, and error associated with interpolating between sample points and extrapolating into other areas where no data are present. As each new parameter is added to a model, the error of the model estimate increases. Eventually, the increased accuracy due to additional parameters is not detectable within the error associated with the model.

Throughout the text of this report, potential additions to the model are indicated in a text box like this one. At this point, these additions are not included in order to keep the model as simple as possible.

This model begins with the fewest possible parameters and coefficients. If necessary, addition of other processes may be included.

2.6 Choice of Performance Criteria and Technique

The performance criteria require a good match between model output for the state variables and rates to field data. The model should capture the correct range of data. The model output is unlikely to capture the short term variability in state variables as we will usually be comparing the box-wide daily average provided by the model to field data which represent a specific location at a specific time. Part of model assessment will include averaging field data to better match the spatial and temporal scale of model output.

2.7 Identification of Model Structure and Parameter Values (Calibration)

The acceptable ranges for constants and coefficients were defined by literature values coupled with local knowledge of typical ranges in Long Island Sound.

The structure of the model refers to formulations describing the processes included in the model (Figure 2, page 8). The model will be run many times, allowing parameters to randomly vary within their ranges; this will yield a family of predictions, providing an estimate of the range in predictions provided by the model – this is termed "stochastic simulations" (Kremer 1983).

2.8 Conditional Verification of Model Output

Conditional verification of the model was conducted at every step where model output was generated. This process involves examining the output to verify data values relative to what is known about the system.

2.9 Quantification of Uncertainty

213

214 Uncertainty in models can have many sources, including an incomplete understanding of the system and
215 sparse data, the two sources most likely to affect this model. To quantify the degree of these
216 uncertainties, model outputs are compared to the field data available. From this assessment, estimates
217 of the fraction of model predictions which will accurately predict eelgrass success were determined.

2.10 Model Evaluation (Skill Analysis)

218

219 Evaluation of the model output relative to the available field data was used to assess the skill of the
220 model. The accuracy of the model was determined by examining the model output relative to the
221 location and mass of existing naturally occurring eelgrass beds and macroalgae. State variables are
222 compared to water quality data available for Niantic River. A number of skill metrics appropriate to this
223 model are employed. These are presented in Sections 6 (page 66) and 7 (page 66).

3 Model Choice Justification

224

3.1 Watershed Models

225

226 The watershed model used for this project is the Long Island Sound Nitrogen Loading Model (Vaudrey et
227 al. 2013), which uses land use and population to estimate nitrogen load and applies attenuation factors
228 for nitrogen removal as the groundwater travels through the watershed. The watershed portion of the
229 model characterizes the nitrogen load reaching the edge of the estuary. This watershed model is used to
230 run scenarios, changing the nitrogen contribution to the estuary as land use changes. It does this by
231 providing a fractional modifier – comparing the load at baseline conditions to the load estimated via
232 land-use changes. This process if further described in Section 7.2 (page 66).

233 In the in-estuary model, the nitrogen input from the watershed is characterized as the nitrogen
234 concentration in incoming water multiplied by the volume of the incoming freshwater. The watershed
235 model can be used to reduce or increase this input by comparing the changed nitrogen load to the
236 default load and applying that fraction to the incoming freshwater's nitrogen concentration. There is not
237 a direct link between the watershed model and the in-estuary model – the user of the in-estuary model
238 needs to specify by what fraction they want to change the nitrogen concentration.

239 Watershed models will not be reviewed further; we will use the LIS NLM because it is the only model
240 which has already been applied to the Long Island Sound embayments. The comparison in Table 2 is
241 provided to show the similarity among the coefficients used for the various watershed models. Three
242 watershed models were reviewed by Howes et al. (2001) as part of the Massachusetts Estuary Project:
243 Massachusetts Estuary Project Linked Model, Buzzards Bay Project Nitrogen Loading Methodology, Cape
244 Cod Commission Nitrogen Loading/Critical Loads Methodology. Howes and colleagues reviewed the
245 models by applying them to five embayments in Massachusetts. The Long Island Sound Nitrogen
246 Loading Model (LIS NLM) is also presented in Table 3-1.

3.2 Review of In-Estuary Models

One of the project deliverables was a comparison of the in-estuary model chosen for this project (EcoGEM) and similar models. Each in-estuary model is reviewed for certain key characteristics. While each of these models includes subtle details not presented here, this comparison serves to highlight the differences among the models. Information on the Buzzards Bay and Cape Cod Commission models are summarized from the comparison presented in Howes et al. (2001). These two models essentially lack an in-estuary model. The models are presented side-by-side to facilitate comparison.

The Massachusetts Estuary Project uses the RMA-4 water quality module, coupled with the RMA-2 hydrodynamic model. The documentation on this model is vague in the online technical information and is not well described by Howes et al. (2001). Looking into the water quality modeling section of an embayment technical report provides more detail on the actual application of the model (e.g. Chp. 6 of Howes et al. 2006). Vaudrey and colleagues created EcoGEM, information is provided from personal experience and is documented in Vaudrey (2014).

261 *Table 3-1: Review of key parameters in four watershed nitrogen load models.*
262 *The first three are taken from Table III-1 in Howes et al. (2001). The LIS NLM information is from Vaudrey. The MA Estuary*
263 *Project Linked Model is also considered in Section 3.2, Review of In-Estuary Models (page 11).*

Parameter	Buzzards Bay Project Nitrogen Loading Methodology	Cape Cod Commission Nitrogen Loading Methodology	MA Estuary Project Linked Model	Long Island Sound Nitrogen Loading Model (LIS NLM)
LOADING FACTORS (as delivery to estuary, includes attenuation)				
Septic Systems	2.67 kg N / person / y	2.67 kg N / person / y	1.80 kg N / person / y	1.54 ± 0.5 kg N / person / y [e]
Lawns	1.7 kg N / lawn / y [a]	1.7 kg N / lawn / y [a]	1.36 kg N / lawn / y [a]	0.8 ± 0.08 kg N / lawn / y [d]
Precipitation to impervious surface that reaches groundwater	0.75 mg/L [b]	0.75 mg/L [b]	0.75 mg/L [b]	0.81 mg/L
Precipitation to roadways that reaches groundwater	1.5 mg/L [b]	1.5 mg/L [b]	1.5 mg/L [b]	0.81 mg/L
ATTENUATION FACTORS				
attenuation in freshwater systems and surface water inflows	30%	0%	30 to 60%	50 to 70%
attenuation in groundwater	30%	0%	0% [c]	0 to 88% [f]

264 [a] Nitrogen added to residential lawns assumed to be 3 lb / 1000 square feet, with lawn sizes assumed to be 5000 square feet. Leaching is
265   assumed to be 20% in Linked Model, 25% on Buzzards Bay model, and 25% in Cape Cod Commission model
266 [b] Only 90% of precipitation to surface reaches groundwater
267 [c] A series of studies conducted in MA estuaries indicates attenuation in groundwater does not occur.
268 [d] Units of LIS NLM output have been converted to be consistent with results from Howes et al. (2001). The LIS NLM varies lawn size by
269   watershed and zone within watershed. Fertilizer N applied is also varied with different regions within LIS, with Long Island and the Western
270   Sound having higher application rates. The value shown includes all attenuation, the load to the estuary is shown; it is the average and
271   standard error for all embayments. The value for Niantic River watershed is 0.74 ± 0.05 kg N / lawn.
272 [e] Units of LIS NLM output have been converted to be consistent with results from Howes et al. (2001). The LIS NLM identifies population on
273   septic within each zone of the watershed and applies attenuation factors according to zone. The value shown includes all attenuation, the
274   load to the estuary is shown.
275 [f] Attenuation depends upon land use category and location within the watershed.
276

277

3.2.1.1 Buzzards Bay Project Nitrogen Loading Methodology

3.2.1.1.1 Required Inputs

- estimates of nitrogen load from the watershed
- estimate of freshwater flushing time

3.2.1.1.2 Hydrodynamics

Not included. Freshwater flushing time is used to evaluate the residence time of nitrogen in the estuary.

3.2.1.1.3 Nutrient Inputs from Boundaries

Only includes the nutrient load as generated by the watershed loading model, which includes groundwater and surface water. Nutrient inputs are distributed to the whole system as a bulk number.

3.2.1.1.4 Time Frame

Annual estimate.

3.2.1.1.5 Calibration

None.

3.2.1.1.6 Verification

None.

3.2.1.1.7 Setting Nitrogen Thresholds

The thresholds are determined by allowing the estimated nitrogen load from the watershed to flush conservatively though the estuary. No in-estuary processes are included.

3.2.1.2 Cape Cod Commission Nitrogen Loading/Critical Loads Methodology

3.2.1.2.1 Required Inputs

- estimates of nitrogen load from the watershed
- estimate of freshwater flushing time

3.2.1.2.2 Hydrodynamics

Not included. Freshwater flushing time is used to evaluate the residence time of nitrogen in the estuary.

3.2.1.2.3 Nutrient Inputs from Boundaries

Only includes the nutrient load as generated by the watershed loading model, which includes groundwater and surface water. Nutrient inputs are distributed to the whole system as a bulk number.

3.2.1.2.4 Time Frame

Annual estimate.

3.2.1.2.5 Calibration

None.

3.2.1.2.6 Verification

None.

3.2.1.2.7 Setting Nitrogen Thresholds

The thresholds are determined by allowing the estimated nitrogen load from the watershed to flush conservatively though the estuary. No in-estuary processes are included.

3.2.1.3 Linked Model – used in Massachusetts Estuary Project

3.2.1.3.1 Required Inputs

- boundary conditions and dispersion coefficients output as a table from RMA-2
- estimates of nitrogen load from the watershed
- measurements of benthic flux of nitrogen during summer
- measurements of nitrogen in the water column during summer

3.2.1.3.2 Hydrodynamics

Uses a finely resolved, 2-D hydrodynamic model (RMA-2), which would include thousands of grid cells when applied to Niantic River. Each of these grid cells is equivalent to the coarsely resolved ecological model mentioned for the EcoGEM model.

3.2.1.3.3 Nutrient Inputs from Boundaries

Includes nutrients entering from freshwater surface flow, marine boundary (e.g. Long Island Sound for Niantic River), and groundwater. Nutrient inputs are distributed to each grid cell as appropriate. For example, groundwater enters throughout the spatial area of the embayment

3.2.1.4 EcoGEM Box Model

3.2.1.4.1 Required Inputs

- boundary conditions and dispersion coefficients from the Officer Box Model approach to determining hydrodynamics
- light, wind, temperature
- estimates of nitrogen load from the watershed
- estimates of benthic flux of nitrogen
- measurements of state variables in the incoming water and within the estuary: salinity, chlorophyll, nitrogen, phosphorus, benthic carbon, dissolved oxygen

3.2.1.4.2 Hydrodynamics

Uses a coarsely resolved, 3-D box model approach to determining mixing within the embayment, with three boxes representing the NRE. This coarse resolution is more appropriate to the scale of ecological processes, allowing us to average over larger scales and verify model estimates with field data (Kremer et al. 2010). Ideally, a fine-scale hydrodynamic model would be used to estimate the mixing among the three boxes. NRE was well-mixed, both vertically and horizontally, thus the Officer box model approach which been used in many estuaries was not appropriate (Officer 1980; Officer and Kester 1991). The Officer approach could be applied to embayments with a greater range of salinity values along the embayment. For NRE, a simpler approach was used, employing a dilution scheme with an estimate of return flow (Plew et al. 2018).

3.2.1.4.3 Nutrient Inputs from Boundaries

Includes nutrients entering from freshwater surface flow, marine boundary (e.g. Long Island Sound for Niantic River), groundwater, and atmospheric deposition directly to the embayment surface. Nutrient inputs are distributed to each model box as appropriate. For

while surface flow enters at the location of streams and rivers.

3.2.1.3.4 Time Frame

The model has a spin-up of 28 days, followed by 7 days for the model run. The 28-day period allows the model domain to reach steady state, this period is not considered model output.

3.2.1.3.5 Calibration

Calibration of the model is in reference to the nitrogen concentrations measured in the water column. The dispersion coefficients are tuned until the model output matches the in-estuary concentration.

3.2.1.3.6 Verification

To verify the model is operating as expected, salinity output from the model are compared to salinity data from the estuary.

3.2.1.3.7 Setting Nitrogen Thresholds

Only nitrogen is modeled directly. Dissolved oxygen, eelgrass, and benthic infauna (when eelgrass was not present) are used to set targets for nitrogen loads, using actual data from the system. A site within the system is chosen as a sentinel site such that improvement in water quality in that location will restore habitat to the desired condition. For example, eelgrass may be desired at an inner station (landward). To set a nitrogen threshold, the nitrogen level at existing eelgrass beds in that system are used to set the target nitrogen concentration for the water column. The nitrogen load from the watershed is adjusted until the desired condition is achieved at the sentinel station.

example, groundwater enters throughout the spatial area of the embayment while surface flow enters at the location of streams and rivers.

3.2.1.4.4 Time Frame

The model will cover multiple years, and the model will be responsive to changes in temperature, light, and wind.

3.2.1.4.5 Calibration

Calibration of the model is in reference to the chlorophyll, nutrients, and dissolved oxygen measured in the water column. The respiratory coefficient of the water column and benthos are the only items tuned to achieve a goodness of fit.

3.2.1.4.6 Verification

To verify the model is operating as expected, salinity output from the model are compared to salinity data from the estuary.

3.2.1.4.7 Setting Nitrogen Thresholds

The model provides estimates of nutrients, chlorophyll, and dissolved oxygen. Macroalgae and seagrass will be added to the model. A result of the model is an estimate of the light attenuation coefficient in the water column. Estimates of the light reaching the bottom will predict success for eelgrass. Scenarios of changing nutrient loads (adjusting the nitrogen loads relative to the watershed model) in the context of increasing temperatures will provide estimates for nitrogen thresholds responsive to predicted water column warming.

278

3.3 Summary of Model Choice Justification

WATERSHED MODEL

> The Long Island Sound Nitrogen Loading Model (LIS NLM) will be used to determine the watershed loading rate for nitrogen for scenario runs. Changes in land use result in changes to the nitrogen load. The revised nitrogen input relative to the default is used as a fractional adjuster in the interface of the in-estuary model; the two models (watershed and in-estuary) are not dynamically linked. Further evaluation of the other three watershed models presented in Table 3-1 (page 12) is beyond the scope of this project. In addition, the LIS NLM model is the only one which has already been applied to the LIS embayment.

IN-ESTUARY MODEL

> The Buzzards Bay and Cape Cod Commission models essentially do not have an in-estuary model. We will have estimates of the flushing time of the embayment, and can thus apply these methods for setting criteria (basically, a flushing of the nitrogen through the system).

> The benefit of the Linked Model used in the MA Estuary Project is the application of a fine-scale hydrodynamic model. Application of that model is beyond the scope of this project in terms of both time and resources.

> The EcoGEM model, used in this project, operates over multiple years and can estimate the impacts of climate factors on water quality.

> We will compare estimates using a procedure similar to the Linked Model approach by substituting the mixing coefficients derived from the simplified hydrodynamic model approach used for EcoGEM.

4 Hydrodynamic Model Development

An overview of the hydrodynamic and biogeochemical models are provided in Section 2.4 (page 8).

Niantic River Estuary is divided into three boxes for both the hydrodynamic model and the biogeochemical model (Figure 3). The final choice for hydrodynamics in the model was a simple dilution scheme to drive mixing. This section reviews the attempt to use the more refined Officer box model equations and the justification for using a dilution scheme instead of the Officer box model equations.
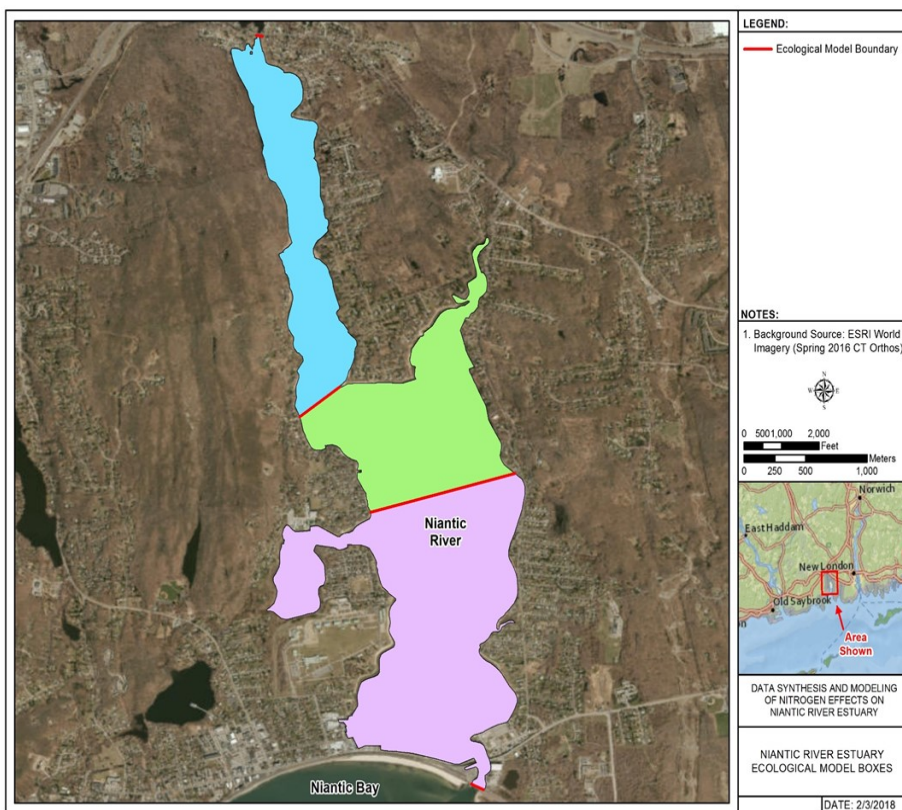
PROJECT: \NianticRiverGIS\Projects\DataReport\Figure X Niantic River_EcoModel_Boxes.mxd

306
307 *Figure 3: Model domain and box delineations.*
308 *Each colored area represents a box in the model domain. The red lines indicate boundaries between boxes, with the freshwater*
309 *input at the north, and with Niantic Bay at the south.*

4.1   Officer Box Model Approach

311   The physical mixing was first modelled using the Officer box model approach and available data for
312   salinity and freshwater flow (Hagy et al. 2000; Officer 1980, eqns. 80-86; Officer and Kester 1991,
313   Hansen-Rattray parameter). This approach estimates physical exchanges between adjacent elements
314   using data on freshwater inputs to the estuary and the corresponding salinity within the estuary and at
315   the ocean boundary.

316   This method did not work for NRE because the estuary is often vertically and horizontally well-mixed
317   (Figure 4), though Niantic Bay shows more frequent stratification. As the salinity difference approaches
318   zero, the Officer equations are not able to accurately estimate exchange. The end result in the ecological

319 model was that salt builds up in the estuary, achieving salinities over 100 ppt. The Officer box model
320 approach is mentioned here because other embayments may have sufficient salinity differences to allow
321 for the use of Officer's approach.

322 The Officer box model approach requires daily salinity values in each box of the model domain and at
323 the boundaries. For systems where the Officer box model approach is likely to work, a source of
324 modeled salinity data for Long Island Sound is reviewed in Appendix A.

325

326
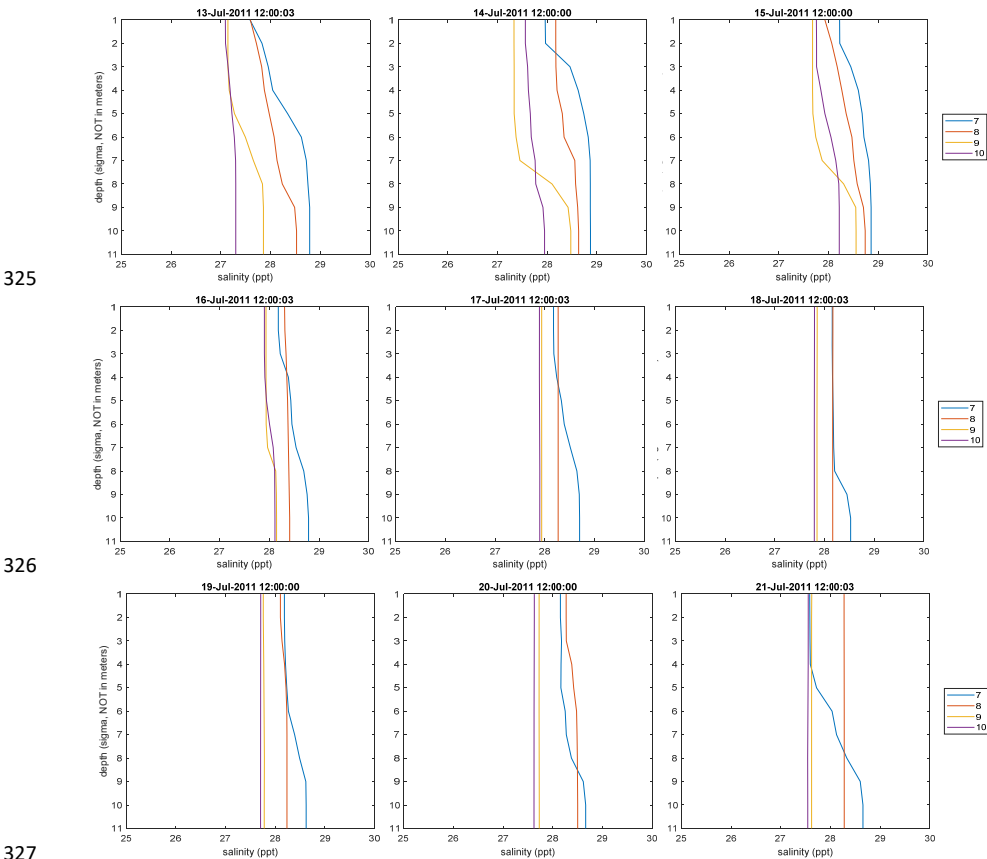
327
328 *Figure 4: NYHOPS modeled salinity profiles.*
329 *Salinity at the 11 depths modeled by the NYHOPS model; note, these are not in meters, but instead the water column is divided*
330 *into 11 layers. Box 7 corresponds to Niantic Bay, 8 to the lower basin, 9 to the upper basin, and 10 to the arm (Figure 42). This*
331 *series of was randomly chosen to illustrate the water column is often well-mixed.*

4.2 Simplified Mixing Approach

A recent paper reviewed simple dilution models for use in water quality models and identified conditions under which more complex hydrodynamic models are required (Plew et al. 2018). In short, the criteria involve calculating an indicator (I) as:

$$I = Q_f * T / P \qquad\qquad (eqn. 1)$$

where Q_f is the freshwater inflow (m^3 sec^{-1}), T is the tidal period (sec), and P is the volume of the tidal prism. For Niantic River, freshwater inflow from all three streams was calculated from USGS gage data, using an extrapolation from nearby gages (see the Data Synthesis section of the report for methods). The tidal period is 12.42 hours, which equates to 44,712 seconds. The volume of the tidal prism was calculated from the average tidal range of 0.7 m and the area of NRE of 2.96 km, which equates to 2,069,256 m^3. For NRE, the value of the indicator, I, is 0.025. Less than 0.1 is well-mixed and less than 0.25 is reasonably well-mixed (Plew et al. 2018).

The simplified scheme balances volumes entering and leaving a box on a given day (Figure 5). The salt concentration in the sending box is multiplied by the volume to yield the amount of salt transported among boxes. Salinity in the box is calculated at the end of the day by balancing the salt inputs and outputs. Plew et al. (2018) provide a method for calculating return flow, which is the amount of water that leaves an estuary and immediately returns (Figure 6). They suggest this is more of a "tuning factor" than a known number.
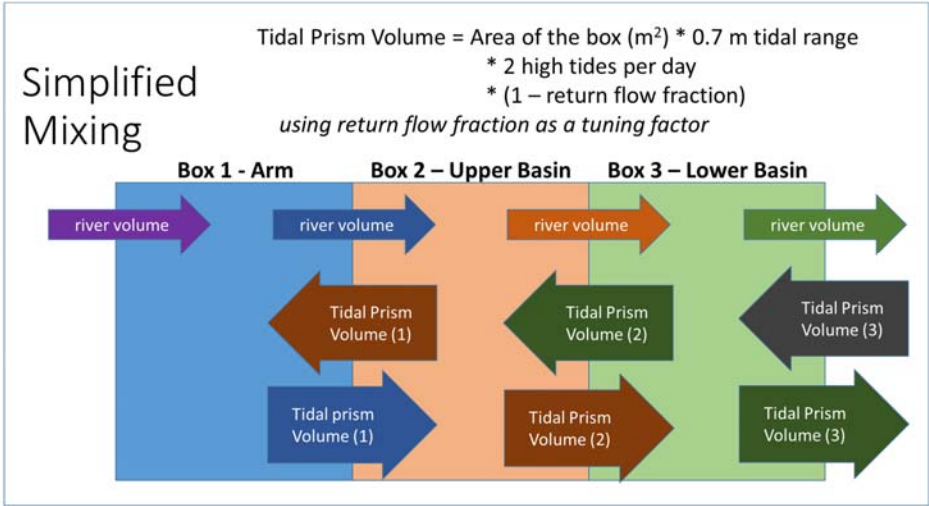
Figure 5: Simplified Mixing
Colors of the arrows indicate the concentration of the state variable associated with the flow.

353   The change in salinity for each day (dydt) was calculated as follows for each box (Figure 5):

354   $dydt_{box1} =$ RivFlux * RiverBoundaryConditions
355   - RivFlux * $Yconc_{box1}$
356   + $SurfArea_{box1}$ * TPfactor * (1-$ReturnFlowFrac_{box1}$) * $Yconc_{box2}$
357   - $SurfArea_{box1}$ * TPfactor * (1-$ReturnFlowFrac_{box1}$) * $Yconc_{box1}$

358   $dydt_{box2} =$ RivFlux * $Yconc_{box1}$
359   - RivFlux * $Yconc_{box2}$
360   + $SurfArea_{box2}$ * TPfactor * (1-$ReturnFlowFrac_{box2}$) * $Yconc_{box3}$
361   - $SurfArea_{box2}$ * TPfactor * (1-$ReturnFlowFrac_{box2}$) * $Yconc_{box2}$
362   + $SurfArea_{box1}$ * TPfactor * (1-$ReturnFlowFrac_{box1}$) * $Yconc_{box1}$
363   - $SurfArea_{box1}$ * TPfactor * (1-$ReturnFlowFrac_{box1}$) * $Yconc_{box2}$

364   $dydt_{box3} =$ RivFlux * $Yconc_{box2}$
365   - RivFlux * $Yconc_{box3}$
366   + $SurfArea_{box3}$ * TPfactor * (1-$ReturnFlowFrac_{box3}$) * OceanBoundaryConditions
367   - $SurfArea_{box3}$ * TPfactor * (1-$ReturnFlowFrac_{box3}$) * $Yconc_{box3}$
368   + $SurfArea_{box2}$ * TPfactor * (1-$ReturnFlowFrac_{box2}$) * $Yconc_{box2}$
369   - $SurfArea_{box2}$ * TPfactor * (1-$ReturnFlowFrac_{box2}$) * $Yconc_{box3}$

370   Where:
371   RivFlux (m^3) = the freshwater input from the three streams estimated from nearby USGS gages using a
372   relationship developed using time periods when freshwater streams into Niantic River were
373   gaged. This relationship is discussed in the Data Synthesis section of this report.
374   Yconc (ppt, kg m^{-3}) = the salinity value in each box at the end of the previous day.
375   RiverBoundaryCondidtions = boundary conditions in the river; for salt, the salinity is 0 ppt.
376   OceanBoundaryConditions = boundary conditions in Niantic Bay, salinity (ppt) is obtained from the
377   NYHOPS model; this value is forced, not modeled.
378   TPfactor (m d^{-1}) = 1.3527 m d^{-1} = 0.7 m per tidal prism * 2 tidal prisms per day * (24 h/24.84 h); Just
379   under two tidal cycles per day, so adjusted for this.
380   ReturnFlowFrac (unitless) = fraction of water leaving a box that returns to the box within that day, due
381   to return flow associated with incoming tides. The base value was calculated using the formula
382   for the return flow fraction ("b") provided in Plew et al. (2018), which results in a value which
383   varies with freshwater flow into the system (Figure 6). A tuning factor was applied to the base
384   value, as recommended by Plew et al. (2018). Because the mixing equations use "1 – return flow
385   fraction" to indicate the amount leaving the box and not returning, a smaller tuning factor
386   results in a larger return flow. The tuning factors were determined by minimizing the difference
387   between the modeled salinity and the NYHOPS salinity output, keeping in mind that the NYHOPS
388   salinity overestimates salinity in the arm (box 1) when compared to field data. The unitless
389   tuning factors were: box 1 = 0.001, box 2 = 0.2, box 3 = 0.4; these factors were multiplied by the
390   base value for the return flow fraction shown in Figure 6.
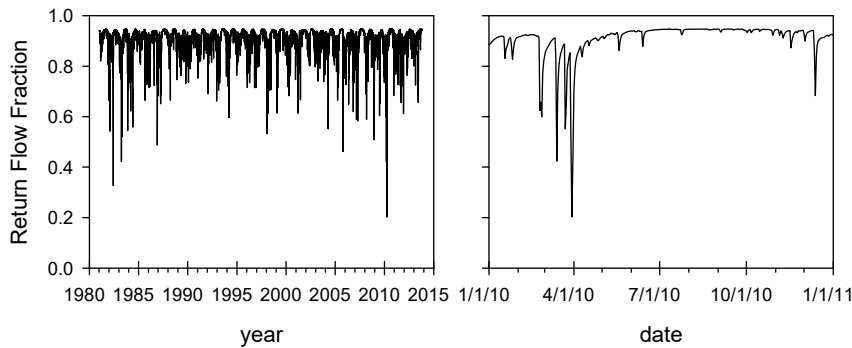
391
392 *Figure 6: Return Flow Fraction for years with NYHOPS model output, 1981 to 2013.*
393 *(Left panel) Return flow fraction by day. The values vary with freshwater input to Niantic River Estuary. (Right panel) Return flow*
394 *fraction by day for the year 2010. Return Flow Fraction is calculated as $b = 0.949e^{(-1.679x)}$, where $x = Q_f T / P$, Q_f = freshwater*
395 *inflow ($m^3 s^{-1}$), T = tidal period (12.42 h = 44,712 s), and P is the volume of the tidal prism (m^3).*

396 The salinity output of EcoGEM, modeled using the equations shown above, were compared to the
397 NYHOPS model salinity output (Figure 7). The NYHOPS model includes output for 1/1/1981 to 10/31/13,
398 a total of 11,992 days. The NYHOPS model tends to overestimate the salinity in the Arm - box 1
399 (Appendix A, page 70), thus higher values of the difference between NYHOPS and EcoGEM salinity are
400 preferred in box 1.
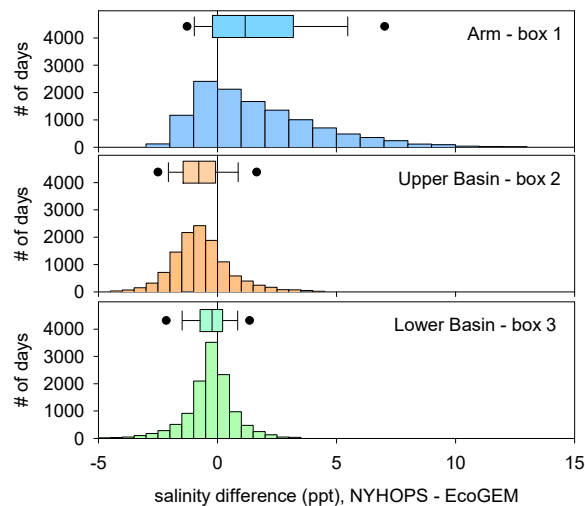
Figure 7: Difference in NYHOPS modeled salinity and EcoGEM salinity model output.

Histograms of 11,992 days (1/1/81 to 10/31/13) of salinity modeling using the simple mixing model in EcoGEM relative to the NYHOPS model output. A boxplot of the same data is at the top of each panel. The box indicates the 25th percentile, median, and 75th percentile of data. The whiskers are at the 10th and 90th percentiles with the black dots indicating the 5th and 95th percentiles. The return flow fraction was optimized to minimize the error in EcoGEM relative to NYHOPS, taking into consideration that NYHOPS overestimates salinity in box 1 relative to field data (thus, skewing to the right in box 1 is preferred).

401
402

5 Biogeochemical Model Development

403

404 An overview of the hydrodynamic and biogeochemical models are provided in Section 2.4 (page 8).

405 The model is structured with three boxes in Niantic River Estuary (Figure 3, page 17). Material is input
406 from the river source at the head (northern-most section) of the model and is exchanged across the
407 southern boundary with Niantic Bay. Each box includes a single layer; original attempts included two
408 layers, but the Niantic River Estuary is vertically well-mixed, so one layer was chosen as a better
409 representation of the system.

410 Relatively few processes and coefficients constitute the model, thus the term intermediate-complexity
411 model (Figure 8, page 23). Formulations are based on empirically derived relationships from the
412 literature. Eight state variables are modeled: salt, phytoplankton biomass, macroalgae biomass, eelgrass
413 biomass, labile nitrogen (inorganic and labile organic), labile phosphorus (inorganic, labile organic, and
414 particulate), benthic carbon, and dissolved oxygen; these are defined below and described further in this
415 section (Section 5). Differential equations define the daily rate of change in each state variable. The
416 differential equation solver used in the model is MatLab's *ode45*, which uses a Runge-Kutta 4th/5th order
417 integration scheme. The change due to mixing is not included in the differential equations of the
418 biogeochemical portion of the model, the mixing occurs once per day in accordance with the method
419 used to create the GEM matrices of mixing coefficients. Constants and coefficients used in the model
420 formulations are detailed in Section 5.2 (page 31).

> **Commented [VJ3]:** verify this is correct for the revised dilution model, in code

421 OVERVIEW OF STATE VARIABLES

422 <u>Salt</u> is not modeled in the ecological portion of the model. Changes in salt are due solely to mixing.

423 <u>Phytoplankton</u> biomass (g C) is modeled as the gross primary production, minus the 24-hour
424 phytoplankton community respiration, minus the heterotrophic respiration of phytoplankton. The
425 heterotrophic respiration of the phytoplankton biomass is modeled using respiratory coefficients,
426 versus modeling zooplankton grazing dynamics. The heterotrophic respiration is partitioned into the
427 fraction of phytoplankton biomass respired in the water column (with nutrients regenerated to the
428 water column) and the fraction delivered to the benthos (fueling benthic metabolism). Exchange of
429 phytoplankton biomass across the open boundaries and among the elements is handled in the
430 mixing routine.

431 <u>Macroalgae</u> biomass (g C) is modeled as the gross primary production, minus the 24-hour respiration,
432 minus the heterotrophic respiration of macroalgae. The heterotrophic respiration is modeled using
433 respiratory coefficients and includes consumption, death, and decay of the algae. Heterotrophic
434 respiration is assumed to be occurring mostly at the sediment-water interface. Macroalgae are not
435 allowed to exchange among boxes, they are assumed to be stationary on the bottom. Some fraction
436 of macroalgae production will be sequestered in the estuarine sediments.

437

Figure 8: Overview of Model Processes
Processes within the model are indicated by the blue arrows with the basis for the formulation shown in black italicized text. The state variables are nitrogen, phosphorus, sediment organic carbon, phytoplankton, macroalgae, seagrass, and oxygen. Black arrows indicate transport of state variables across the boundary of the model domain. For example, N enters via river and groundwater input from the watershed and from atmospheric deposition to the surface of the embayment. N is exchanged with Niantic Bay / Long Island Sound via hydrodynamics and is lost to the atmosphere via denitrification. Note, the black arrows do not always point to the symbol for the state variable to which they are contributing in order to keep the graphical display uncluttered, but their contribution is assigned to those pools. C is carbon, N is nitrogen, P is phosphorus, O_2 is oxygen, T is temperature, OM is organic matter or biomass. The "≡" symbol indicates equivalency, that the N and P are calculated stoichiometrically from C.

Eelgrass biomass (g C) is modeled as the gross primary production, minus the 24-hour respiration, minus the heterotrophic respiration of eelgrass. The heterotrophic respiration is modeled using respiratory coefficients and includes consumption, death, and decay of the eelgrass. Heterotrophic respiration is assumed to be occurring mostly at the sediment-water interface. Eelgrass are not allowed to exchange among boxes, they are assumed to be stationary on the bottom. Some fraction of eelgrass production will be sequestered in the estuarine sediments.

Nitrogen (g N, dissolved inorganic) is modeled as N from atmospheric deposition, N mixed into or out of the element (from freshwater, Niantic Bay, or neighboring model elements), plus the N regenerated to the water column from the sediments as a result of benthic metabolism, plus the N regenerated to the water column from pelagic heterotrophy, plus the N regenerated to the water column due to phytoplankton community respiration, minus the N assimilated by phytoplankton production. A C : N ratio is used to convert these processes originally defined in terms of C to N. Exchange of N across the open boundaries and among the elements is handled in the mixing routine.

Phosphorus (g DIP, dissolved inorganic) is modeled as P mixed into or out of the element (from freshwater, Niantic Bay, or neighboring model elements), P regenerated to the water column from the sediments as a result of benthic metabolism, plus the P regenerated to the water column from

465   pelagic heterotrophy, plus the P regenerated to the water column due to phytoplankton community
466   respiration, minus the P assimilated by phytoplankton production. A C : P ratio is used to convert
467   these processes originally defined in terms of C to P. Exchange of P across the open boundaries and
468   among the elements is handled in the mixing routine.

469   <u>Benthic carbon</u> (g C) is modeled as the C delivered to the benthos from the water column, minus the
470   benthic metabolism. No physical mixing of benthic C is included in the model as benthic processes
471   are not subject to mixing among elements.

472   <u>Oxygen</u> (g O_2) is modeled through stoichiometric relationships between metabolic processes listed
473   above and O_2 production or consumption. Oxygen change is the sum of atmospheric exchange of
474   oxygen across the air-sea interface, plus the O_2 produced through primary productivity by the
475   phytoplankton and macrophytes, minus the O_2 demand by phytoplankton and macrophyte
476   respiration, minus the O_2 demand by heterotrophic water column respiration of phytoplankton and
477   macrophytes, minus the O_2 demand from benthic metabolism. Exchange of O_2 across the open
478   boundaries and among the elements is handled in the mixing routine.

5.1   Constants and Coefficients Related to Primary Producers

480   Availability of light, temperature, and nitrogen limit the specific growth rate of the primary producers
481   (μ). The specific growth rate (d^{-1}) during a time step is determined by calculating and comparing the
482   specific growth rate based temperature, light and nitrogen. Only one of these factors is limiting to
483   growth during any given time step, so the minimum specific growth rate from among the options (light,
484   temperature, nitrogen) is used during a time step. Thus, the competition between the three groups of
485   primary producers is driven by their physiological ability to take in N, grow at certain light levels, or grow
486   at certain temperatures. This section describes how the competition for available nitrogen is handled in
487   the model.

488   The Michaelis-Menten equation is an equation useful for describing enzymatic reaction rates. It has
489   been applied to nutrient uptake by primary producers (Brush and Nixon 2010; Gurney and Nisbet 1998;
490   Touchette and Burkholder 2000; Wang et al. 2014; Ward et al. 2012). This equation assumes that the
491   substrate (nitrogen) reaches equilibrium on a much faster rate than biomass is formed. For primary
492   producers, this is a valid assumption. The realized uptake rate, U (substrate per unit biomass), is
493   calculated based on nitrogen (N):

494      $$U \; = \; U_{max} \, \frac{[substrate]}{(k+[substrate])} \qquad\qquad \text{(eqn. 2)}$$

495   Where U_{max} is the maximum attainable uptake rate of the
496   substrate (substrate per unit biomass), k is the half saturation
497   constant for uptake, and *[substrate]* is the concentration of the
498   substrate (N). Please note, in most presentations of this
499   relationship, U is denoted by the variable V; in the NREEM model
500   description, V refers to volume, so the letter U is used instead.
501   The same equation applies to all three groups of primary
502   producers (P = phytoplankton, E = eelgrass, M = macroalgae):
503   phytoplankton ($U_{P\text{-}N}$), eelgrass ($U_{E\text{-}N}$), macroalgae ($U_{M\text{-}N}$).

A similar relationship could be applied to phosphorus; to keep the model simple, we assume that P is not limiting and thus do not include it.

504 *Table 5-1: Michaelis-Menten equation coefficients.*
505 *Michaelis-Menten equation coefficients for the three groups of primary producers based on nitrogen concentration. The values*
506 *shown in colored bold text are used in NREEM.*

	Maximum Attainable Uptake Rate (U_{max}) of Nitrogen (μmol N g-DW^{-1} h^{-1})	Half Saturation Constant (k) for Nitrogen (mmol N m^{-3})	Information Necessary for Unit Conversion: g C / g-DW	Maximum Attainable Uptake Rate (U_{max}) of Nitrogen (gN$_{uptake}$ gC$_{biomass}^{-1}$ d^{-1}) (for sample calculation, see [C])	Half Saturation Constant (k) for Nitrogen (gN m^{-3})
MACROALGAE					
Ulva lactuca[A]	84.3	15	0.28	0.101	0.210
Ulva lactuca[B]	NH_4^+: 450 NO_3^-: 116	NH_4^+: 85 NO_3^-: 34	0.3 [D]	0.504 0.130	1.190 0.476
Ulva prolifera[B]	NH_4^+: 285 NO_3^-: 124	NH_4^+: 25.1 NO_3^-: 15.1	0.3 [D]	0.319 0.139	0.351 0.211
Ulva linza[B]	NH_4^+: 250 NO_3^-: 109	NH_4^+: 37 NO_3^-: 23	0.3 [D]	0.280 0.122	0.518 0.322
Ulva AVERAGE				**0.228**	**0.468**
Ulva RANGE				**0.101-0.504**	**0.210-1.19**
Graciliaria tikvahiae[A]	52.7	15	0.26	0.068	0.210
Gracilaria folifera[B]	NH_4^+: 23.8 NO_3^-: 9.7	NH_4^+: 1.6 NO_3^-: 2.5	0.22 [D]	0.036 0.015	0.022 0.035
Gracilaria pacifica[B]	NH_4^+: 21.5 NO_3^-: 6	NH_4^+: 50.9 NO_3^-: 26.8	0.22 [D]	0.033 0.009	0.713 0.375
Gracilaria gracilis[B]	NO_3^-: 35	NO_3^-: 5.6	0.22 [D]	0.053	0.078
Gracilaria tenuistipitata[B]	NO_3^-: 37.2	NO_3^-: 61.5	0.22 [D]	0.057	0.861
Gracilaria AVERAGE				0.039	0.328
Gracilaria RANGE				0.009-0.068	0.022-0.861
Cladophora montagneana[B]	NH_4^+: 130 NO_3^-: 42	NH_4^+: 20.7 NO_3^-: 1.4	0.35 [D]	0.125 0.040	0.290 0.020
Cladophora AVERAGE				0.083	0.155
Cladophora RANGE				0.040-0.125	0.02-0.29
SEAGRASS AND PHYTOPLANKTON					
Zostera marina[E]	leaf, NH_4^+: 20.5 root, NH_4^+: 211	leaf, NH_4^+: 9.2 root, NH_4^+: 104	0.336 [F] ± 0.0031	**leaf: 0.021** root: 0.211	**leaf: 0.129** root: 1.456
Ruppia maritima[E]	leaf, NH_4^+: 243-270 root, NH_4^+: 48-56	leaf, NH_4^+: 9.0-17.7 root, NH_4^+: 2.8-12.6	0.336 [F] ± 0.0031	leaf: 0.243-0.270 root: 0.048-0.056	leaf: 0.126-0.248 root: 0.039-0.176
phytoplankton [G]		NO_3^- & NH_4^+: 2.4 range: 0.38-7.09 NO_3^- : 2.9 range: 0.59-7.09 NH_4^+ : 1.9 range: 0.38-4.52		**NO_3^- & NH_4^+ = 1.68** **range = 0.17-4.12** NO_3^- : 2.22 range: 0.34-4.12 NH_4^+ : 1.13 range: 0.17-2.10	**NO_3^- & NH_4^+ = 0.03** **range = 0.01-0.10** NO_3^- : 0.04 range: 0.008-0.099 NH_4^+ : 0.03 range: 0.005-0.063

507 [A] (Brush and Nixon 2010)
508 [B] (Wang et al. 2014; and works reviewed therein)

509 [C] $\frac{gN_{uptake}}{gC_{biomass} \cdot d} = \frac{84.3\ \mu mol\ N}{gDW \cdot h}\ \frac{24\ h}{d}\ \frac{14\ \mu g\ N}{\mu mol\ N}\ \frac{g\ N}{10^6\ \mu g\ N}\ \frac{gDW}{0.28\ gC}$

510 [D] Estimated from Long Island Sound %C data for the genus.
511 [E] (Touchette and Burkholder 2000; and works reviewed therein)
512 [F] (Duarte 1990)
513 [G] (Ward et al. 2012); estimates were available for a range of sizes (cell volume) and types of phytoplankton
514

515 For modeling the growth of phytoplankton, macroalgae, and eelgrass, the Michaelis-Menten equation
516 will be used to determine the rate of nutrient acquisition by each group (phytoplankton, macroalgae,

517 eelgrass). A review of typical values for maximum attainable uptake rate and half saturation coefficient
518 for nitrogen is provided in Table 5-1. This realized uptake rate will be translated into the fraction of the
519 nutrient pool available to each group. However, the Michaelis-Menten equation will not be used to
520 assess growth. Other equations which incorporate important controls on growth for each group will be
521 employed.

522 As an illustration of the relationships among groups of primary producers and the impact on nitrogen
523 demand by each group is plotted for a gradient of water column nitrogen concentrations typical of
524 Niantic River Estuary (Figure 9). While phytoplankton have a faster realized nitrogen uptake rate than
525 macroalgae and seagrass, once the biomass of the three groups is factored in, eelgrass and macroalgae
526 can demand more of the available nitrogen because of their greater biomass. The eelgrass and
527 macroalgae grow slowly compared to phytoplankton, but they also survive longer (lower death and
528 decay rate) and remain in the estuary whereas phytoplankton is exchanged with Long Island Sound
529 through mixing.
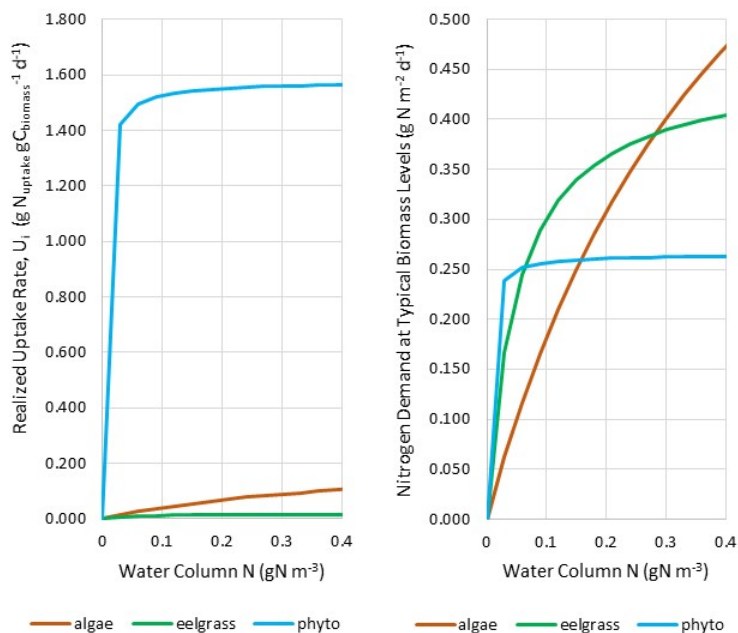
530
531 *Figure 9: Michaelis-Menten relationships for primary producers versus nitrogen.*
532 *Left panel: Curves describe the impact of limiting factors on the maximum attainable uptake rate for each class of primary*
533 *producers. Right panel: Nitrogen demand based on typical biomass levels found in NRE: 4.5 gC m^{-2} algae; 24.5 gC m^{-2} eelgrass;*
534 *0.168 gC m^{-2} phytoplankton.*

535 Modeling macroalgae and eelgrass growth require an understanding of typical carbon to nitrogen ratios
536 (C:N, molar ratio). For estuarine macrophytes, we assume phosphorus is not limiting. Millstone
537 Environmental Lab has collected macrophytes from their trawl station in Niantic River since July 2012,

538   with trawls conducted every two weeks throughout the year (Figure 10, page 27). Macroalgae is
539   collected from one location, thus comparisons are not confounded by the potential impact of varying
540   nutrient supply in different locations within Niantic River Estuary. Carbon content varies by species, but
541   is generally stable throughout the year. Nitrogen content varies by season and thus drives the variability
542   in the C:N molar ratio. Individual species typically show a similar range in values interannually (Figure 10,
543   page 27), allowing for grouping of all samples by month (Figure 11, page 28).
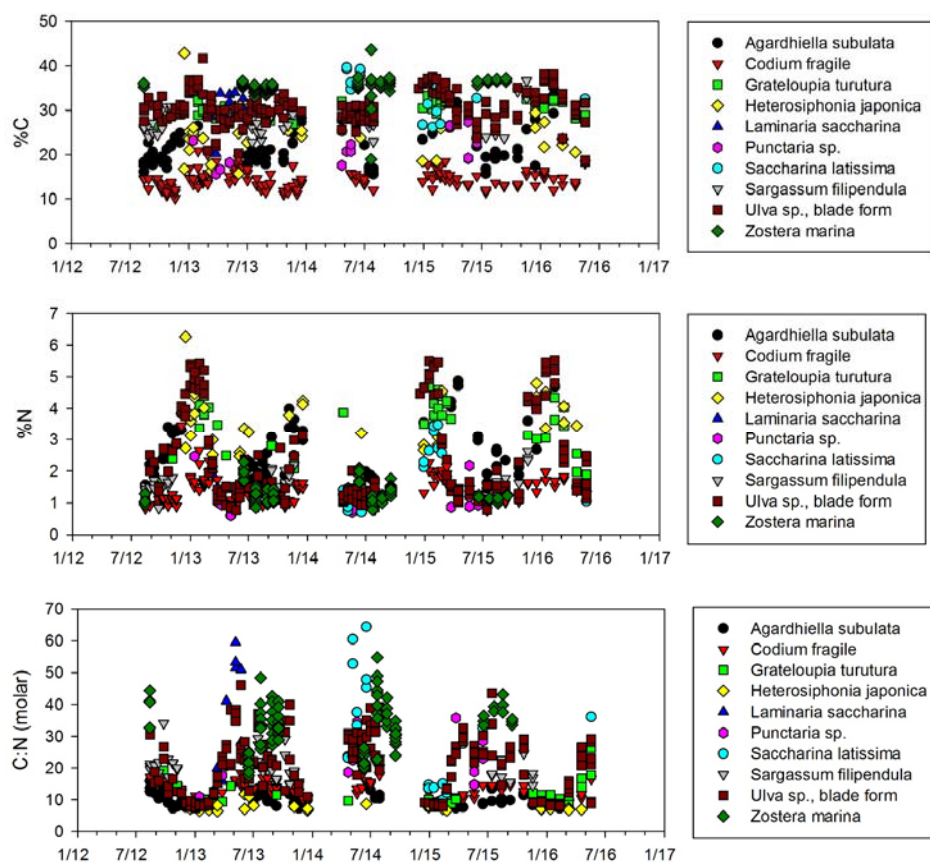
544
545   *Figure 10: C : N molar ratio of macrophytes.*
546   *Macrophytes are collected during Millstone Environmental Lab's biweekly trawl survey in Niantic River. Analysis of macrophyte*
547   *samples are ongoing, explaining the gaps in the data. Only species with 12 or more samples are included in the analysis for the*
548   *model.*
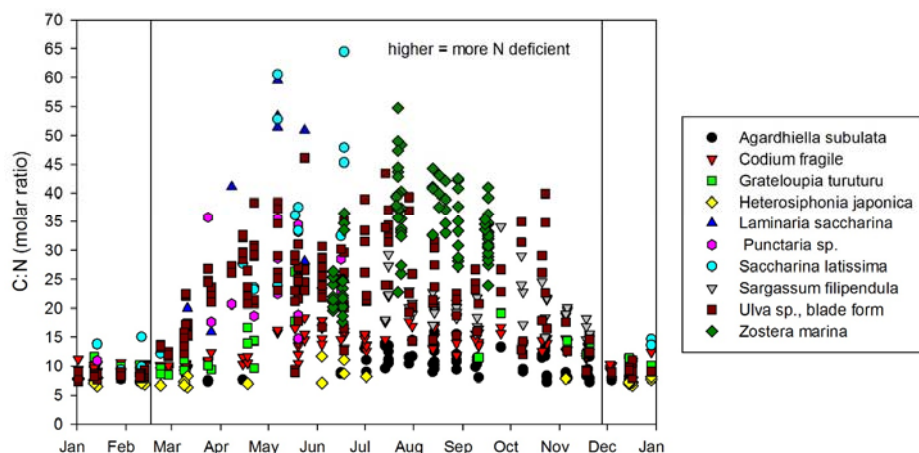
549
550 *Figure 11: C:N molar ratio by season.*
551 *Data from 2012 to 2016 were combined into a single plot with samples plotted by month and date. The lines at February 17 and*
552 *December 28 mark the boundaries of the winter season, when nitrogen is not limited.*

553 Examination of the C:N molar ratio by day of the year (ordinal date) illustrates the impact of growth rate
554 on the internal deficiency of nitrogen in macrophytes (Figure 11, page 28). The winter months represent
555 the ideal C:N ratio for macrophyte growth. During the spring, summer, and fall months, the increased
556 amount of light and warmer temperatures allow for increased growth rates. Macrophytes are capable of
557 luxury uptake of nitrogen (Brush and Nixon 2010);
558 when nitrogen is plentiful, they take in excess
559 nitrogen and store it internally. When nitrogen in the
560 environment is lower, they can access these internal
561 pools of nitrogen. The winter values represent the
562 optimal (minimum) C:N molar ratio (Table 5-2, page
563 29). The maximum summer values represent the C:N
564 molar ratio required by each species. The three
565 highest C:N molar ratios for each species were used
566 to calculate the maximum allowable C:N molar ratio
567 (Table 5-2, page 29). Use of daily varying C:N and C:P
568 ratios based on local field data accomplish the same
569 end as modeling luxury uptake of nutrients.

Adding luxury uptake and internal storage of nitrogen to the macroalgae pool increases the complexity of the model. These steps may be taken if necessary, following the methods of Brush and Nixon (2010). If luxury uptake is added, the C:N of the macrophytes will be modeled versus determined based on field data.

570 *Agardhiella subulata* and *Ulva* sp., blade form are the dominant macroalgae species found throughout
571 Niantic River, with *Codium fragile* also commonly found in the southern portions of the river (Vaudrey
572 2007; Vaudrey et al. 2019). The average C:N molar ratio was determined for each ordinal date by using a
573 third order polynomial regression of C:N molar ratio on ordinal date for the period of 2/17 through
574 11/28 (Table 5-3, page 30; Figure 12, page 30). For the winter, C:N molar ratio was set to the minimum
575 C:N molar ratio (Table 5-2, page 29).

576 *Zostera marina* in NRE exhibits a C:N of 18.6 in June (average of lowest three values) ranging to a high
577 value (average of highest three values) of 51 in late July (Figure 11, page 28). The June value of 18.6 C:N
578 coincides with a worldwide review of C:N ratios for seagrasses not experiencing nutrient limitation
579 (Duarte 1990) of 16 C:N and the overall pattern of increasing C:N in late summer has been observed
580 elsewhere in Long Island Sound eelgrass beds (Vaudrey et al. 2009). The average C:N molar ratio was
581 determined for each ordinal date by using a third order polynomial regression of C:N molar ratio on
582 ordinal date for the period of 2/17 through 11/28 (Table 5-3, page 30; Figure 13, page 31). For the
583 winter, C:N molar ratio was set to the minimum C:N molar ratio (Table 5-2, page 29).

584 *Table 5-2: C:N molar ratios of macrophytes.*
585 *All available samples from the winter were used in calculating the optimal C:N molar ratios. The highest three C:N molar ratios*
586 *from the summer period were used for calculating the maximum C:N. The bold font identifies the species with greatest biomass*
587 *in Niantic River Estuary. Samples were collected by Millstone Environmental Lab during biweekly trawl surveys at one location in*
588 *Niantic River Estuary.*

	Average C:N (molar ratio)	Standard Deviation of C:N (molar ratio)	Standard Error of C:N (molar ratio)	Number of Samples
WINTER				
Agardhiella subulata (red)	**8.3**	**1.0**	**0.3**	**12**
Ulva sp., blade form (green)	**8.6**	**0.6**	**0.1**	**44**
Codium fragile (green)	**10.0**	**0.8**	**0.1**	**32**
Heterosiphonia japonica (red)	*7.3*	*0.5*	*0.1*	*19*
Grateloupia turuturu (red)	*9.3*	*1.2*	*0.3*	*15*
Saccharina latissima (brown)	*12.2*	*2.7*	*1.0*	*7*
SUMMER				
Agardhiella subulata (red)	**15.3**	**0.7**	**0.4**	**3**
Codium fragile (green)	**19.4**	**1.0**	**0.6**	**3**
Ulva sp., blade form (green)	**43.2**	**3.1**	**1.8**	**3**
Zostera marina (vascular) - max	**50.7**	**3.5**	**2.0**	**3**
Zostera marina (vascular) - min	**18.6**	**1.0**	**0.6**	**3**
Grateloupia turuturu (red)	*21.1*	*4.6*	*2.6*	*3*
Heterosiphonia japonica (red)	*10.5*	*1.6*	*0.9*	*3*
Laminaria saccharina (brown)	*54.8*	*4.2*	*2.4*	*3*
Punctaria sp. (brown)	*35.2*	*0.7*	*0.4*	*3*
Saccharina latissima (brown)	*59.2*	*5.9*	*3.4*	*3*
Sargassum filipendula (brown)	*30.8*	*2.8*	*1.6*	*3*

589

Table 5-3: Results of Polynomial Regression of C:N on ordinal date.

Non-winter data for C:N molar ratios were regressed on ordinal date. Statistical results are fully reported in Sections 12.1 (page 94), 12.2 (page 95), and 12.3 (page 96).

format of the regression equation → f = y0 + a(x) + b(x²) + c(x³)								
	Aghardiella subulata				*Ulva* sp., blade form			
	coefficient	std. error	t	P	coefficient	std. error	t	P
y0	2.1855	6.3945	0.3418	0.7337	-3.9563	6.6285	-0.5969	0.5515
a	0.0575	0.1069	0.5379	0.5929	0.4356	0.1305	3.3375	0.0011
b	3.22×10^{-5}	0.0005	0.0589	0.9532	-0.0018	0.0008	-2.3526	0.0199
c	-4.16×10^{-7}	8.66×10^{-7}	-0.5322	0.5964	2.05×10^{-6}	1.37×10^{-6}	1.4877	0.1389
Adjusted R^2	0.30				0.24			
Standard Error of the Estimate	1.78				6.64			
F-statistic	10.59				17.48			
P	<0.0001				<0.0001			
	Zostera marina							
y0	-440.2775	129.848	-3.391	0.0010				
a	5.643	1.800	3.135	0.0023				
b	-0.0214	0.0082	-2.6162	0.0104				
c	2.56×10^{-5}	1.22×10^{-5}	2.106	0.0380				
Adjusted R^2	0.47							
Standard Error of the Estimate	5.90							
F-statistic	29.62							
P	<0.0001							
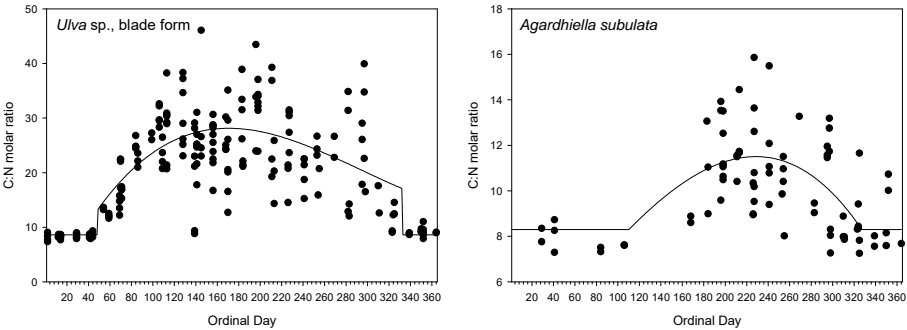
Figure 12: C:N molar ratio for seaweeds, modeled versus field data.

Winter field data were set to the minimum average C:N molar ratio. For each ordinal date, a C:N molar ratio was calculated using a third order polynomial regression (Table 5-3, page 30), indicated by the black lines. The C:N molar ratio for each date is presented in Section 11.1, (page 85).
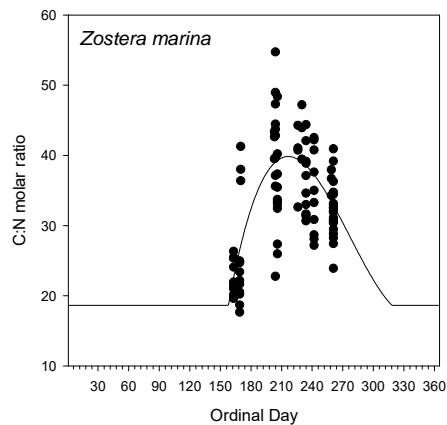
Figure 13: C:N molar ratio for eelgrass, modeled versus field data. Winter field data were set to the minimum average C:N molar ratio. For each ordinal date, a C:N molar ratio was calculated using a third order polynomial regression (Table 5-3, page 30), indicated by the black line. The C:N molar ratio for each date is presented in Section 11.1, (page 85).

601

5.2   Constants and Coefficients - Summary

603 Constants and coefficients used in the model are presented in Table 31 (page 31). References and
604 descriptions in the Table explain the derivation of these values. A longer description is available in
605 Vaudrey (2016).

606 *Table 5-4: Constants and Coefficients*
607 ==need to add values for algae and eelgrass==

variable name	typical value	units	description	reference
$c_{B\text{-}phyto}$	42 (30 to 60)	g C : g Chl	carbon to chlorophyll, for phytoplankton	Valiela (1995), Cloern et al. (1995), Brush et al. (2002)
$c_{N\text{-}phyto}$	6.625	moles C : moles N	conversion of C to N, for phytoplankton	Redfield Ratio; Kremer and Nixon (1978)
$c_{P\text{-}phyto}$	106	moles C : moles P	conversion of C to P, for phytoplankton	Redfield Ratio; Kremer and Nixon (1978)
$c_{N\text{-}eelg}$	changes daily (18 to 40)	moles C : moles N	conversion of C to N, for eelgrass	see Section 5.1 (page 24) and Appendix C (page 85)
$c_{P\text{-}eelg}$	435 (200 to 800)	moles C : moles P	conversion of C to P, for eelgrass	Duarte (1992)
$c_{N\text{-}algae}$	changes daily (8 to 28)	moles C : moles N	conversion of C to N, for macroalgae	see Section 5.1 (page 24) and Appendix C (page 85)
$c_{P\text{-}algae}$	800 (300 to 1000)	moles C : moles P	conversion of C to P, for macroalgae	Duarte (1992)
r_P	0.52 (0.02 to 1.2)	d^{-1}	phytoplankton autotrophic respiration as a fraction of phytoplankton stock	Oviatt and Smith field data (*pers. comm.*), corresponds to Falkowski and Woodhead (1992)
r_{M0}	7.875 x 10^{-4}	d^{-1}	macroalgae autotrophic respiration rate at 0°C	

variable name	typical value	units	description	reference
r_{MQ}	0.15	°C^{-1}	macroalgae autotrophic thermal respiratory quotient (Q$_{10}$ for respiration)	
g_0	0.047	d^{-1}	water column phytoplankton grazing rate at 0°C	*optimized value*
g_Q	0.095	°C^{-1}	water column phytoplankton grazing thermal respiratory quotient (Q$_{10}$ for respiration)	Brush's (2002) Greenwich Bay model, from Sampou & Kemp (1994)
g_{M0}	0.01	d^{-1}	grazing rate on macroalgae at 0°C	Brush and Nixon (2010)
g_{MQ}	0.122	°C^{-1}	macroalgae grazing thermal respiratory quotient (Q$_{10}$ for respiration)	Brush and Nixon (2010)
φ	0.238 (0.23 to 0.25)	1/d	fraction of phytoplankton NPP24 delivered to the benthos	Nixon (1981) = 0.238 NPP24 Brush (2002) = 0.25 NPP24 Kemp et al (2005) = 0.24 phyt_bio
b_0	0.00489 (0.001 to 0.2)	°C^{-1}	benthic respiration (remin) coeff at 0°C	*optimized value*
b_Q	0.14	d^{-1}	benthic thermal respiratory quotient (Q$_{10}$ for respiration)	Brush (2002) based Greenwich Bay model value.
σ	0.4	unitless	fraction of the sediment N denitrified	Kremer used a straight fraction of 0.5 in the CLUE model
$\dot{\omega}$	1.3 (1 to 1.4)	moles O$_2$: moles C	photosynthetic quotient for phytoplankton, O$_2$ produced : C assimilated	Valiela (1995) Smith and Oviatt (*pers. comm.*) photosynthetic equation
ω_p	0.89 (narrowly constrained)	moles C : moles O$_2$	respiratory quotient for phytoplankton, Org C respired : O$_2$ consumed	Williams and del Giorgio (2005) Hedges et al. (2002) Williams and Robertson (1991) Smith and Oviatt (*pers. comm.*)
ω_g	0.97 (0.78 to 1.16)	moles C : moles O$_2$	respiratory quotient for phytoplankton grazing, Org C respired : O$_2$ consumed	Hernández-León and Ikeda (2005) Smith and Oviatt (pending)
ω_s	1 : 30.5 (1:14.8 to 1:46.2)	moles N : moles O$_2$	respiratory quotient for sediment, N regenerated : O$_2$ consumed	Fulweiler and Nixon's sediment core data, this project
K_{phyto}	0.017 (0.015 to 0.019)	m^{-1} (ug/L)$^{-1}$	diffuse attenuation coeff. due to phytoplankton	
K_0	0.527 (0.512 to 0.542)	m^{-1}	diffuse attenuation coefficient due to water	
d_{dry}	6	Kg N ha^{-1} y^{-1}	dry deposition	Clark and Kremer (2005)
d_{wet}	30 (9 – 200)	uM N	nitrogen concentration in wet precipitation	Clark and Kremer (2005) Nat'l. Atm. Deposition Program

608

5.3 Description of Model Formulations

5.3.1 Light Available at Depth

The productivity of phytoplankton, macroalgae, and eelgrass form the basis of many of the formulations in the ecological model. Light is an important forcing factor as it is one of the primary factors affecting primary production. The light attenuation factor (K, m^{-1}) is calculated as the sum of the contribution from the water (K_0) and the phytoplankton (K_p), which are defined in Table 5-4 (page 31). Field data from Narragansett Bay, RI were used to validate the choice of model for calculating K and for the decision of the intercept term (K_0) which describes the light attenuation due to non-phytoplankton related properties of the water (Vaudrey 2016). This data set from Narragansett Bay included 202 profiles of light in the water column gathered with a Li-Cor LI193SA Spherical Underwater Quantum Sensor coupled with a Li-Cor Quantum deck sensor. While some data are available for local Long Island Sound embayments, no data set matches the number of profiles and consistency with which these Narragansett Bay data were collected. The CTDEEP cruises have a similar dataset collected over a long time frame, but those collections are in deeper, more open waters. The field data were used to estimate an average and range of values for K_0 and K_p (Table 5-4, page 31) and indicated a linear model was the best choice:

$$K = K_0 + \frac{1000 K_P B_P}{c_B V} \qquad \text{(eqn. 3)}$$

where B_P is the phytoplankton biomass in each element (gC element^{-1}), V is the volume of each element (m^3), and c_B is the carbon to chlorophyll mass ratio (unitless). The K is calculated for both surface and bottom elements, using the light available at the surface of the element.

5.3.1.1 Correction to Photic Zone Depth in Shallow Systems

The depth of the photic zone was calculated using the Lambert-Beer equation,

$$I_z = I_0 e^{-Kz} \qquad \text{(eqn. 4)}$$

where z is depth (m), K is the diffuse attenuation coefficient (m^{-1}, eqn. 3), I_0 is the light at the surface, and I_z is the light at depth z. The depth of the photic zone was defined as the depth receiving 1% of the incident irradiance at the surface of the water column.

The polynomial regressions in Table 5-5 (page 34) are used to correct the photic zone depth in cases where light reaches the bottom of the element. Light decays in the water in an exponential fashion with depth. Thus, taking a fraction of the photic zone attributed to the depth of a layer would yield an incorrect estimate of the total light received integrated over the water column depth of the element.

I_o (E m^{-2} d^{-1})	Regression
1 - 10	$\%P_t = -1.20E^{-6}(\%Z_p)^4 + 4.25E^{-4}(\%Z_p)^3 - 5.85E^{-2}(\%Z_p)^2 + 3.80(\%Z_p)$
11 – 20	$\%P_t = 9.06E^{-7}(\%Z_p)^4 - 8.85E^{-5}(\%Z_p)^3 - 1.66E^{-2}(\%Z_p)^2 + 2.64(\%Z_p)$
21 – 30	$\%P_t = 1.30E^{-6}(\%Z_p)^4 - 2.25E^{-4}(\%Z_p)^3 - 1.45E^{-3}(\%Z_p)^2 + 2.10(\%Z_p)$
31 – 40	$\%P_t = 1.15E^{-6}(\%Z_p)^4 - 2.30E^{-4}(\%Z_p)^3 + 3.28E^{-3}(\%Z_p)^2 + 1.82(\%Z_p)$
41 – 50	$\%P_t = 8.97E^{-7}(\%Z_p)^4 - 1.99E^{-4}(\%Z_p)^3 + 4.22E^{-3}(\%Z_p)^2 + 1.67(\%Z_p)$
51 – 60	$\%P_t = 6.84E^{-7}(\%Z_p)^4 - 1.68E^{-4}(\%Z_p)^3 + 3.99E^{-3}(\%Z_p)^2 + 1.59(\%Z_p)$
61 - 70	$\%P_t = 4.80E^{-7}(\%Z_p)^4 - 1.34E^{-4}(\%Z_p)^3 + 3.31E^{-3}(\%Z_p)^2 + 1.53(\%Z_p)$
71 - 80	$\%P_t = 3.15E^{-7}(\%Z_p)^4 - 1.06E^{-4}(\%Z_p)^3 + 2.56E^{-3}(\%Z_p)^2 + 1.48(\%Z_p)$
81 - 90	$\%P_t = 1.75E^{-7}(\%Z_p)^4 - 8.04E^{-5}(\%Z_p)^3 + 1.75E^{-3}(\%Z_p)^2 + 1.45(\%Z_p)$
91 - 100	$\%P_t = 7.80E^{-8}(\%Z_p)^4 - 6.21E^{-5}(\%Z_p)^3 + 1.12E^{-3}(\%Z_p)^2 + 1.43(\%Z_p)$

643

5.3.2 Balancing Production Among the Three Groups of Primary Producers

645 Checks in the model prevent the primary producers (phytoplankton, macroalgae, eelgrass) from growing
646 beyond the availability of the limiting nutrient in the water column, nitrogen or phosphorus. The
647 available stock of each nutrient is checked at each time step. The C : N and C : P ratios are used to
648 confirm that N and P are sufficient to support the predicted growth. If a nutrient is limiting, growth is
649 limited to that which is supported by the available stock.

650 The competition for nitrogen among the three primary
651 producers takes into account the biomass of each group
652 in the box model as well as the nitrogen stock in the
653 water column. When nitrogen stock is low,
654 phytoplankton will have a competitive edge due to their
655 higher realized uptake rate at low concentrations. But
656 at higher nitrogen stocks, eelgrass and macroalgae will
657 get a higher fraction of the available nitrogen due to
658 slightly increased uptake rates, though their affinity for
659 nitrogen is still low compared to phytoplankton. The
660 fraction of N available to each group is calculated as:

Seagrass is able to access nutrients stored in the sediment. At present, the seagrass growth is modeled using only the water column nutrients. If necessary, a separate state variable for benthic nitrogen could be added to allow seagrass access to this source.

661
$$U_i = B_i \cdot U_{max_i} \frac{substrate}{(k_i \cdot V + substrate)} \qquad \text{(eqn. 5)}$$

662 Where U_i (g N element^{-1} d^{-1}) is the realized uptake rate based on the Michaelis-Menten coefficients for
663 the group (Table 5-1; U_{max}, gN gC$_{biomass}^{-1}$ d^{-1}; k_i, gN m^{-3}), V is the volume of the element (m^3), and
664 *substrate* is the stock of nitrogen in the element (gN element^{-1}).

665 The fraction assigned to each group of primary producers is determined by:

666 $$fraction\ of\ N_i\ =\ \frac{U_i}{(U_P + U_M + U_E)}$$ (eqn. 6)

5.3.3 Phytoplankton Gross Primary Production and Autotrophic Respiration

668 Phytoplankton growth is modeled using a BZI (biomass-photic zone depth-incident irradiance)
669 relationship which has been applied in many estuarine ecosystems (see reviews in: Brawley et al. 2003;
670 Brush and Brawley 2009; Brush et al. 2002). The temperature range in Niantic River Estuary should not
671 limit growth of phytoplankton and is not included in the assessment of production, though it is included
672 in respiration. The empirical BZI (biomass-photic zone depth-incident irradiance) model predicts
673 estuarine phytoplankton daytime net primary production (β, as mg C m^{-2} d^{-1}) from the existing standing
674 stock of phytoplankton (B_P, as chl a, mg m^{-3}), depth of the photic zone (Z, m), and surface irradiance (I_0, E
675 m^{-2} d^{-1}) (Brawley et al. 2003; Brush et al. 2002).

676 $$\beta = 200 + 0.76 B_P Z I_0$$ (eqn. 7)

677 If the depth of the model element is less than the photic zone depth, a correction (eqn. 8) is applied to
678 equation 7. The correction factor, Z_{corr} (fraction), is calculated using polynomial regression equations
679 predicting net primary production occurring in various fractions of the photic depth, as presented in
680 Brush and Brawley (2009) and detailed in Section 5.3.1.1, (page 33).

681 $$\beta_{corr} = \beta Z_{corr}$$ (eqn. 8)

682 The daytime net primary production (β_{corr}, mg C m^{-2} d^{-1}) is converted to units appropriate to the model
683 (β_{day}, g C element^{-1} d^{-1}) separately for each element, where V is the volume of the element (m^3), and T is
684 the thickness or depth of the element (m):

685 $$\beta_{day} = \frac{\beta_{corr} V}{1000 T}$$ (eqn. 9)

686 To calculate the 24-hour net primary production (β_{24}), the phytoplankton respiration during the
687 nighttime must be estimated. Phytoplankton respiration is calculated using a constant fraction (r_P, d^{-1}) of
688 the phytoplankton stock (B_P, g C element^{-1}), where the length of night (Θ) is expressed as a fraction of
689 the 24-hour day.

690 $$\beta_{24} = \beta_{day} - r_P B_P \theta$$ (eqn. 10)

691 The 24-hour phytoplankton respiration (g C element^{-1}) is calculated as:

692 $$R_P = r_P B_P$$ (eqn. 11)

693 If the sum of the oxygen demand by all primary producers is greater than the oxygen available in the
694 water column dissolved oxygen pool, primary producers will die. The amount of death in each class of
695 primary producer will be determined by first looking at the net oxygen production by each class ($G_i - R_i$);
696 if it is positive, that class of primary producers does not sustain any oxygen-related death. If the net
697 oxygen production by a class of primary producers is negative, the negative net production may
698 potentially be converted into a loss term, to bring the system back to a 0 mg/L level of oxygen. Multiple

699 demands are placed on the oxygen pool: autotrophic respiration, heterotrophic respiration, and benthic
700 respiration. These demands will be balanced, apportioning death or reduction in function to each
701 process proportional to the demand and the deficit in oxygen – all processes will compete on equal
702 footing for oxygen.

703 The theoretical gross primary production (g C element^{-1} d^{-1}) of phytoplankton (G_{Pt}) is calculated from β_{day}
704 by adding an estimate of the phytoplankton autotrophic respiration during the day, where length of day
705 (1-Θ) is expressed as a fraction of the 24-hour day:

706
$$G_{Pt} = \beta_{day} + R_P(1 - \Theta) \qquad \text{(eqn. 12)}$$

707 The actual gross primary production (g C element^{-1} d^{-1}) of phytoplankton (G_P) will be the minimum value
708 of G_{Pt} and the maximum attainable growth based on the nitrogen available to the phytoplankton.

709
$$G_P = min\left(G_{Pt}, \left[\frac{U_P}{U_P+U_E+U_M} \cdot N \cdot c_{N-phyto} \cdot \frac{12\ gC}{1\ mole\ C} \cdot \frac{1\ mole\ N}{14\ gN}\right]\right) \qquad \text{(eqn. 13)}$$

710 where U_P, U_E, and U_M are the nitrogen utilization of each class of primary producers (equation 2, page
711 24); N is the nitrogen in the element (gN element^{-1}); and $c_{N-phyto}$ is the C:N molar ratio for phytoplankton.

712 ### 5.3.4 Macroalgae Gross Primary Production and Autotrophic Respiration

713 The model for macroalgae production will follow the methods of Brush and Nixon (2010) with a number
714 of simplifications. Brush and Nixon (2010) modeled the thick mats of macroalgae (*Ulva* sp. and *Gracilaria*
715 sp.) in Greenwich Bay, RI, dividing the mats into 11 vertical
716 layers and modeling attenuation of light as you progress down
717 through the mat. Niantic River does not currently host thick
718 mats of algae, except possibly in the depths of the channel in
719 the lower basin. While *Aghardiella subulata* covers much of the
720 northern most portion of the estuary, in the shallow regions, it
721 is not especially thick. Loss of light within the depth of the
722 macroalgae mat will not be modeled. Brush and Nixon (2010)
723 modeled algae by using the maximum uptake rate coupled
724 with substrate availability and competition among primary
725 producers. The production is further controlled by
726 temperature. They included luxury uptake and storage of
727 nutrients within the macroalgae; in the NREEM, use of daily
728 varying C:N and C:P ratios based on local field data accomplish
729 the same end as modeling luxury uptake of nutrients. For
730 simplicity, only *Ulva* sp. is modeled in the NREEM; alternate
731 equations for *Agardhiella* sp. could be added in at a later time,
732 using Brush and Nixon's (2010) equations for *Gracilaria*.

Additional modifications to the macroalgae model could include modeling Ulva *and* Aghardiella *species as two separate pools with separate uptake rates, adding light limitation in thick mats of macroalgae, and adding in luxury uptake of nutrients (which would mean that C:N is modeled, not specified based on field data). To keep the model simple, these processes are not currently included.*

733 For macroalgae, the growth rate will be determined as the minimum specific growth rate among light
734 (μ_{M-I}) and nutrient availability(μ_{M-N}) (Equation 2, page 24; Table 5-1, page 25) and the impact of
735 temperature on growth rate (presented below).

736 *5.3.4.1 Gross Primary Production of Macroalgae*

737 Temperature impacts both the gross primary production (GPP) and respiration (R) rates of the
738 macroalgae. The maximum attainable GPP (GPP_{max}) is an exponential temperature-dependent function
739 up to an optimum value above which the GPP_{max} declines rapidly to zero; the equation follows that used
740 for *Ulva* by Brush and Nixon (2010). Brush and Nixon's (2010) equations for GPP were in units of mg O_2
741 versus mg C used in the NREEM.

742 The max attainable biomass specific GPP based on temperature (GPP_T, mg O_2 gD.W.$^{-1}$ h^{-1}) becomes:

743
$$GPP_T = 0.51 \, e^{(0.195 - 0.000007 \, e^{0.36\epsilon})\epsilon} \qquad \text{(eqn. 14)}$$

744 where ϵ is temperature (°C). The rate is initially calculated in hours as the intensity of the sunlight
745 impacts the rate of productivity, calculated as the daily total insolation divided by the number of hours
746 of light on a given day.

747 Brush and Nixon (2010) calculate the GPP per layer of macroalgae, where a layer is 1 cm thick. For the
748 NREEM, we assume that productivity is well-represented by a single layer. In embayments with thicker
749 mats of macroalgae, the calculation by layer can be added in, which allows for light attenuation as you
750 move down in the mat of algae. Gross primary production of macroalgae is driven by a photosynthesis-
751 irradiance relationship, yielding an hourly value for GPP (GPP_{TI}, mg O_2 gD.W.$^{-1}$ h^{-1}):

752
$$GPP_{TI} = GPP_T \left(1 - e^{-\left(\frac{\alpha I}{GPP_T}\right)} \right) \qquad \text{(eqn. 15)}$$

753 where GPP_T is the macroalgae temperature-dependent maximum attainable GPP (Equation 14, Figure
754 14) (mg O_2 gD.W.$^{-1}$ h^{-1}), I is instantaneous incident irradiance at the bottom of the water column (μmol
755 m^{-2} s^{-1}), and α (mg O_2 gDW^{-1} h^{-1} (μmol m^{-2} s^{-1})$^{-1}$) is a coefficient set to 0.18 based on measurements in
756 *Ulva* (Brush and Nixon 2010).
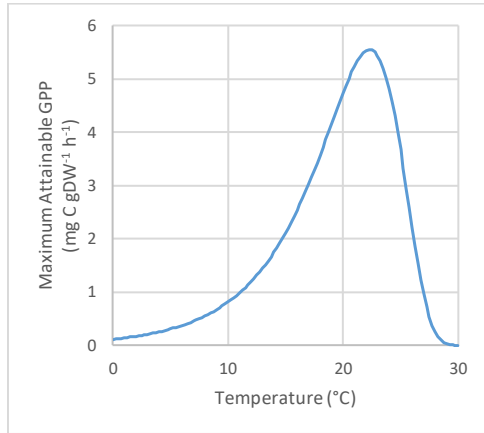
Figure 14: Macroalgae Maximum Attainable Gross Primary Production
Temperature depended maximum attainable gross primary production of macroalgae, as calculated from Equation 15.

757
758

759   To convert GPP_{TI} (mg O_2 gD.W.$^{-1}$ h^{-1}) to units of the rate of change for the state variable in the model (g C
760   element^{-1} d^{-1}), conversions are needed. To convert oxygen to carbon, a molar ratio of 1.7 O_2 : C was
761   derived by balancing the following production/respiration equation using the average C : N ratio of 20
762   for macroalgae (1.6 O_2 : C is equivalent to an RQ of 0.59):

763         $640\ CO_2 + 1382\ H_2O + 32\ NO_3 + 2\ PO_4 = (CH_2O)_{640}(NH_3)_{32}(H_3PO_4)_2 + 1059\ O_2$ (eqn. 16)
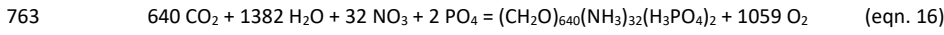
764   The fraction of carbon in seaweed dry weight was set at: 0.25 g C / 1 g dry weight. This value was based
765   on the %C in *Ulva* sp. and *Agardhiella subulata* in NRE (Figure 10, page 27). Carbon content remains
766   relatively steady across years and across seasons. *Agardhiella subulata* is typically around 20% C while
767   *Ulva* is typically around 30% C. The value of 25% was chosen as representative of both species, with a
768   range of 18% to 35%.

769   The theoretical gross primary production of macroalgae (G_{Mt}, g C element^{-1} d^{-1}) becomes:

770         $G_{Mt} = GPP_{TI}\ \dfrac{gD.W.}{0.25\ gC}\ \dfrac{1\ mmole\ O_2}{32\ mg\ O_2}\ \dfrac{1\ mmole\ C}{1.7\ mmole\ O_2}\ \dfrac{12\ mg\ C}{1\ mmole\ C}\ \dfrac{1\ g\ C}{1000\ mg\ C}\ \dfrac{24\ h}{d}\ (1 - \theta)\ B_M$ (eqn. 17)

771   where GPP_{TI} (mg O_2 gD.W.$^{-1}$ h^{-1}) is the gross primary production determined based on light and
772   temperature (equation 15, page 37), where the length of day (*1 - θ*) is expressed as a fraction of the 24-
773   hour day, and B_M is the biomass of macroalgae in the box (gC element^{-1}).

774   The actual gross primary production (g C element^{-1} d^{-1}) of macroalgae (G_M) will be the minimum value of
775   G_{Mt} and the maximum attainable growth based on the nitrogen available to the macroalgae.

776         $G_M = min\left(G_{Mt}, \left[\dfrac{U_M}{U_P + U_E + U_M} \cdot N \cdot c_{N-algae} \cdot \dfrac{12\ gC}{1\ mole\ C} \cdot \dfrac{1\ mole\ N}{14\ gN}\right]\right)$ (eqn. 18)

777 where U_P, U_E, and U_M are the nitrogen utilization of each class of primary producers calculated as the
778 minimum based on available light and nitrogen (equation 2, page 24); N is the nitrogen in the element
779 (gN element^{-1}); and $c_{N\text{-}algae}$ is the C:N molar ratio for macroalgae (Table 5-4, page 31).

780 *5.3.4.2 Autotrophic Respiration of Macroalgae*

781 An exponential function of temperature was developed by Brush and Nixon (2010) to describe
782 autotrophic respiration of macroalgae. Their equation for *Ulva* was based on a sparse data set and used
783 a Q_{10} of 0.15°C^{-1} and a respiration rate at 0°C of 0.035 mg O_2 gD.W.$^{-1}$ h^{-1}. The following equation converts
784 the respiration rate at 0°C (r_{M0}) to units consistent with the NREEM (d^{-1}):

785
$$r_{M0} = 7.412 \; x \; 10^{-4} = \frac{0.035 \; mg \; O_2}{gD.W. \; h} \; \frac{gD.W.}{0.25 \; gC} \; \frac{1 \; mmole \; O_2}{32 \; mg \; O_2} \; \frac{1 \; mmole \; C}{1.7 \; mmole \; O_2} \; \frac{12 \; mg \; C}{1 \; mmole \; C} \; \frac{1 \; g \; C}{1000 \; mg \; C} \; \frac{24 \; h}{d} \qquad \text{(eqn. 19)}$$

786 The autotrophic respiration of macroalgae (gC element^{-1} d^{-1}) is modeled as (Figure 15):

787
$$R_M = r_{M0} \; e^{(r_{MQ} \; \epsilon)} \; B_M \qquad \qquad \text{(eqn. 20)}$$

788 where r_{M0} is the macroalgae autotrophic respiration rate at 0°C (d^{-1}, Table 5-4, page 31), r_{MQ} is the
789 macroalgae autotrophic thermal respiratory quotient (Q_{10} for respiration) (°C^{-1}, Table 5-4, page 31), ϵ is
790 the temperature (°C), and B_M is the biomass of macroalgae (gC element^{-1}).

791 Autotrophic respiration returns N and P to the water column, in stoichiometric balance with C.

792 If the sum of the oxygen demand of all primary producers is greater than the oxygen available in the
793 water column dissolved oxygen pool, primary producers will die. The amount of death in each class of
794 primary producer will be determined by first looking at the net oxygen production by each class ($G_i - R_i$);
795 if it is positive, that class of primary producers does not sustain any oxygen-related death. If the net
796 oxygen production by a class of primary producers is negative, the negative net production may
797 potentially be converted into a loss term, to bring the system back to a 0 mg/L level of oxygen. Multiple
798 demands are placed on the oxygen pool: autotrophic respiration, heterotrophic respiration, and benthic
799 respiration. These demands will be balanced, apportioning death or reduction in function to each
800 process proportional to the demand and the deficit in oxygen – all processes will compete on equal
801 footing for oxygen.
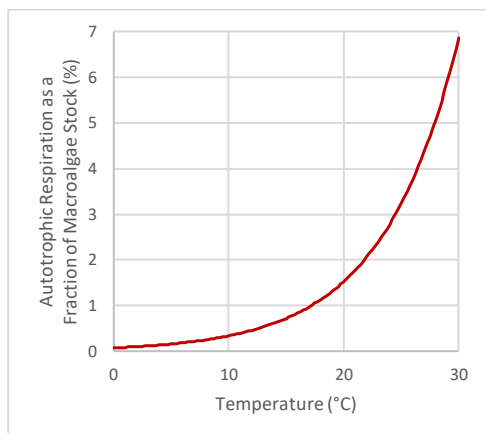
Figure 15: Macroalgae Autotrophic Respiration
Temperature dependent autotrophic respiration of macroalgae calculated using Equation 20. Presented as a fraction of the stock of macroalgae biomass.

802

5.3.5 Eelgrass Gross Primary Production and Autotrophic Respiration

804 For eelgrass, the growth rate of eelgrass will be determined as the minimum specific growth rate among
805 light ($\mu_{E\text{-}I}$) and nitrogen ($\mu_{E\text{-}N}$) (Equation 2, page 24; Table 5-1, page 25) and the impact of temperature on
806 growth rate (presented below).

5.3.5.1 Gross Primary Production of Eelgrass

808 In northern latitudes, a unimodal pattern of growth may be observed, if the warmest summer
809 temperatures remain in the optimal range for growth, usually 15°C to 20°C (Lee et al. 2007). Above 20°C,
810 eelgrass growth declines quickly with increases in temperature (Figure 16, page 41).

811 For eelgrass, the specific growth rate based on temperature ($\mu_{E\text{-}\epsilon}$, d^{-1}) through the upper limit of optimal
812 temperature (20°C) for growth is modeled as:

813
$$\mu_{E-\epsilon} = (-7 \times 10^{-6})\epsilon^3 + 0.002\,\epsilon^2 - 0.003\,\epsilon + (6 \times 10^{-6}) \qquad \text{(eqn. 21)}$$

814 where ϵ is the water column temperature. This model for seagrass specific growth with temperature
815 was calculated from a set of data provided by Zimmerman and colleagues (1989). For temperatures
816 above 20°C, the specific growth rate is modeled as an exponential decay:

817
$$\mu_{E-\epsilon} = 17709\,e^{(-0.5\epsilon)} \qquad \text{(eqn. 22)}$$

818
819 *Figure 16: Example of Eelgrass Gross Primary Production.*
820 *For this example, all values were calculated based on a standing stock of 30 gC m^{-2} for eelgrass biomass. Up to 20°C, a third*
821 *order polynomial equation is used to predict specific growth rate (Equation 21, page 40). Above 20°C, an exponential decay*
822 *predicts specific growth rate (Equation 22, page 40).*

823 The theoretical gross primary production of eelgrass (G_{Et}, g C element^{-1} d^{-1}) becomes:

824 $$G_{Et} = \mu_{E-\epsilon} \; B_E \qquad \text{(eqn. 23)}$$

825 where $\mu_{E-\epsilon}$ (d^{-1}) is the specific growth rate of eelgrass based on temperature and B_E is the biomass of
826 eelgrass in the element (gC element^{-1}).

827 The actual gross primary production (g C element^{-1} d^{-1}) of eelgrass (G_E) will be the minimum value of G_{Et}
828 and the maximum attainable growth based on the nitrogen and light available to the eelgrass.

829 $$G_E = min\left(G_{Et}, \left[\frac{U_M}{U_P+U_E+U_M} \cdot N \cdot c_{N-eelg} \cdot \frac{12 \, gC}{1 \, mole \, C} \cdot \frac{1 \, mole \, N}{14 \, gN} \right] \right) \qquad \text{(eqn. 24)}$$

830 where U_P, U_E, and U_M are the nitrogen utilization of each class of primary producers based on available
831 nitrogen (equation 2, page 24); N is the nitrogen in the element (gN element^{-1}); and c_{N-eelg} is the C:N
832 molar ratio for eelgrass (Table 5-4, page 31).

833 *5.3.5.2   Autotrophic Respiration of Eelgrass*

834 A review by Duarte and Cebrián (1996) concluded that seagrass autotrophic respiration accounts for
835 57.1 ± 5.7% of gross primary production. This fraction will be used to estimate autotrophic respiration
836 (R_E, gC element^{-1} d^{-1}) for eelgrass:

837 $$R_E = 0.571 \, G_E \qquad\qquad \text{(eqn. 25)}$$

838 where G_E is the gross primary production of eelgrass (gC element^{-1} d^{-1}).

839 Autotrophic respiration returns N and P to the water column, in stoichiometric balance with C.

Commented [VJ8]: This will be changed – will be modeling eelgrass GPP & R using a Q10 relationship, modified by light availability

840 If the sum of the oxygen demand of all primary producers is greater than the oxygen available in the
841 water column dissolved oxygen pool, primary producers will die. The amount of death in each class of
842 primary producer will be determined by first looking at the net oxygen production by each class ($G_i - R_i$);
843 if it is positive, that class of primary producers does not sustain any oxygen-related death. If the net
844 oxygen production by a class of primary producers is negative, the negative net production may
845 potentially be converted into a loss term, to bring the system back to a 0 mg/L level of oxygen. Multiple
846 demands are placed on the oxygen pool: autotrophic respiration, heterotrophic respiration, and benthic
847 respiration. These demands will be balanced, apportioning death or reduction in function to each
848 process proportional to the demand and the deficit in oxygen – all processes will compete on equal
849 footing for oxygen.

5.3.6 Heterotrophic Processes

851 The primary producer biomass (B_P, B_M, B_E) is depleted through two external pathways: consumption by
852 grazers (B_{g-P}, B_{g-M}, B_{g-E}) and delivery to the benthos (B_{b-P}, B_{b-M}, B_{b-E}). These pathways encompass the sum
853 of heterotrophic processes acting on the primary producers. The resulting estimates of heterotrophic
854 processes are compared to the total stock available, such that the heterotrophic processes do not
855 exceed the available primary producer biomass. This check is necessary as the sum of the processes
856 could be greater than the stock available, especially as the consumption by grazers is calculated using
857 the running average of biomass stock. Nitrogen and phosphorus associated with the B_{g-i} and B_{b-i} are
858 determined using the C : N : P molar ratio (Table 5-4, page 31). Nitrogen and phosphorus in the biomass
859 respired through heterotrophic processes are assumed to be regenerated to the water column. In
860 reality, some of the N and P will be in complex organic molecules with a lag time in the return of the
861 nutrients to the inorganic pools. To maintain the simplicity of the model, this lag is assumed to be
862 nonexistent.

863 If the sum of the oxygen demand of autotrophic respiration and heterotrophic processes from all
864 primary producer is greater than the oxygen available in the water column dissolved oxygen pool,
865 primary producers will die and heterotrophic processes will be reduced. Multiple demands are placed on
866 the oxygen pool: autotrophic respiration, heterotrophic respiration, and benthic respiration. These
867 demands will be balanced, apportioning death or reduction in function to each process proportional to
868 the demand and the deficit in oxygen – all processes will compete on equal footing for oxygen.

5.3.6.1 Phytoplankton Heterotrophic Processes - Grazing

870 The grazing on the phytoplankton stock (B_{g-P}) is estimated using a multi-day running average of the
871 phytoplankton stock ($\overline{B_P}$) and a water column grazing coefficient developed using a Q_{10} relationship.

872 $$B_{g-P} = g_O\, e^{(\epsilon g_Q)}\, \overline{B_P} \qquad\qquad \text{(eqn. 26)}$$

873 where ϵ is the water column temperature, which is provided as output from the NYHOPS model; g_Q (°C^{-1})
874 is the thermal respiratory quotient and g_O (d^{-1}) is the water column grazing rate at 0°C (Table 5-4, page
875 31).

876 Heterotrophic processes will be reduced if sufficient oxygen is not available in the water column pool to
877 fuel all autotrophic respiration and heterotrophic processes.

5.3.6.2   Phytoplankton Heterotrophic Processes - Death / Delivery to the Benthos

879   The amount of phytoplankton delivered to the benthos (B_b) is based on an empirically derived statistical
880   relationship between the primary production and benthic remineralization (Nixon 1981). Nixon's (1981)
881   formulation was presented in terms of the annual production and annual benthic remineralization, thus
882   the intercept has been divided by the number of days in a year.

883   $$B_{b-P} = \frac{15}{365} + \ 0.238\ \beta_{24} \hspace{3cm} \text{(eqn. 27)}$$

884   The B_{b-P} describes the amount of phytoplankton stock from an element that will be delivered to the
885   benthos.

886   The NREEM does not currently include a surface and bottom element in each box. If two layers are
887   added to this model, an adjustment of phytoplankton delivery to the bottom will be required. Some of
888   the surface element phytoplankton biomass may be delivered to the benthos of the surface element
889   and some may pass through the boundary between vertical elements and be delivered to the benthos of
890   the bottom element. The fraction of the surface element B_{b-P} delivered to the surface element benthos
891   versus the bottom element benthos is determined by comparing the area of the surface element
892   relative to the area of the interface between the surface and bottom element.

893   Heterotrophic processes will be reduced if sufficient oxygen is not available in the water column pool to
894   fuel all autotrophic respiration and heterotrophic processes.

895   *5.3.6.3   Macroalgae Heterotrophic Processes - Grazing*

896   Grazing rates on macroalgae are highly variable (Brush and Nixon, 2010). Brush and Nixon (2010)
897   employed a temperature dependent model for grazing which they later modified to extend high grazing
898   rates until later in the fall. As a first pass, grazing will be modeled using the temperature dependent
899   grazing rate and adjusted as needed at a later time.

900   The grazing rate on macroalgae biomass is modeled as (B_{g-M}, g C element^{-1}) (Figure 17):

901   $$B_{g-M} = \ g_{M0}\ \ e^{(g_{MQ}\ \epsilon)}\ B_M \hspace{3cm} \text{(eqn. 28)}$$

902   where g_{M0} is the rate of grazing on macroalgae at 0°C (d^{-1}, Table 5-4, page 31), g_{MQ} is the grazing on
903   macroalgae thermal respiratory quotient (Q$_{10}$ for respiration) (°C^{-1}, Table 5-4, page 31), ϵ is the
904   temperature (°C), and B_M is the biomass of macroalgae (gC element^{-1}). The coefficients for this
905   relationship (g_{M0}, g_{MQ}) were based on the work of Brush and Nixon (2010), but can be changed to better
906   reflect NRE, if changing them improves model performance at predicting macroalgae biomass.

907   Heterotrophic processes will be reduced if sufficient oxygen is not available in the water column pool to
908   fuel all autotrophic respiration and heterotrophic processes.
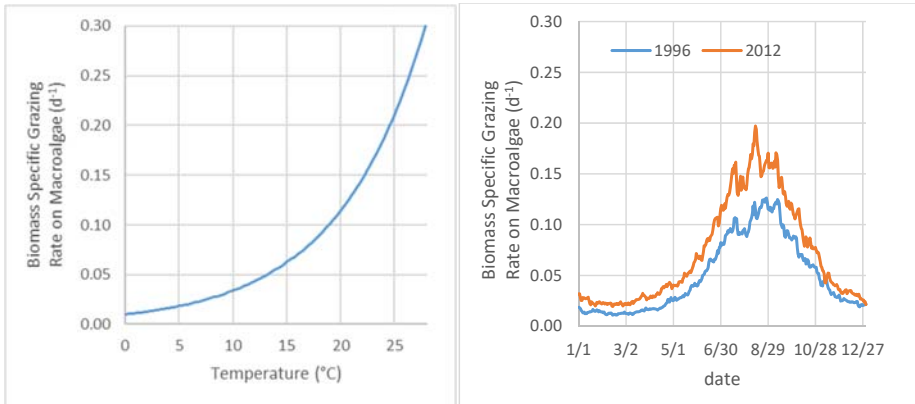
909
910 *Figure 17: Grazing Rate on Macroalgae.*
911 *Grazing rate on macroalgae is a function of temperature. The panel on the right shows how grazing rate varies over the course*
912 *of a year using a warm year (2012) and a cold year (1996).*

913 *5.3.6.4   Macroalgae Heterotrophic Processes - Death / Delivery to the Benthos*

914 Macroalgae autotrophic respiration in excess of the oxygen available will produce death of the
915 macroalgae sufficient to bring the water column oxygen pool into balance (not negative, but only going
916 as low as 0 mg/L). See the section on oxygen for how this will be handled (Section 5.3.8, page 46). When
917 autotrophic respiration is greater than the oxygen available, this loss term is included:

918 $$B_{b-M} = R_M - \left[\frac{(net\ oxygen\ demand)}{(total\ oxygen\ demand)}\ (O_2\ availabe\ to\ M)\ \frac{moles\ O_2}{32\ g\ O_2}\ \frac{moles\ C}{1.7\ moles\ O_2}\ \frac{12\ g\ C}{moles\ C} \right] \qquad \text{(eqn. 29)}$$

919 where R_M is the 24-hour respiration of macroalgae (gC element^{-1}).

Note, Brush and Nixon (2010) applied a similar scheme, but only included death when the respiration allowed by oxygen availability was 10% of the target respiration for five days. If macroalgae death is too high, this alteration could be applied. In an effort to maintain simplicity in the model, this caveat was not included.

As a simplification, no other death of macroalgae is currently included in the model. If greater complexity is needed to adequately simulate the situation in NRE, a temperature dependent loss of macroalgae will be considered following the methods of Brush and Nixon (2010) or Solidoro et al. (1997).

920

Commented [VJ9]: compare heterotrophic processes to ranges from Duarte 1995

need to check this equation

5.3.6.5   Eelgrass Heterotrophic Processes – Loss of Leaves (Death / Delivery to the Benthos)

922   Grazing on eelgrass is assumed to be zero. However, eelgrass does shed a leaf every five to twelve days
923   during the growing season (plastochrone interval). This is a natural process of the plant, not a death of
924   the plant.

925   The first iteration of the model includes a simplification: if we assume plants typically have six leaves,
926   one sixth of the plant is shed every ten days. This equates to a loss of
927   0.016 d^{-1}. A second simplification, we will assume that the leaves stay within
928   the embayment and decay and that no outside leaves are introduced to the
929   embayment.

930    $$B_{g-E} = 0.016 \ B_E \qquad \text{(eqn. 30)}$$

931   No additional death term is added to eelgrass. Under high temperatures, GPP
932   is reduced or goes to zero. Under low light, the GPP is reduced or goes to
933   zero. The shedding of leaves will account for the reduction in eelgrass
934   biomass.

If necessary, a more catastrophic death of eelgrass could be triggered by very high temperature or prolonged periods of very low light.

935   ## 5.3.7   Benthic Processes

936   If the sum of the oxygen demand from autotrophic respiration and heterotrophic processes by all
937   primary producer is greater than the oxygen available in the water column dissolved oxygen pool,
938   primary producers will die and heterotrophic processes will be reduced. Multiple demands are placed on
939   the oxygen pool: autotrophic respiration, heterotrophic respiration, and benthic respiration. These
940   demands will be balanced, apportioning death or reduction in function to each process proportional to
941   the demand and the deficit in oxygen – all processes will compete on equal footing for oxygen.

942   The benthic metabolism (S_M) is estimated using the accumulated benthic stock of carbon (S) and a
943   benthic respiratory coefficient developed using a Q$_{10}$ relationship:

944    $$S_M = b_O \ e^{(\epsilon b_Q)} \ S \qquad \text{(eqn. 31)}$$

945   where ϵ is the water column temperature, which is provided as output from the ROMS model or
946   modeled based on ordinal date, b_Q (°C^{-1}) is the benthic thermal respiratory quotient and b_0 (d^{-1}) is the
947   benthic respiratory rate at 0°C (Table 5-4, page 31).

948   Benthic metabolism is considered in terms of carbon, with respiration of nitrogen and phosphorus
949   related to carbon metabolism through a C : N (c_N) and C : P (c_P) molar ratio (Table 5-4, page 31)
950   converted to a mass ratio. These C : N and C: P molar ratios within the sediment are weighted to reflect
951   the source of the delivery to the benthos (phytoplankton, macroalgae, eelgrass) taking into account the
952   amount of material that remains in the benthos. We assume bacterial respire organic matter with a ratio
953   of 106 : 16 : 1 for C : N : P. If N or P are not sufficient, benthic metabolism is reduced and carbon-rich
954   organic matter builds up in the sediment.

Commented [VJ10]: bacteria will need a certain C:N:P to respire material
do not allow respiration to exceed available N
or, model the sediment nutrient pools separately
--really need to add separate pools, it seems...

955   A fraction of the benthic nitrogen is removed from the model domain through denitrification.
956   Denitrification is modeled as a constant fraction of the carbon metabolism (σ, Table 5-4, page 31). The

957 metabolized nitrogen not lost through denitrification is assumed to be regenerated to the water column
958 (N_S).

959 $$N_S = \frac{S_M (1-\sigma)}{c_N}$$ (eqn. 32)

960 ### 5.3.8 Oxygen

961 Oxygen is coupled to all processes through stoichiometric relationships of $C : O_2$. This relationship is
962 termed a respiratory quotient (RQ) for $C : O_2$ and a photosynthetic quotient (PQ) for $O_2 : C$.

963 In the NREEM, when oxygen stocks are low in the water column, primary producers may die and
964 heterotrophic processes may cease, to keep oxygen levels from going negative. If the oxygen levels
965 approach zero, the model triggers a routine that compares the oxygen demand from each source as a
966 fraction of the total oxygen demand. Each oxygen demand receives that fraction of the available oxygen.

967 Specifically, for autotrophic respiration, the respiration demand for each class of primary producers is
968 first compared to the oxygen produced by the primary producer for that day. If the demand is less than
969 what the primary producer produced, it may take that oxygen from the pool and the available oxygen in
970 the pool is recalculated for the other demands.

971 Autotrophic respiration demands in excess of what the primary producer generated that day are then
972 compared to all other oxygen demands. Each demand is awarded the oxygen equivalent to the fraction
973 of the demand out of the total demands (recalculated after autotrophic respiration has been handled as
974 described in the previous paragraph).

975 Atmospheric exchange and boundary conditions occur at the end of the day; they are not included in
976 the daily iteration of changes to state variables.

977 Contributors:

978 - atmosphere
979 - boundary conditions
980 - gross primary production

981 Detractors:

982 - atmosphere
983 - boundary conditions
984 - autotrophic respiration
985 - grazing
986 - death / delivery to benthos
987 - benthic processes (decay)

988

5.3.9 Atmospheric Deposition as a Source of Nitrogen

Atmospheric deposition (N_A) contributes nitrogen to the estuary in the form of wet and dry deposition to the surface elements. Wet deposition is estimated as the product of the precipitation (ρ, m d^{-1}) and the average concentration of dissolved inorganic nitrogen in rain water (d_{wet}, gN m^{-3}, Table 5-4, page 31). Dry deposition is based on an annual average flux (d_{dry}, gN m^{-2} d^{-1}, Table 5-4, page 31), based on the work of Clark and Kremer (2005). Given the degree in uncertainty in atmospheric deposition nitrogen concentrations, the uncertainty in the final results due to N deposition were assessed by running the model using three concentrations: 30 μM, 50 μM, and 100 μM. The effect on model output was negligible, and for most parameters, insignificant. A slight difference was seen in the nitrogen concentration, but this did not translate into higher productivity or greater oxygen demand.

$$N_A = (\rho d_{wet} + d_{dry})\alpha \qquad \text{(eqn. 33)}$$

where N_A is the nitrogen delivered from atmospheric deposition (gN element^{-1} d^{-1}), ρ is precipitation (m d^{-1}), d_{wet} is nitrogen concentration in wet deposition (gN m^{-3}), d_{dry} is the average dry deposition (gN m^{-2} d^{-1}), and α is the surface area of the upper element (m^2).

5.3.10 Differential Equations

Eight differential equations are solved for each model day to estimate the daily change in stocks. The variables indicated in the differential equations were defined in equations 9 through 33; constants and coefficients were defined in Table 5-4 (page 31).

$$\frac{dB_P}{dt} = G_P - R_P - B_{g-P} - B_{b-P} \qquad \text{(eqn. 34)} \quad \textit{phytoplankton}$$

$$\frac{dB_M}{dt} = G_M - R_M - B_{g-M} - B_{b-M} \qquad \text{(eqn. 35)} \quad \textit{macroalgae}$$

$$\frac{dB_E}{dt} = G_E - R_E - B_{g-E} - B_{b-E} \qquad \text{(eqn. 36)} \quad \textit{eelgrass}$$

$$\frac{dS}{dt} = B_b - S_M \qquad \text{(eqn. 37)} \quad \textit{benthic carbon}$$

$$\frac{dN}{dt} = N_S + N_A + \frac{B_{g-P}+R_P-G_P}{c_{N-phyto}} + \frac{B_{g-M}+R_M-G_M}{c_{N-algae}} + \frac{B_{g-E}+R_E-G_E}{c_{N-eelg}} \qquad \text{(eqn. 38)} \quad \textit{nitrogen}$$

$$\frac{dP}{dt} = \frac{S_M}{c_P} + \frac{B_{g-P}+R_P-G_P}{c_P} + \frac{B_{g-M}+R_M-G_M}{c_P} + \frac{B_{g-E}+R_E-G_E}{c_P} \qquad \text{(eqn. 39)} \quad \textit{phosphorus}$$

The oxygen dynamics are modeled through stoichiometric relationships based on the production and respiration terms in the model converted from molar units to mass ($\acute{\omega}$, ω_p, ω_g, ω_s; Table 5-4, page 31). In addition, oxygen exchanges between the surface layer and the atmosphere (O_{atm}) are modeled following the equations of Garcia and Gordon (1992).

$$\frac{dO}{dt} = O_{atm} + G\acute{\omega} - \frac{R}{\omega_p} - \frac{B_g}{\omega_g} - \frac{N_S}{\omega_S} \qquad \text{(eqn. 40)} \quad \textit{oxygen}$$

Commented [VJ11]: need to revise

1018 Field data in the rivers and ocean boundaries were used to determine concentration of state variables
1019 entering the model domain. The volume of river and ocean water entering the domain were determined
1020 as part of the hydrodynamic modeling component. The user interface allows for nutrient inputs to be
1021 increased or decreased overall or for a specific component such as nutrients from fertilizers. This
1022 flexibility allows for hindcasting and forecasting scenarios related to changes in nutrient loads.

1023 5.4 Forcing Functions

1024 Data for the period of 1/1/81 to 12/31/16 are included for all forcing functions. When additional years
1025 were available, they were included in the MatLab file, to allow for expansion of the model time frame at
1026 a later point.

1027 Temperature, light, and wind were taken from the Millstone meteorological dataset, discussed in the
1028 statistical portion of this project (Figures 18, 19, 20). Dates included span from 1/1/1976 to 12/31/16.

1029 Light data must be in units of Einsteins per square meter per day ($E\ m^{-2}\ d^{-1}$) for the productivity
1030 equation. This unit is equivalent to moles of photons per square meter per day ($mol\ m^{-2}\ d^{-1}$).

1031 Precipitation data (Figure 21) came from the NOAA National Centers for Environmental Information
1032 website, using the "Climate Data Online" order form to access the data
1033 (https://www.ncdc.noaa.gov/cdo-web/). Data from the Groton station were preferentially used
1034 (GROTON, CT US (GHCND:USC00063207)). Data from the Groton airport were used when data from the
1035 Groton station were unavailable (1491 days out of 11953 days = 12% of the time) (GROTON NEW
1036 LONDON AIRPORT, CT US (GHCND:USW00014707)). Data currently available in the model source files
1037 are 1/1/1981 to 1/16/18.
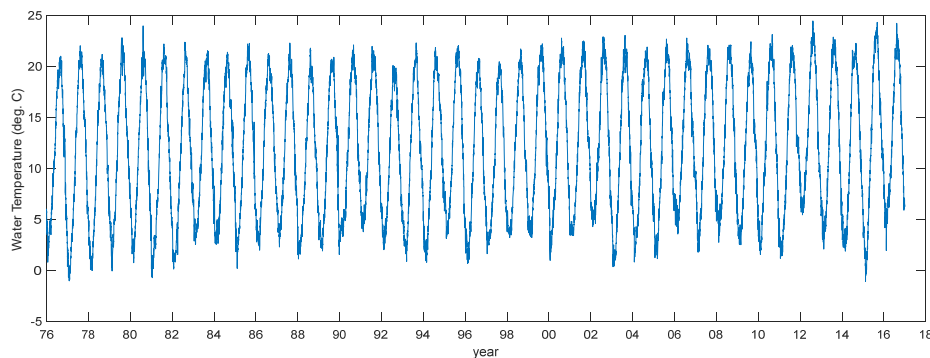
1038
1039 *Figure 18: Water Temperature*
1040 *Data shown are from Millstone's Meteorological dataset. Temperature is measured at the Plant intake. An offset is not currently*
1041 *applied to account for warmer temperatures in the Niantic River boxes; this may be included at a later time.*
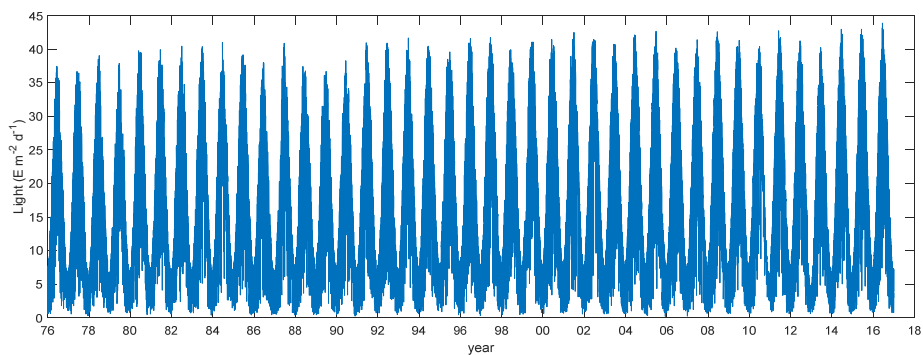
1042
1043 *Figure 19: Light*
1044 *Data shown are from Millstone's Meteorological dataset. E m^{-2} d^{-1} = mol m^{-2} d^{-1}*
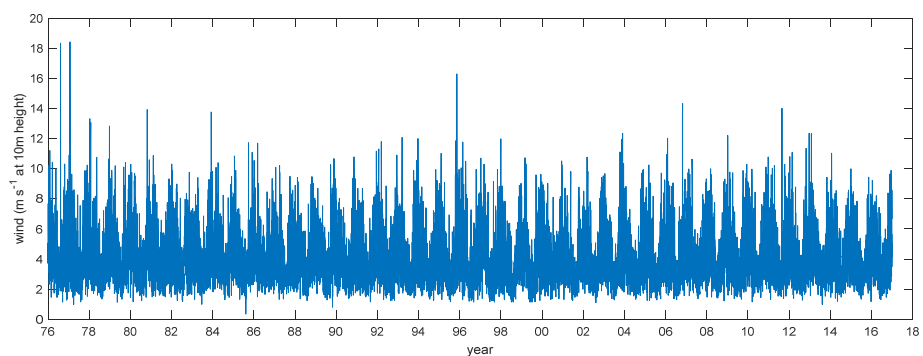
1045
1046 *Figure 20: Wind Speed*
1047 *Data shown are from Millstone's Meteorological dataset.*
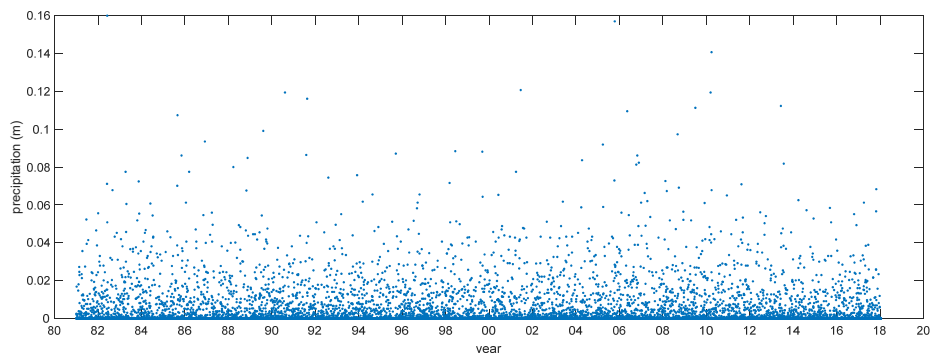
Figure 21: Precipitation
Precipitation data are from NOAA data sources for Groton. The average precipitation over the record shown is 0.0034 m per day
(= 0.34 cm per day = 0.13 inches per day).

5.5 Boundary Conditions

Boundary conditions refers to the state variables located outside of the model domain but contributing to the model. These conditions are forced using real data. The boundaries exist at the river, with freshwater input, and at the mouth, with input from the Niantic Bay area.

- Benthic carbon, macroalgae, and seagrass are not exchanged across the boundaries as these are benthic state variables – they do not move with the exchange of water.
- Salt is set to zero in the river and the NYHOPS model is used to set the salinity in Niantic Bay (Figure 22). NYHOPS provides salinity from 1/1/81 to 10/31/13. Salinity from 10/31/13 to 12/22/18 was estimated from a linear regression of salinity on river flow Appendix A, page 70).
- Oxygen is assumed to be at 100% saturation in the freshwater inputs and Niantic Bay; details are provided below on how this quantity is estimated (Section 5.5.1, page 52).
- Phytoplankton is set to zero in the river because freshwater phytoplankton should not survive in the estuary. Data collected by CTDEEP are used to estimate phytoplankton in Niantic Bay; details are provided below on how this quantity is estimated (Section 5.5.2, page 53).
- Nutrients (nitrogen and phosphorus) are estimated from USGS data for the river and from CTDEEP data for Niantic Bay; details are provided below on how these quantities are estimated (Section 5.5.2, page 53; Section 5.5.2, page 53).
- In the User Interface Excel file, the user has the option of using dissolved inorganic nutrients or dissolved total nutrients (inorganic + organic). If organic nutrients are chosen, the user also must designate the fraction of riverine organic matter expected to be labile (available to biological processes within the residence time of the embayment). Riverine organic N lability is typically 10% to 30% for groundwater originating from a variety of land use categories and 30% to 60% for atmospheric deposition from urban runoff (Table 5-6). Completely forested watersheds tend to have a lower fraction of bioavailable N while atmospheric deposition not filtered through groundwater tends to be more highly bioavailable (Petrone et al. 2009; Seitzinger et al. 2002). Organic P is currently set with a range from 0.5 to 0.9, though this is likely much lower. For

1078	phosphorus, the particulate phosphorus is included in the estimate of dissolved organic
1079	phosphorus in the User Interface Excel file, as P binds tightly to sediment in freshwater and is
1080	liberated in salt water due to chemical (especially pH) differences in the freshwater versus the
1081	estuary (Bianchi 2007; O'Mara et al. 2019). It is assumed that oceanic organic N and P are largely
1082	refractory, as the marine organisms have been working on the breakdown for quite some time.
1083	Organic N in the oceanic waters is assigned a lability of 10% and organic P is assigned a lability of
1084	2%.

1085 *Table 5-6: Fraction of DON that is Bioavailable.*
1086 *A brief review of the bioavailability of DON. Text in grey indicate seasonal data that the authors summarized into an annual*
1087 *estimate (black text).*

source	watershed type	Location	DON that is bioavailable, % (avg ± std dev; or range)	citation
groundwater – spring	agricultural (animals)	NJ, USA	44 ± 4.7	(Seitzinger et al. 2002)
groundwater – summer	agricultural (animals)	NJ, USA	32 ± 9.7	(Seitzinger et al. 2002)
groundwater – fall	agricultural (animals)	NJ, USA	14 ± 5.5	(Seitzinger et al. 2002)
groundwater – annual	agricultural (animals)	NJ, USA	30 ± 14	(Seitzinger et al. 2002)
groundwater – winter	mixed (ag., natural)	TX, USA	15 - 38	(Wu et al. 2019)
groundwater – summer	mixed (ag., natural)	TX, USA	9 - 15	(Wu et al. 2019)
groundwater – annual	mixed (ag., natural)	TX, USA	9 - 38	(Wu et al. 2019)
groundwater – summer	mixed (ag, natl, urban)	AUS	20 - 44	(Petrone et al. 2009)
groundwater – spring	forest	NJ, USA	12 ± 14	(Seitzinger et al. 2002)
groundwater – summer	forest	NJ, USA	35 ± 19	(Seitzinger et al. 2002)
groundwater – fall	forest	NJ, USA	26 ± 12	(Seitzinger et al. 2002)
groundwater – annual	forest	NJ, USA	24 ± 17	(Seitzinger et al. 2002)
groundwater – summer	forest	AUS	4	(Petrone et al. 2009)
atm. dep. – spring	urban/suburban runoff	NJ, USA	68 ± 7.3	(Seitzinger et al. 2002)
atm. dep. – summer	urban/suburban runoff	NJ, USA	50 ± 7.4	(Seitzinger et al. 2002)
atm. dep. – fall	urban/suburban runoff	NJ, USA	59 ± 11	(Seitzinger et al. 2002)
atm. dep. – annual	urban/suburban runoff	NJ, USA	59 ± 11	(Seitzinger et al. 2002)
atm dep. – summer	100% urban, drains	AUS	27 - 46	(Petrone et al. 2009)

1088
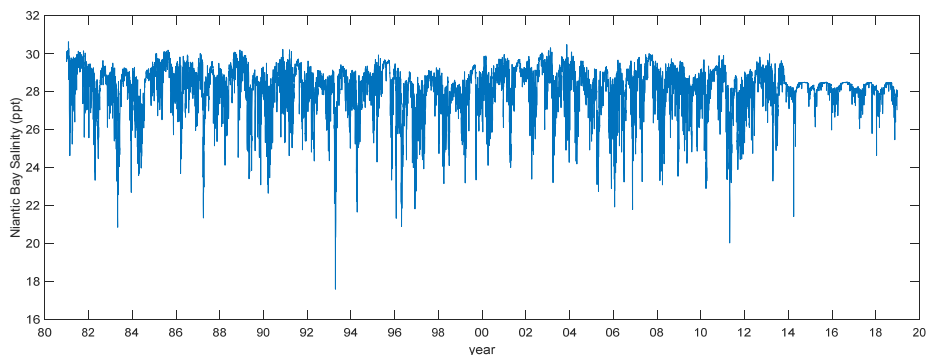
1089
1090 *Figure 22: Salinity of the Ocean Boundary.*
1091 *NYHOPS provides salinity from 1/1/81 to 10/31/13. Salinity data from 10/31/13 to 12/22/18 were estimated from a linear*
1092 *regression of salinity on river flow Appendix A, page 70).*

1093 ### 5.5.1   Boundary Conditions – oxygen

1094 Oxygen data are not consistently available for the river nor for the ocean (Niantic Bay) boundaries. The
1095 assumption of 100% saturation was applied to both boundaries, with saturation calculated as a function
1096 of temperature and salinity, per the equations applied in the model (see Section 5.3.10, page 47).

1097 In short, water density was calculated from salinity and water temperature using the "Seawater Version
1098 3.0" toolbox in MatLab. Salinity in the river was set at 0 ppt, salinity in Niantic Bay was set using the
1099 boundary conditions (Figure 22). Equations for oxygen at equilibrium were applied to temperature,
1100 salinity, and density data (Garcia and Gordon 1992). Temperature data were not available for 2017 &
1101 2018; these dates were set equal to the temperature in 2016 on the corresponding date. The date range
1102 spans from 1/1/1981 to 12/22/2018 (Figure 23).

Page **52** of **127**
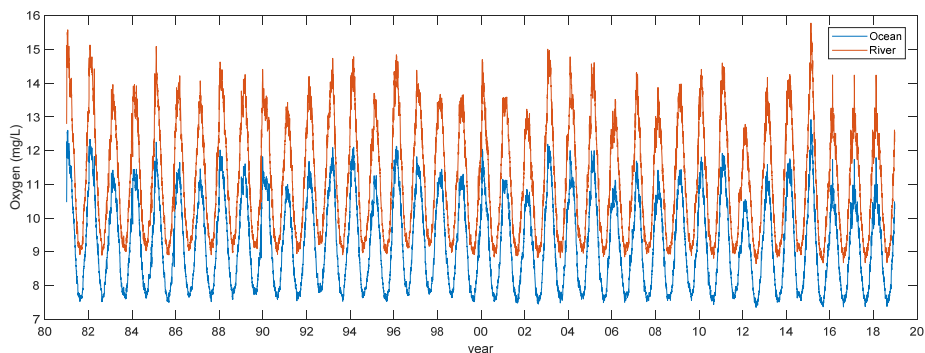
1103
1104 *Figure 23: Oxygen Concentration in the River and Ocean Boundaries.*
1105 *Oxygen at equilibrium was used as the boundary condition. Density is calculated in MatLab form temperature and salinity. A set*
1106 *of equations are used to estimate oxygen equilibrium from temperature, salinity, and density. Temperature data were not*
1107 *available for 2017 & 2018; these dates were set equal to the temperature in 2016 on the corresponding date. The difference*
1108 *between the river and the ocean are due to salinity differences as the same temperature was used for both.*

1109 ### 5.5.2 Ocean Boundary – phytoplankton and nutrients

1110 CTDEEP data from stations K2 and M3 were used to estimate phytoplankton and nutrient
1111 concentrations in Niantic Bay. These two stations are located in Long Island Sound, to the east and west
1112 of Niantic Bay (Figure 24). Data are available from 1991 through 2017. With a few exceptions that are
1113 addressed later in this section, data are collected monthly throughout the year.
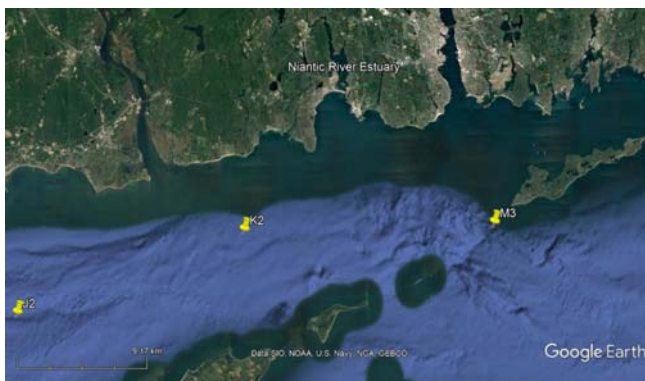
1114
1115 *Figure 24: CTDEEP Station Locations.*
1116 *Locations of CTDEEP stations in the vicinity of Niantic River Estuary are noted by yellow tags, with station name indicated.*

1117 These two stations will be considered representative of the water in Niantic Bay. To confirm this
1118 decision, data for each available parameter were plotted by station for visual confirmation of
1119 comparability and trends (Appendix B, page 75). The parameters compared include: chlorophyll *a*, total

Page **53** of **127**

1120   dissolved phosphorus, dissolved inorganic phosphorus, particulate phosphorus, total dissolved nitrogen,
1121   dissolved ammonium, dissolved nitrate plus nitrite, and particulate nitrogen.

1122   Data from the two stations were compared using a paired t-test to confirm that phytoplankton and
1123   nutrients were similar among the stations on a given date; results of the t-test are referenced on the
1124   plots available in Appendix B (page 75). The two stations were similar across all parameters; thus the
1125   average of the two stations on a particular date is used when data are available at both stations and
1126   data from either station may be used if one station does not have data on a particular day.

1127   To determine if trends occurred over the 26-year data record, data from 1991 through 1993 were
1128   averaged by season and subtracted from all data based on season (winter = December, January,
1129   February; spring = March, April, May; summer = June, July, August; fall = September, October,
1130   November), see Appendix B (page 75). These plots provided a first glimpse of possible trends; the figures
1131   were reviewed visually, no statistics were run on these results because 1991-1993 may not be
1132   representative of the appropriate base condition and the seasonal averaging may have issues that would
1133   confound statistical analysis.

1134   The next step was to determine how to interpolate between the monthly data and what value to use
1135   when sampling events occurred more than a month apart. The visual investigation of trends suggested
1136   that no parameter showed a strong trend over the 26-year dataset, though some periods of years were
1137   higher or lower than the 1991-1993 seasonal averages (Appendix B, page 75). For modeling purposes,
1138   daily estimates of the parameters are determined by drawing a straight line between sampling events –
1139   a linear interpolation of the monthly data to daily data. To account for longer time intervals between
1140   sampling events, if the time interval between sampling dates is greater than 40 days, an alternate
1141   method of estimating the daily data is needed. A sinusoidal curve often fits annual nutrient and
1142   chlorophyll data; this was confirmed by plotting the data on the ordinal date, for all 26 years of data
1143   (Figure 25).

1144

1145
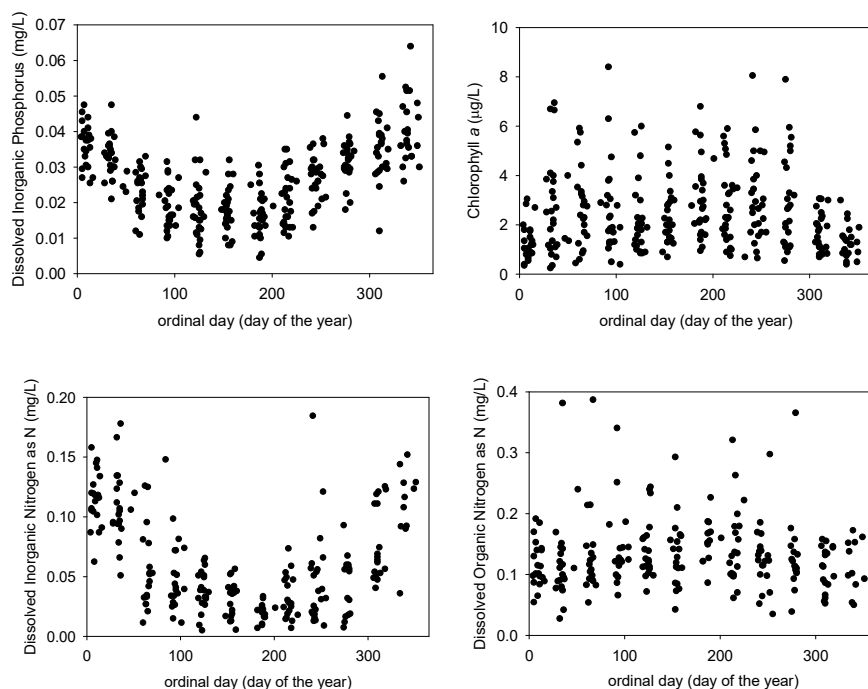
1146 *Figure 25: Boundary Conditions versus Ordinal Date*
1147 *Each panel plots all available parameter data from 1991 to 2017 CTDEEP surveys as the average of stations M3 and K2 versus*
1148 *the ordinal date. All data follow a sinusoidal pattern over the annual cycle with DON showing the weakest sinusoidal pattern.*

1149 A MatLab function written by Chad Greene in 2018 titled "Sine Fit" was designed to fit a least-squares
1150 estimate of a sinusoid to time series data that have a periodicity of 1 year. The routine was designed for
1151 climatological data with more than 1 year of data. The routine generates the terms of the sinusoidal
1152 equation (amplitude, phase shift) and assumes a period of 1 year (Table 5-7). The routine also estimates
1153 a linear trend over the entire time series and calculates the root mean square error (a measure of
1154 goodness of fit) for the sine curve relative to the data; for all parameters, the linear trend was not
1155 ecologically meaningful (Table 5-7).

1156 The sine equation used to estimate daily parameter values when sampling dates were more than 40
1157 days apart and prior to the start of CTDEEP sampling efforts was:

1158 $\qquad$ y(date) = amplitude * sin (period * date + phase shift) – constant offset $\qquad$ (eqn. 41)

1159 where the amplitude, phase shift, and constant offset are provided in Table 5-7 and the period is
1160 equivalent to 1 year, calculated as $2\pi/365$. Plots of daily data are provided in Figures 26 through 30.

Page **55** of **127**

1161 *Table 5-7: Results of Sinusoidal Fit to Boundary Conditions*
1162 *Data represent the output from the MatLab function SineFit. The period for the sine curve is 365 days. Dates were coded as*
1163 *MatLab numbers where 1/1/1991 = 727199. In the column headings, "amount" equates to the units shown in the first column,*
1164 *by parameter.*

parameter	amplitude (amount)	phase shift (day of year corresponding to max value)	constant offset on the y-axis = mean of the data (amount)	estimate of the linear trend (amount / year)	estimate of the linear trend (amount / 26-year period)	root mean square error (amount, lower is better)
chlorophyll *a* (µg/L)	0.4859	187.233	2.4134	0.02760	0.717	1.50
DIN (mg/L)	0.0429	0.211	0.0614	-0.00079	-0.021	0.03
DON (mg/L)	0.0172	181.609	0.1347	-0.00088	-0.023	0.07
DIP (mg/L)	0.0110	337.00	0.0269	0.00034	0.009	0.01
DOP (mg/L)	0.0011	296.327	0.0103	0.00008	0.002	0.01

1165
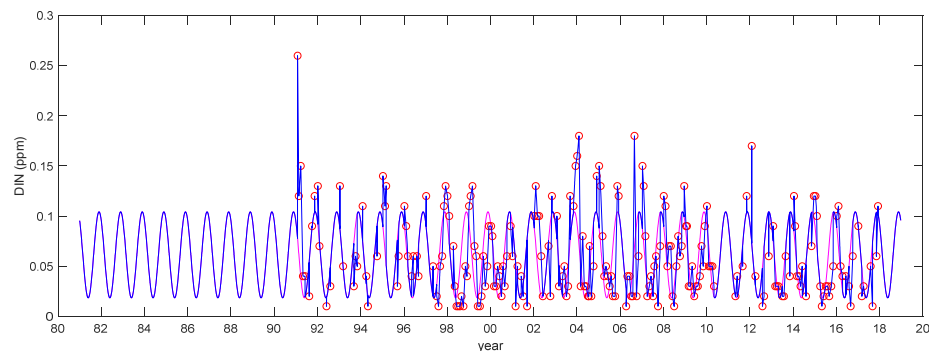
1166
1167 *Figure 26: DIN Daily Data – Boundary Conditions*
1168 *Red circles show the CTDEEP data, the average of station M3 and K2. The pink line in the background shows the sine curve fit to*
1169 *the data (Table 5-7). The blue line is the daily data used in the model. When CTDEEP sample dates are within 40 days of each*
1170 *other, the linear interpolation between data are used to estimate the daily data. If sampling events are more than 40 days*
1171 *apart, the more conservative estimate of the sine curve is used to estimate the daily data. ppm = mg/L = g/m³, as N*

1172
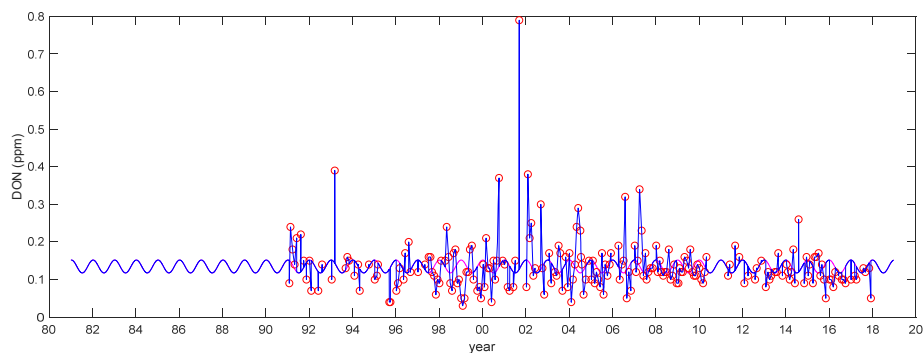
1173
1174 *Figure 27: DON Daily Data – Boundary Conditions*
1175 *Red circles show the CTDEEP data, the average of station M3 and K2. The pink line in the background shows the sine curve fit to*
1176 *the data (Table 5-7). The blue line is the daily data used in the model. When CTDEEP sample dates are within 40 days of each*
1177 *other, the linear interpolation between data are used to estimate the daily data. If sampling events are more than 40 days*
1178 *apart, the more conservative estimate of the sine curve is used to estimate the daily data. ppm = mg/L = g/m³, as N*

1179
1180 *Figure 28: DIP Daily Data – Boundary Conditions*
1181 *Red circles show the CTDEEP data, the average of station M3 and K2. The pink line in the background shows the sine curve fit to*
1182 *the data (Table 5-7). The blue line is the daily data used in the model. When CTDEEP sample dates are within 40 days of each*
1183 *other, the linear interpolation between data are used to estimate the daily data. If sampling events are more than 40 days*
1184 *apart, the more conservative estimate of the sine curve is used to estimate the daily data. ppm = mg/L = g/m³, as P*
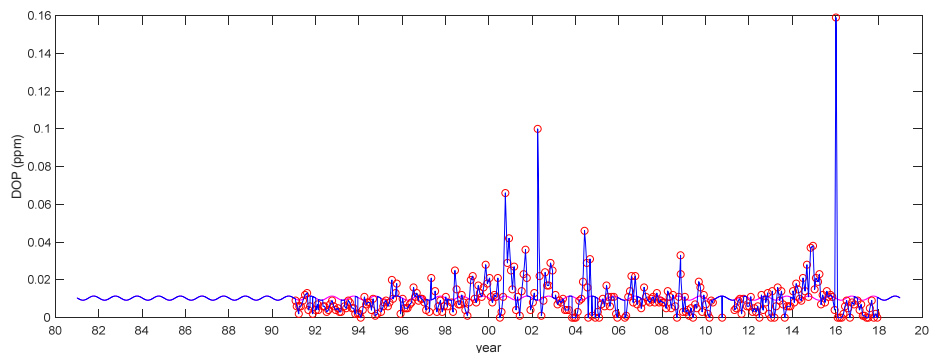
1185
1186 *Figure 29: DOP Daily Data – Boundary Conditions*
1187 *Red circles show the CTDEEP data, the average of station M3 and K2. The pink line in the background shows the sine curve fit to*
1188 *the data (Table 5-7). The blue line is the daily data used in the model. When CTDEEP sample dates are within 40 days of each*
1189 *other, the linear interpolation between data are used to estimate the daily data. If sampling events are more than 40 days*
1190 *apart, the more conservative estimate of the sine curve is used to estimate the daily data. ppm = mg/L = g/m³, as P*

1191
1192 *Figure 30: Chlorophyll a Daily Data – Boundary Conditions*
1193 *Red circles show the CTDEEP data, the average of station M3 and K2. The pink line in the background shows the sine curve fit to*
1194 *the data (Table 5-7). The blue line is the daily data used in the model. When CTDEEP sample dates are within 40 days of each*
1195 *other, the linear interpolation between data are used to estimate the daily data. If sampling events are more than 40 days*
1196 *apart, the more conservative estimate of the sine curve is used to estimate the daily data. The exception was between*
1197 *2/27/1998 and 4/14/98, a 46-day difference, where linear interpolation was applied rather than the sine curve due to unusually*
1198 *low values in 1998. NOTE – the unit used for phytoplankton biomass in the model is gC m⁻³. Data are imported from the User*
1199 *Excel interface as chlorophyll a (µg/L), converted to gCHL m⁻³, then converted to gC m⁻³ using the C:CHL ratio defined in the*
1200 *model. This insures that if the C:CHL ratio is changed in the model, that change is propagated through the chlorophyll data for*
1201 *the boundary condition. ppb = µg/L = mg/m³*

1202 ### 5.5.3 River Boundary – nutrients

1203 Nutrient data from the incoming water collected by USGS, Millstone Environmental Lab (MEL), and the
1204 Niantic River Watershed Commission (NRWC) between 2008 and 2017 were used to estimate the

1205 nutrient concentrations in the incoming freshwater riverine and groundwater sources (Figure 31). Data
1206 are available from USGS for 8/20/08 to 9/11/12, from MEL for 4/15/15 to present, and from NRWC from
1207 4/13/12 to present; only data through the end of 2016 were analyzed, though more data are now
1208 available for later years.

1209
1210 *Figure 31: Station Locations of Latimer Brook Nutrient Data.*
1211 *The stations designated as MEL, USGS, and NRWC, 14 were used to estimate nutrient concentrations in the incoming freshwater*
1212 *from all riverine and groundwater sources.*
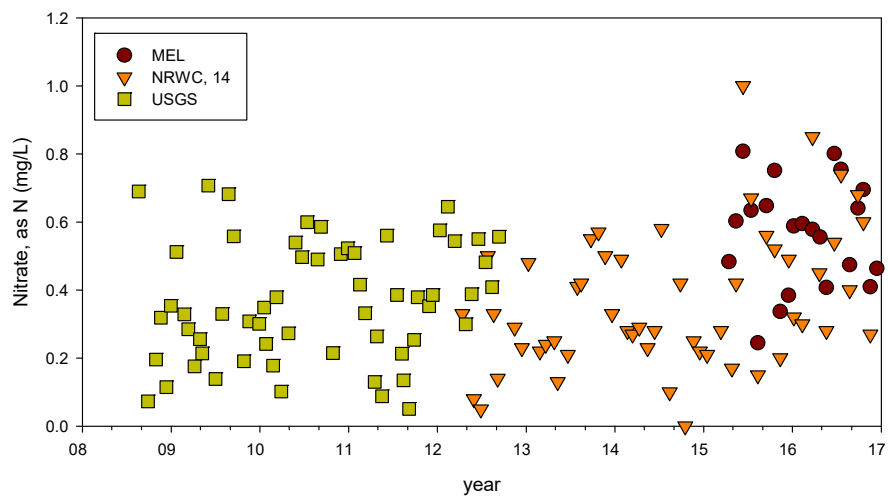
1213
1214   *Figure 32: Nitrate data for Latimer Brook.*
1215   *Nitrate is the only nitrogen species collected by all three groups. USGS and MEL collect other species of N, NRWC does not.*
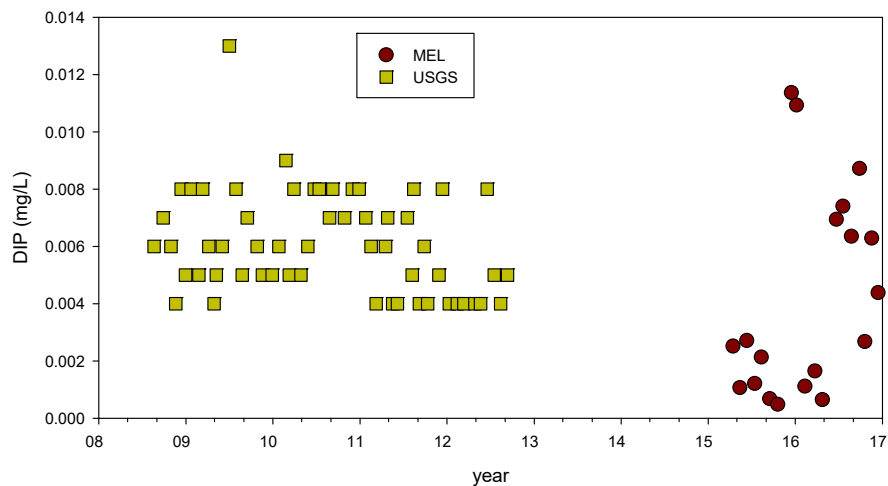
1216
1217   *Figure 33: DIP data for Latimer Brook.*
1218   *Dissolved inorganic phosphorus (DIP, ortho-phosphate as P) is collected only by USGS and MEL.*

Page **60** of **127**

1219 Nitrogen species included in this model include dissolved inorganic nitrogen (DIN) which is the sum of
1220 nitrate (NO_3^-), nitrite (NO_2^-), and ammonium (NH_4^+); and dissolved organic nitrogen (DON). Phosphorus
1221 species include dissolved inorganic phosphorus (as ortho-phosphate, PO_4^-), dissolved organic
1222 phosphorus (DOP), and particulate phosphorus (PP). The USGS data is the only set which includes
1223 information on all species, MEL and NRWC are both missing some of the data (Table 5-8).

1224 *Table 5-8: Summary of Nutrient Data Availability in Latimer Brook, as used in the model.*
1225 *Data are collected monthly for the date ranges shown. Data for DON will be available from MEL, once reanalyzed.*

Nutrient Species	USGS	MEL	NRWC
nitrate (NO_3^-)	8/20/08 to 9/11/12	4/15/15 to 12/14/16	4/13/12 to 11/17/16
nitrite (NO_2^-)	8/20/08 to 9/11/12	4/15/15 to 12/14/16	
ammonium (NH_4^+)	8/20/08 to 9/11/12	4/15/15 to 12/14/16	
dissolved inorganic N (DIN)	8/20/08 to 9/11/12	4/15/15 to 12/14/16	estimated from NO_3^-
dissolved organic N (DON)	8/20/08 to 9/11/12	TBD	
dissolved inorganic P (PO_4^-)	8/20/08 to 9/11/12	4/15/15 to 12/14/16	
dissolved organic P (DOP)	8/20/08 to 9/11/12		
particulate phosphorus (PP)	8/20/08 to 9/11/12		

1226

1227 Using the USGS data, we can compare the relative contributions of the nitrogen species to the total
1228 dissolved nitrogen. When looking at only DIN, nitrate accounts for an average of 94% of the dissolved
1229 inorganic nitrogen, with a range of 84% to 98% (Figure 34). For this reason, the NRWC nitrate data was
1230 determined to be a good estimate of DIN, without adjustments.
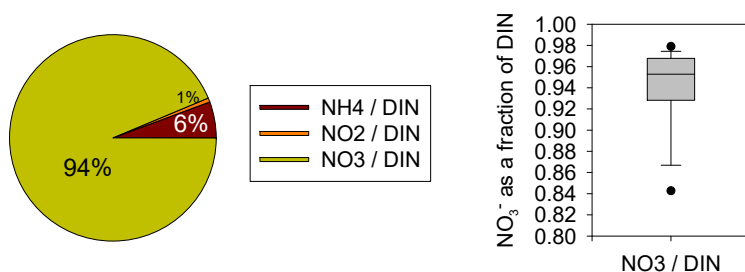
1231
1232 *Figure 34: Nitrate as a Fraction of DIN.*
1233 *USGS monthly data from Latimer Brook for the period of 8/20/2008 to 9/11/2012 were used to evaluate nitrate as a fraction of*
1234 *DIN, to ascertain is nitrate was a good estimate of DIN. The pie chart on the left shows the average relative contribution of each*
1235 *species to DIN. The box plot on the right shows the data distribution: the lower end of the box is the 25th percentile, the upper*
1236 *edge is the 75th percentile, the line in the box indicates the median (50th percentile) with whiskers representing the 10th and 90th*
1237 *percentile and the points indicating the 5th and 95th percentiles.*

1238

1239 The USGS dataset provides four years of monthly data for Latimer Brook nutrients. To apply the
1240 sinusoidal modeling approach used for the ocean boundary data (Section 5.5.2, page 53), we want to
1241 maximize the amount of data available. It was determined that nitrate is a sufficient proxy of DIN data in
1242 the previous paragraph; the question now is the amount of DON present in the incoming freshwater. For
1243 the four years of monthly data, the data indicates DON accounts for 26% to 49% of the TDN (Figure 35),
1244 using the 25th and 75th percentiles as indicators, with a median of 33%. We can widen this range by using
1245 the 10th and 90th percentiles, which yield a range of 20% to 63% for DON as a fraction of TDN. The
1246 median of 33% (DON / TDN) will be used to estimate DON, where DON is equal to DIN * 33 / 67 (see pie
1247 chart in Figure 35). While there is a fair bit of error in this estimate of DON, recall from the introduction
1248 of this section that riverine organic N ranges from a lability if 0.1 (fraction) for groundwater to 0.6 for
1249 atmospheric deposition. Thus, only 10 to 60% of the DON entering from the freshwater sources
1250 contribute to productivity in the model, reducing the impact of the error.
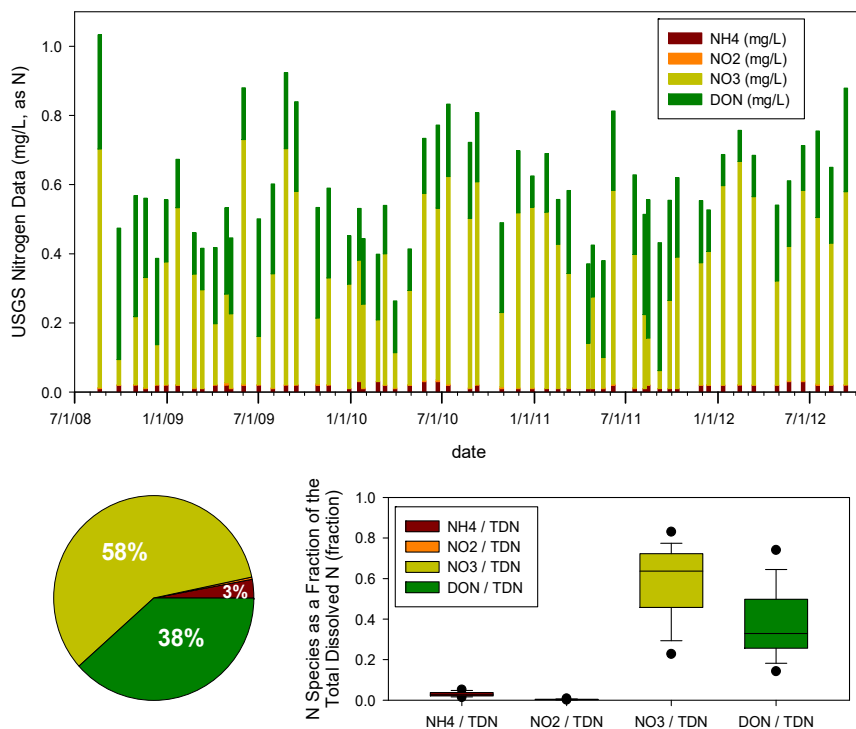
1251
1252 *Figure 35: USGS Nitrogen Data from Latimer Brook.*
1253 *USGS monthly data from Latimer Brook for the period of 8/20/2008 to 9/11/2012 were used to evaluate the species distribution*
1254 *of nitrogen, specifically looking at the contribution of dissolved inorganic nitrogen (DIN) and dissolved organic nitrogen (DON) to*
1255 *the total (TDN). The color coding of the pie chart follows the color scheme of other figures in this panel, with NO_3^- contributing*
1256 *58% to TDN and DON contributing 38% to TDN; NO_2^- accounts for less than 1% of TDN. For the box plots, the lower end of the*
1257 *box is the 25th percentile, the upper edge is the 75th percentile, the line in the box indicates the median (50th percentile) with*
1258 *whiskers representing the 10th and 90th percentile and the points indicating the 5th and 95th percentiles.*

In general, phosphorus in freshwater is tightly bound to sediments, including particulates floating in the river water. Once the particulates encounter salt water, the chemistry of seawater allows for the release of phosphorus from sediment binding sites (Bianchi 2007; O'Mara et al. 2019). Some fraction of this released phosphorus is labile, and thus available to biological processes in the estuary. Thus, particulate phosphorus (PP) is included when estimating the phosphorus input from the riverine and groundwater sources. In the model, PP is grouped with dissolved organic phosphorus (DOP) in the Excel user interface worksheet. At this point, 50% to 90% is assumed to be labile (Bianchi 2007); this figure should be further refined if P is thought to have a bigger influence in this system. PP and DIP are roughly equivalent in amount, with DOP accounting for ~10% of the total phosphorus (TP) (Figure 36).
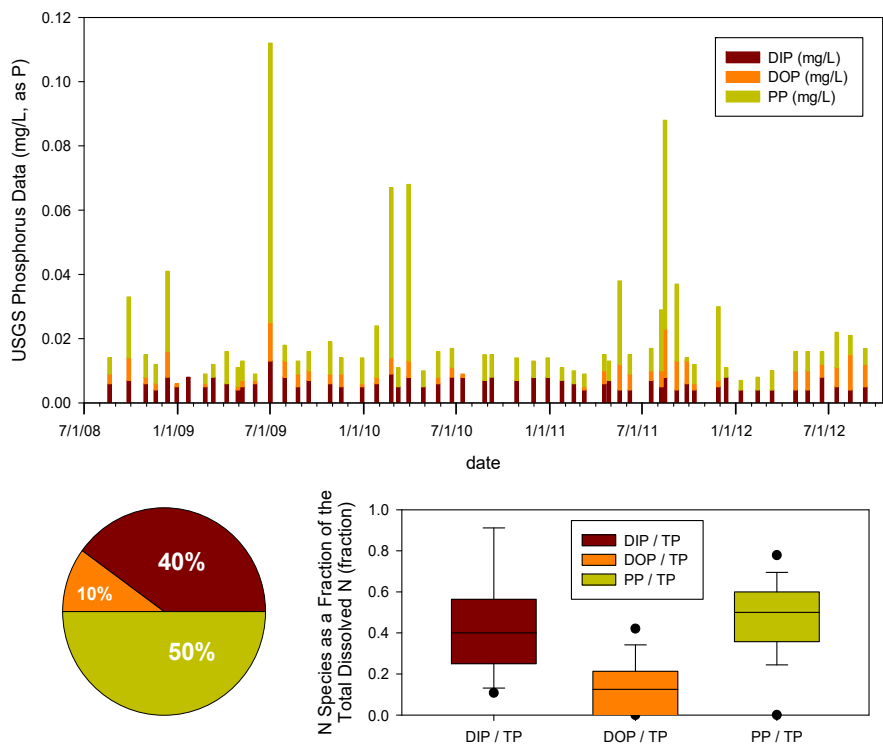
Figure 36: USGS Phosphorus Data from Latimer Brook.
USGS monthly data from Latimer Brook for the period of 8/20/2008 to 9/11/2012 were used to evaluate the species distribution of phosphorus. The color coding of the pie chart follows the color scheme of other figures in this panel, with DIP contributing 40% to TP and PP contributing 50% to TP; DOP accounts for 10% of TP. For the box plots, the lower end of the box is the 25th percentile, the upper edge is the 75th percentile, the line in the box indicates the median (50th percentile) with whiskers representing the 10th and 90th percentile and the points indicating the 5th and 95th percentiles.

1275 The sinusoidal modeling approach used for the ocean boundary data (Section 5.5.2, page 53) was
1276 applied to the riverine data, resulting in estimates of nutrient concentrations in incoming freshwater
1277 (Table 5-9, Figures 37 to 40). The small amplitude of the sine curve relative to the data indicates the sine
1278 curve is not always a good approximation. While the sine curve amplitude is small, it was significant;
1279 thus, the sine model results are used versus using a straight average of data to account for estimates of
1280 nutrient concentrations in years without data.

1281 For the model, DOP + PP is calculated as PP + PP * 10 / 50 (see pie chart in Figure 36).

1282 *Table 5-9: Results of Sinusoidal Fit to River Boundary Conditions*
1283 *Data represent the output from the MatLab function SineFit. The period for the sine curve is 365 days. Dates were coded as*
1284 *MatLab numbers where 1/1/1991 = 727199. Estimate of the trend was only calculated for the eight years with data. In the*
1285 *column headings, "amount" equates to the units shown in the first column, by parameter. For the river, particulate phosphorus*
1286 *(PP) is modeled as P is tightly bound to sediment in freshwater and liberated to some extent in salt water.*

parameter	amplitude (amount)	phase shift (day of year corresponding to max value)	constant offset on the y-axis = mean of the data (amount)	estimate of the linear trend (amount / year)	estimate of the linear trend (amount / 8-year period)	root mean square error (amount, lower is better)
DIN (mg/L)	0.0395	219.6201	0.4074	0.0228	0.1821	0.1884
DON (mg/L)	0.0447	235.8071	0.1723	-0.0103	-0.0821	0.0716
DIP (mg/L)	0.0005	292.4606	0.0055	-0.0004	-0.0032	0.0023
PP (mg/L)	0.0036	181.1713	0.0115	-0.0011	-0.0092	0.0160

1287
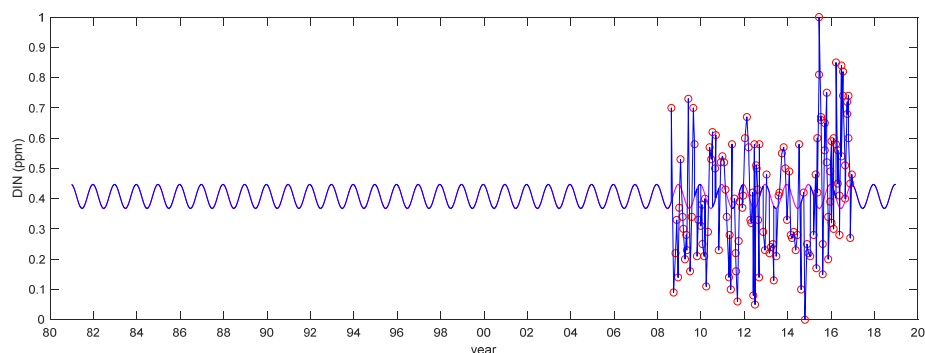
1288
1289 *Figure 37: DIN Daily Data – River Boundary Conditions*
1290 *Red circles show the USGS, MEL, and NRWC data. The pink line in the background shows the sine curve fit to the data (Table*
1291 *5-9). The blue line is the daily data used in the model. When sample dates are within 40 days of each other, the linear*
1292 *interpolation between data are used to estimate the daily data. If sampling events are more than 40 days apart, the more*
1293 *conservative estimate of the sine curve is used to estimate the daily data. ppm = mg/L = g/m³, as N*
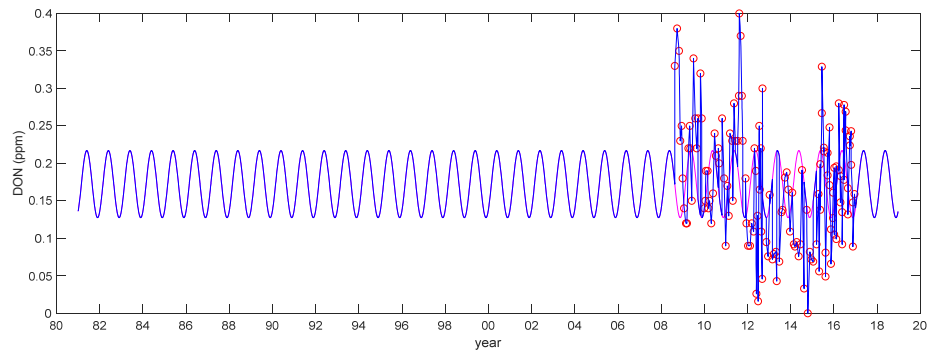
1294
1295 *Figure 38: DON Daily Data – River Boundary Conditions*
1296 *Red circles show the USGS data and DON estimated from DIN for MEL and NRWC data. The pink line in the background shows*
1297 *the sine curve fit to the data (Table 5-9). The blue line is the daily data used in the model. When sample dates are within 40 days*
1298 *of each other, the linear interpolation between data are used to estimate the daily data. If sampling events are more than 40*
1299 *days apart, the more conservative estimate of the sine curve is used to estimate the daily data. ppm = mg/L = g/m³, as N*
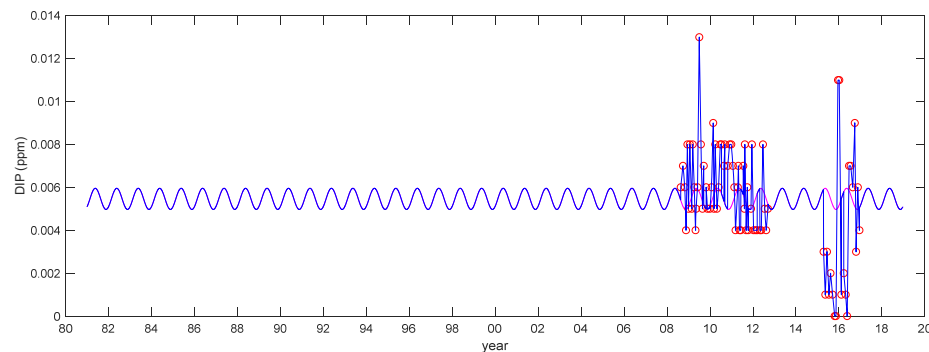
1300
1301 *Figure 39: DIP Daily Data – River Boundary Conditions*
1302 *Red circles show the USGS and MEL data. The pink line in the background shows the sine curve fit to the data (Table 5-9). The*
1303 *blue line is the daily data used in the model. When sample dates are within 40 days of each other, the linear interpolation*
1304 *between data are used to estimate the daily data. If sampling events are more than 40 days apart, the more conservative*
1305 *estimate of the sine curve is used to estimate the daily data. ppm = mg/L = g/m³, as P*
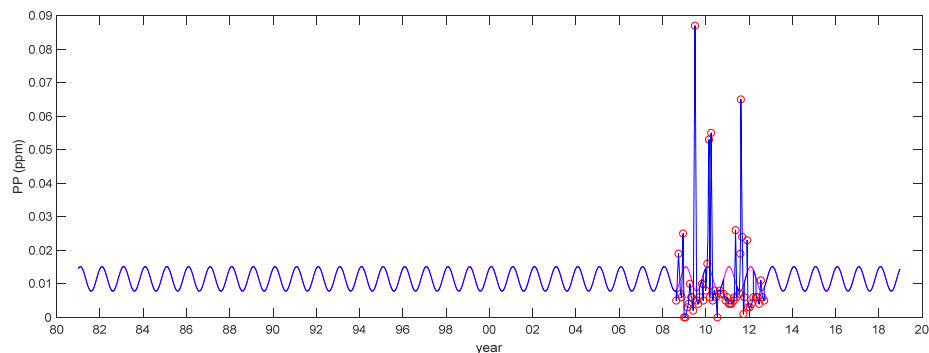
Figure 40: PP Daily Data – River Boundary Conditions
Red circles show the USGS data. The pink line in the background shows the sine curve fit to the data (Table 5-9). The blue line is the daily data used in the model. When sample dates are within 40 days of each other, the linear interpolation between data are used to estimate the daily data. If sampling events are more than 40 days apart, the more conservative estimate of the sine curve is used to estimate the daily data. ppm = mg/L = g/m³, as P

6   Hydrodynamic Model Results

Commented [VJ12]:

6.1   Comparison to Other Estimates of Residence Time

7   Biogeochemical Model Results

Commented [VJ13]:

7.1   Skill Assessment

7.1.1   Skill Metrics - Description

7.2   Scenarios

7.2.1   Using NLM to modify the N load

8 Works Cited

Bianchi, T.S. 2007. *Biogeochemistry of estuaries*. New York: Oxford University Press.

Brawley, J.W., M.J. Brush, J.N. Kremer, and S.W. Nixon. 2003. Potential applications of an empirical phytoplankton production model to shallow water ecosystems. *Ecological Modelling* 160: 55-61.

Brush, M.J. 2002. Development of a numerical model for shallow marine ecosystems with application to Greenwich Bay, RI. Doctoral Dissertation, Univeristy of Rhode Island Narragansett, RI.

Brush, M.J., and J.W. Brawley. 2009. Adapting the light ·biomass (BZI) models of phytoplankton primary production to shallow marine ecosystems. *Journal of Marine Systems* 75: 227–235.

Brush, M.J., J.W. Brawley, S.W. Nixon, and J.N. Kremer. 2002. Modeling phytoplankton production: problems with the Eppley curve and an empirical alternative. *Marine Ecology Progress Series* 238: 31-45.

Brush, M.J., and S.W. Nixon. 2010. Modeling the role of macroalgae in a shallow sub-estuary of Narragansett Bay, RI (USA). *Ecological Modelling* 221: 1065–1079.

Clark, H., and J.N. Kremer. 2005. Estimating direct and episodic atmospheric nitrogen deposition to a coastal waterbody. *Marine Environmental Research* 59: 349-366.

Cloern, J.E., C. Grenz, and L. Vidergar-Lucas 1995. An empirical model of the phytoplankton chlorophyll: carbon ratio - the conversion factor between productivity and growth rate *Limnology and Oceanography* 40: 1313-1321

Duarte, C.M. 1990. Seagrass nutrient content. *Marine Ecology Progress Series* 67: 201-207.

Duarte, C.M. 1992. Nutrient concentration of aquatic plants: Patterns across species. *Limnology and Oceanography* 37: 882-889.

Duarte, C.M., and J. Cebrián. 1996. The fate of marine autotrophic production. *Limnology and Oceanography* 41: 1758-1766.

Falkowski, P.G., and A.D. Woodhead. 1992. Primary productivity and biogeochemical cycles in the sea. New York, NY: Plenum Press.

Garcia, H.E., and L.I. Gordon. 1992. Oxygen solubility in seawater: better fitting equations. *Limnology & Oceanography* 37: 1307-1312.

Gurney, W.S.C., and R.M. Nisbet. 1998. *Ecological Dynamics*. New York: Oxford University Press, Inc.

Hagy, J.D., W.R. Boynton, and L.P. Sanford. 2000. Estimation of net physical transport and hydraulic residence times for a coastal plain estuary using box models. *Estuaries* 23: 328-340.

Hedges, J.I., J.A. Baldock, Y. Gélinas, C. Lee, M.L. Peterson, and S.G. Wakeham. 2002. The biochemical and elemental composition of marine plankton: a NMR perspective. *Marine Chemistry* 78: 47-63.

Hernández-León, S., and T. Ikeda. 2005. Zooplankton respiration. In *Respiration in Aquatic Ecosystems*, ed. P.A. del Giorgio and P.J.l.B. Williams, 57-82. Oxford: Oxford University Press.

Howes, B., S.W. Kelley, J.S. Ramsey, R. Samimy, D. Schlezinger, and E. Eichner. 2006. Linked Watershed-Embayment Model to Determine Critical Nitrogen Loading Thresholds for West Falmouth Harbor, Falmouth, Massachusetts. Massachusetts Estuaries Project, Massachusetts Department of Environmental Protection. Boston, MA.

Howes, B.L., J.S. Ramsey, and S.W. Kelley. 2001. Nitrogen Modeling to Support Watershed Management: Comparison of Approaches and Sensitivity Analysis. prepared for: Massachusetts Department of Environmental Protection Bureau of Resource Protection and U.S. Environmental Protection Agency Region I.Project #00-06/104.

Jakeman, A.J., R.A. Letcher, and J.P. Norton. 2006. Ten iterative steps in development and evaluation of environmental models. *Environmental Modelling & Software* 21: 602-614.

1370 Kremer, J.N. 1983. Ecological implications of parameter uncertainty in stochastic simulation. *Ecological*
1371 *Modelling* 18: 187-207.
1372 Kremer, J.N., and S.W. Nixon. 1978. *A Coastal Marine Ecosystem*. New York: Springer-Verlag.
1373 Kremer, J.N., J.M.P. Vaudrey, D. Ullman, D.L. Bergondo, N. Nasota, C. Kincaid, D.L. Codiga, and M.J.
1374 Brush. 2010. Simulating property exchange in estuarine ecosystem models at ecologically
1375 appropriate scales. *Ecological Modelling* 221: 1080-1088.
1376 Lee, K.S., S.R. Park, and Y.K. Kim. 2007. Effects of irradiance, temperature, and nutrients on growth
1377 dynamics of seagrasses: A review. *Journal of Experimental Marine Biology and Ecology* 350: 144-
1378 175.
1379 Nixon, S.W. 1981. Remineralization and nutrient cycling in coastal marine ecosystems. In *Estuaries and*
1380 *Nutrients*, ed. B.J. Neilson and L.E. Cronin, 111-138. N.J.: Humana Press.
1381 O'Mara, K., J.M. Olley, B. Fry, and M. Burford. 2019. Catchment soils supply ammonium to the coastal
1382 zone - Flood impacts on nutrient flux in estuaries. *Science of the Total Environment* 654: 583-
1383 592.
1384 Officer, C.B. 1980. Box models revisited. In *Estuarine and Wetland Processes with Emphasis on Modeling*,
1385 ed. P. Hamilton and R.B. McDonald, 65-114. New York: Plenum Press.
1386 Officer, C.B., and D.R. Kester. 1991. On estimating the non-advective tidal exchanges and advective
1387 gravitational circulation exchanges in an estuary. *Estuarine, Coastal and Shelf Science* 32: 99-
1388 103.
1389 Petrone, K.C., J.S. Richards, and P.F. Grierson. 2009. Bioavailability and composition of dissolved organic
1390 carbon and nitrogen in a near coastal catchment of South-Western Australia. *Biogeochemistry*
1391 92: 27-40.
1392 Plew, D., J. Zeldis, U. Shankar, and A. Elliott. 2018. Using simple dilution models to predict New Zealand
1393 estuarine water quality. *Estuaries and Coasts* 41: 1643-1659.
1394 Sampou, P.A., and M. Kemp. 1994. Factors regulating plankton community respiration in Chesapeake
1395 Bay. *Marine Ecology Progress Series* 110: 249-258.
1396 Seitzinger, S.P., R.W. Sanders, and R. Styles. 2002. Bioavailability of DON from natural and
1397 anthropogenic sources to estuarine plankton. *Limnology and Oceanography* 47: 353-366.
1398 Solidoro, C., V.E. Brando, C. Dejak, D. Franco, R. Pastres, and G. Pecenik. 1997. Long term simulations of
1399 population dynamics of Ulva r. in the lagoon of Venice. *Ecological modelling* 102: 259-272.
1400 Touchette, B.W., and J.M. Burkholder. 2000. Review of nitrogen and phosphorus metabolism in
1401 seagrasses. *Journal of Experimental Marine Biology and Ecology* 250: 133-167.
1402 Valiela, I. 1995. *Marine Ecological Processes*. New York, New York, U.S.A.: Springer-Verlag New York, Inc.
1403 Vaudrey, J.M.P. 2007. Estimating total ecosystem metabolism (TEM) from the oxygen rate of change: a
1404 comparison of two Connecticut estuaries. Doctoral Dissertation, University of Connecticut
1405 Groton.
1406 Vaudrey, J.M.P. 2014. 2014 working report on the Narragansett Bay EcoGEM model. University of
1407 Connecticut. 68 pp.
1408 Vaudrey, J.M.P. 2016. EcoGEM: Modeling Response of Hypoxia to Changes in Nutrient Inputs to
1409 Narragansett Bay, RI, USA. Department of Marine Sciences, University of Connecticut. prepared
1410 for NOAA CHRP. 122 pp.
1411 Vaudrey, J.M.P., T. Getchis, K. Shaw, J. Markow, R. Britton, and J.N. Kremer. 2009. Effects of oyster
1412 depuration gear on eelgrass (*Zostera marina* L.) in a low density aquaculture site in long island
1413 sound. *Journal of Shellfish Research* 28: 243-250.
1414 Vaudrey, J.M.P., J.K. Kim, C. Yarish, L. Brousseau, C. Pickerell, and J. Eddings. 2013. Comparative analysis
1415 and model development for determining the susceptibility to eutrophication of Long Island
1416 Sound embayments; QAPP Version 2 – September 9, 2013; EPA identifier RFA#: 13110.

1417   University of Connecticut and Cornell Cooperative Extension of Suffolk County. contact:
1418   jamie.vaudrey@uconn.edu.
1419 Vaudrey, J.M.P., J. Krumholz, and C. Calabretta. 2019. Eelgrass success in Niantic River Estuary, CT:
1420   quantifying factors influencing interannual variability of eelgrass (Zostera marina) using a 30-
1421   year dataset. Department of Marine Sciences, Groton, CT. Final report prepared for the Niantic
1422   Nitrogen Work Group. 200 pp.
1423 Wang, C., A. Lei, K. Zhou, Z. Hu, W. Hao, and J. Yang. 2014. Growth and nitrogen uptake characteristics
1424   reveal outbreak mechanism of the opportunistic macroalga Gracilaria tenuistipitata. *PLoS ONE* 9.
1425 Ward, B.A., S. Dutkiewicz, O. Jahn, and M.J. Follows. 2012. A size-structured food-web model for the
1426   global ocean. *Limnology and oceanography* 57: 1877-1891.
1427 Williams, P., and P. del Giorgio. 2005. Respiration in aquatic ecosystems: history and background. In
1428   *Respiration in Aquatic Ecosystems*, ed. P. del Giorgio and P. Williams, 1-17: Oxford University
1429   Press.
1430 Williams, P.J.l.B., and J.E. Robertson. 1991. Over-all planlton oxygen and carbon dioxide metabolism: the
1431   problem of reconciling observations and calculations of photosynthetic quotients. *Journal of*
1432   *Plankton Research* 13: 153-169.
1433 Wu, K., K. Lu, M. Dai, and Z. Liu. 2019. The bioavailability of riverine dissolved organic matter in coastal
1434   marine waters of southern Texas. *Estuarine, Coastal and Shelf Science* 231.
1435 Zimmerman, R.C., R.D. Smith, and R.S. Alberte. 1989. Thermal acclimation and whole-plant carbon
1436   balance in *Zostera marina* L. (eelgrass). *Journal of Experimental Marine Biology and Ecology* 130:
1437   93-109.

1438

1439

9 Appendix A – Salinity Data

The Officer box model approach requires daily salinity values in each box of the model domain and at the boundaries. Given the sparsity of salinity data, modeled salinity from Dr. Nickitas Georgas at Stevens Institute of Technology will be used to inform the development of the box model hydrodynamics. Dr. Georgas uses a model called NYHOPS (New York Harbor Observing and Prediction System) for hindcasting salinity (as well as other parameters) in the Long Island Sound area. Access to model results is available at http://hudson.dl.stevens-tech.edu/maritimeforecast/maincontrol.shtml (on the right hand side, under Region, select Long Island Sound). Dr. Georgas states, "The contributing watershed name in NYHOPS is "Southeast Shoreline 17, CT." It covers 42.54 square miles. Flow is estimated by watershed-area-adjusting the Shetucket near Willimantic gaged USGS daily flow (404 miles). The freshwater yield (discharge in the model) is split into three NYHOPS receiving water cells," within the Niantic River Estuary. One at the very head of the River (where Latimer Brook enters NRE), one at the adjacent cell to the south (where Stony Brook comes in), and one just west of Niantic Bay's mouth from several tributaries. River water temperature is assigned from the nearby Connecticut River at Essex gage. Niantic River has three model boxes, with more boxes in Niantic Bay (Figure 41). Unfortunately, the NYHOPS model does not include the restriction at the south end of Niantic created by the road and train bridge. Comparison of model predictions with salinity data will be used to evaluate the impact of this missing restriction. If the NYHOPS modeled salinity accurately captures the major trends in salinity in Niantic River and Bay, the 35-year model predictions would be of great use to hindcasting the ecological model to explore the pressures impacting the state variables within the system.
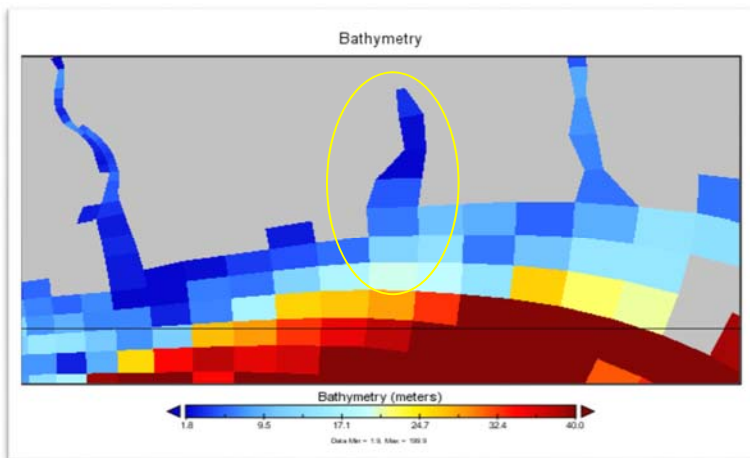
Figure 41: Bathymetry from the NYHOPS model.
Provided by Dr. Nickitas Georgas, Stevens Institute of Technology. Niantic River and Bay are identified by the yellow oval. (Image courtesy of Dr. Georgas.)

Salinity data from the NYHOPS model is modeled at 11 depths, with the distance between each depth changing with the total depth in the model box. For comparison to field data, the surface layer was

1466 calculated as the average of the top five depths and the bottom was calculated as the average of the
1467 bottom six depths.

1468 The NYHOPS data from a box was compared to the corresponding NREEM model box (Figure 42). The
1469 field data used for comparison included any data collected in Niantic River and collated as part of this
1470 project. A key point to remember is that the field data was collected at one location in the box, at one
1471 depth, and at a single point in time whereas the NYHOPS salinity is the daily averaged salinity across the
1472 whole model box for the surface or bottom layer.

1473 In general, the NYHOPS model slightly underestimates salinity with the closest match found in the arm
1474 and the worst match found in Niantic Bay (Figures 43 to 46). The NYHOPS model also misses some low
1475 salinity events in the arm and upper basin (Figures 43 & 44). Overall, the match between the NYHOPS
1476 model output and field data is good, especially considering the mismatch in data type (daily, box-wide
1477 average versus single point data).
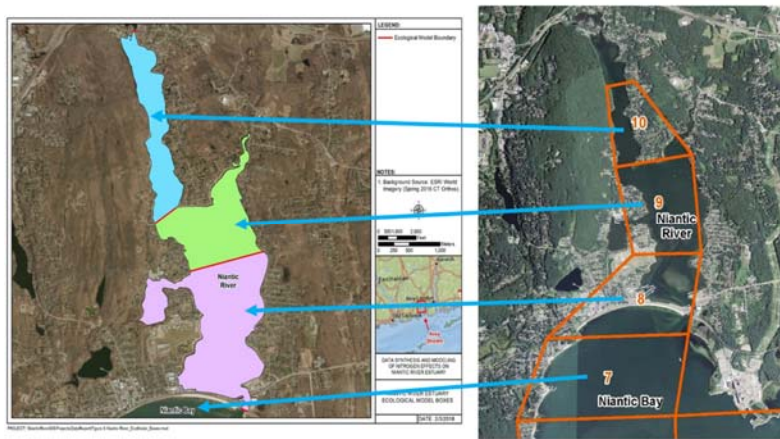
1478
1479 *Figure 42: NYHOPS model boxes vs. NREEM model boxes.*
1480 *Salinity from the NYHOPS model was used to estimate salinity in NRE, to drive hydrodynamic mixing in the model. The figure on*
1481 *the right shows the NYHOPS model boxes with the blue arrows indicating the corresponding NREEM model boxes.*
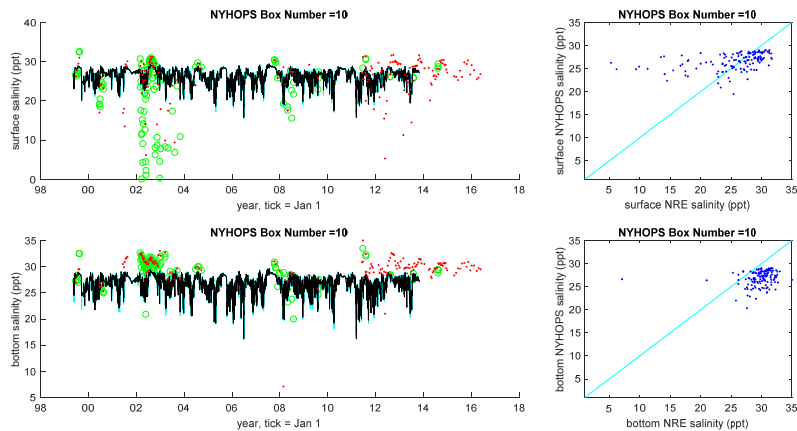
1482
1483 *Figure 43: NYHOPS Salinity vs. Field Salinity – Arm*
1484 *Comparison of the daily and box-wide average surface and bottom layer for NYHOPS salinity to field data in the respective layer*
1485 *(from a single location in the box, a single depth, at one point in time in the day). (LEFT) Depth-averaged NYHOPS model data is*
1486 *shown by the black line with the cyan line indicating the minimum and maximum salinity values for the layer. Red points are*
1487 *field data. Green circles are field data from north of the NYHOPS box (Figure 42). (RIGHT) Plot of NYHOPS data on field data, the*
1488 *identity line (1:1) is shown in cyan.*
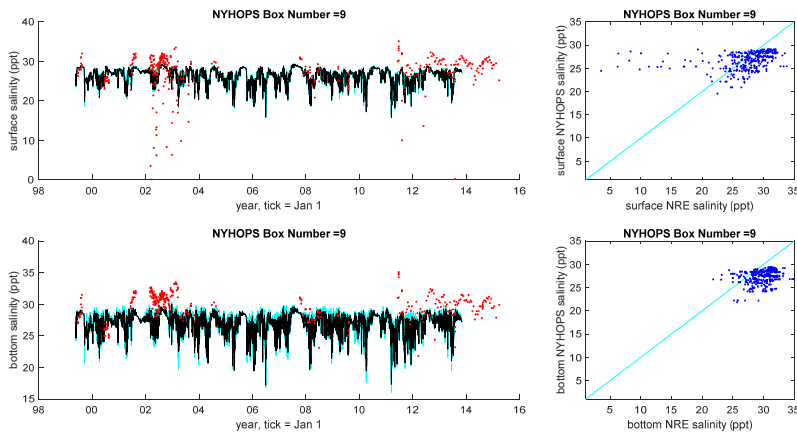
1489
1490 *Figure 44: NYHOPS Salinity vs. Field Salinity – Upper Basin*
1491 *Comparison of the daily and box-wide average surface and bottom layer for NYHOPS salinity to field data in the respective layer*
1492 *(from a single location in the box, a single depth, at one point in time in the day). (LEFT) Depth-averaged NYHOPS model data is*
1493 *shown by the black line with the cyan line indicating the minimum and maximum salinity values for the layer. Red points are*
1494 *field data. (RIGHT) Plot of NYHOPS data on field data, the identity line (1:1) is shown in cyan.*

1495
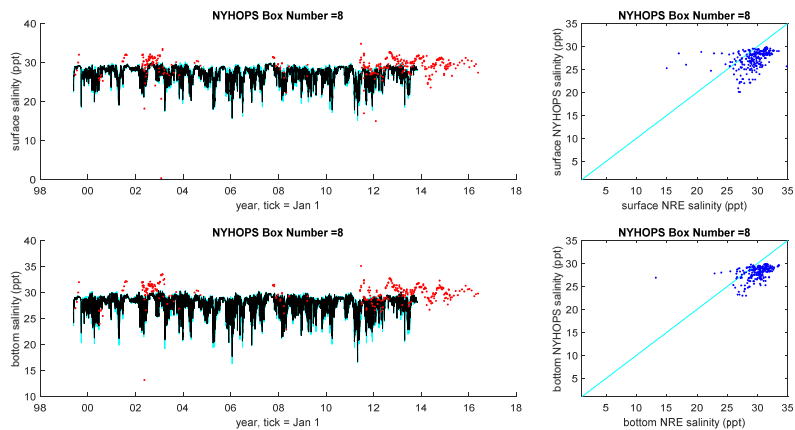
1496
1497   *Figure 45: NYHOPS Salinity vs. Field Salinity – Lower Basin*
1498   *Comparison of the daily and box-wide average surface and bottom layer for NYHOPS salinity to field data in the respective layer*
1499   *(from a single location in the box, a single depth, at one point in time in the day). (LEFT) Depth-averaged NYHOPS model data is*
1500   *shown by the black line with the cyan line indicating the minimum and maximum salinity values for the layer. Red points are*
1501   *field data. (RIGHT) Plot of NYHOPS data on field data, the identity line (1:1) is shown in cyan.*
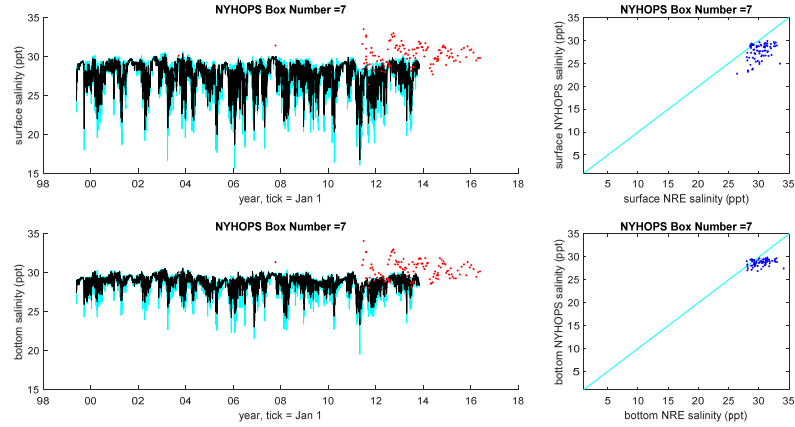
1502
1503   *Figure 46: NYHOPS Salinity vs. Field Salinity – Niantic Bay*
1504   *Comparison of the daily and box-wide average surface and bottom layer for NYHOPS salinity to field data in the respective layer*
1505   *(from a single location in the box, a single depth, at one point in time in the day). (LEFT) Depth-averaged NYHOPS model data is*
1506   *shown by the black line with the cyan line indicating the minimum and maximum salinity values for the layer. Red points are*
1507   *field data. (RIGHT) Plot of NYHOPS data on field data, the identity line (1:1) is shown in cyan.*

9.1   Estimating Niantic Bay Salinity Beyond NYHOPS End Date

1509   NYHOPS has an end date of 10/31/2013, for data in the Niantic River Estuary region. Salinity in the
1510   Niantic Bay is required to run the model. Salinity data in Niantic Bay was estimated from river flow using
1511   a linear regression on all available daily data (1/1/1981 to 10/31/2013). Regression results are shown
1512   below. Statistical analyses were conducted in *JMP 13.0.0*, a SAS product.

1513   Salinity in Niantic Bay (ppt) = River Flow (m^3 d^{-1}) * -0.00000393 + 28.511953

salinity data - Fit Least Squares   Page 1 of 1

Response NB salinity (ppt)

Regression Plot
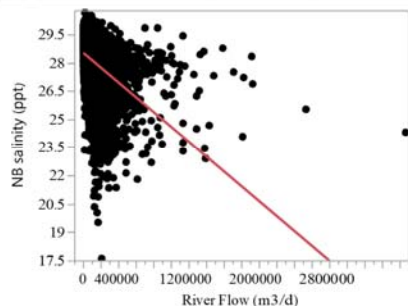
Lack Of Fit

Source	DF	Sum of Squares	Mean Square	F Ratio
Lack Of Fit	1348	4174.477	3.09679	2.4823
Pure Error	10642	13276.446	1.24755	Prob > F
Total Error	11990	17450.923		<.0001*
				Max RSq
				0.3513

Summary of Fit

RSquare	0.147369
RSquare Adj	0.147298
Root Mean Square Error	1.206423
Mean of Response	28.12648
Observations (or Sum Wgts)	11992

Analysis of Variance

Source	DF	Sum of Squares	Mean Square	F Ratio
Model	1	3016.217	3016.22	2072.351
Error	11990	17450.923	1.46	Prob > F
C. Total	11991	20467.140		<.0001*

Parameter Estimates

Term	Estimate	Std Error	t Ratio	Prob>|t|	Lower 95%	Upper 95%
Intercept	28.511953	0.013895	2052.0	<.0001*	28.484717	28.53919
River Flow (m3/d)	-3.93e-6	8.633e-8	-45.52	<.0001*	-4.099e-6	-3.761e-6

1514

10 Appendix B – Boundary Conditions Supplemental Plots
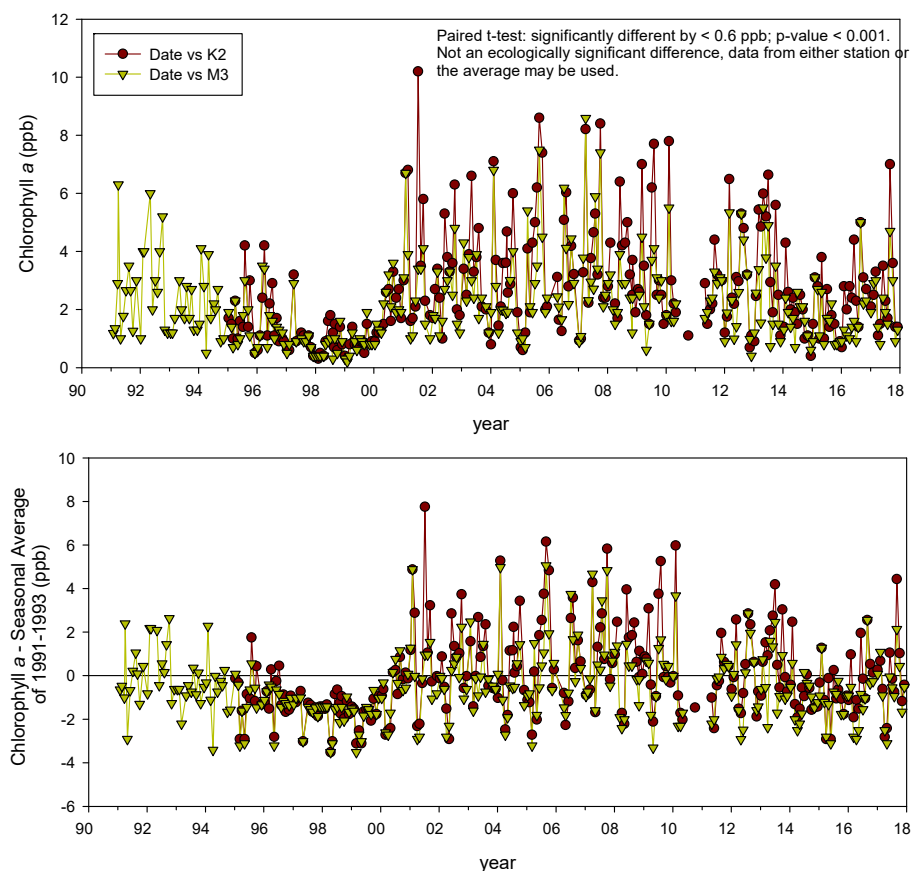
1517 Figure 47: Chlorophyll a, Niantic Bay Boundary Conditions.
1518 The top panel shows the available data from stations M3 and K2 of the CTDEEP Long Island Sound sampling program (see Figure
1519 24, page 53 for a map of station locations). Data were compared by date using a Paired t-test and when the assumption of
1520 normality was not met, a Signed Rank test; results are shown in the in-figure caption. The bottom panel shows the data from the
1521 top panel minus the seasonal average from 1991-1993; data values above the origin indicate increases relative to the 1991-93
1522 period and below indicate decreases.
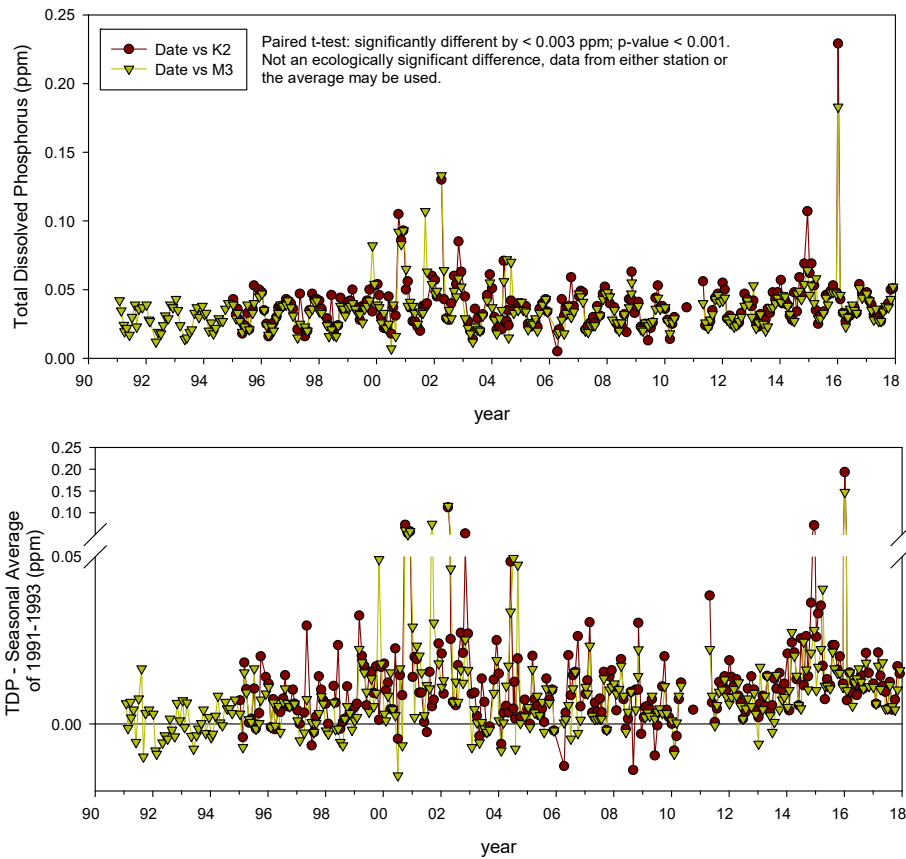
Figure 48: Total Dissolved Phosphorus, Niantic Bay Boundary Conditions.
The top panel shows the available data from stations M3 and K2 of the CTDEEP Long Island Sound sampling program (see Figure 24, page 53 for a map of station locations). Data were compared by date using a Paired t-test and when the assumption of normality was not met, a Signed Rank test; results are shown in the in-figure caption. The bottom panel shows the data from the top panel minus the seasonal average from 1991-1993; data values above the origin indicate increases relative to the 1991-93 period and below indicate decreases.

Paired t-test: significantly different by < 0.003 ppm; p-value < 0.001. Not an ecologically significant difference, data from either station or the average may be used.
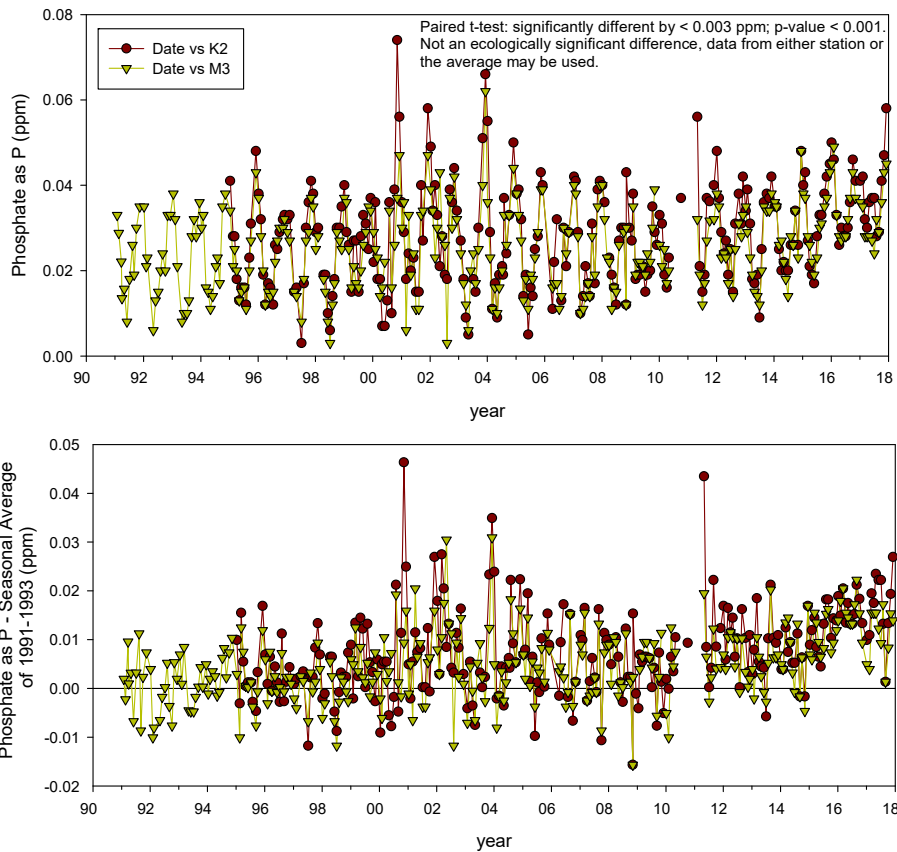
1530
1531 *Figure 49: Dissolved Inorganic Phosphorus, Niantic Bay Boundary Conditions.*
1532 *The top panel shows the available data from stations M3 and K2 of the CTDEEP Long Island Sound sampling program (see Figure*
1533 *24, page 53 for a map of station locations). Data were compared by date using a Paired t-test and when the assumption of*
1534 *normality was not met, a Signed Rank test; results are shown in the in-figure caption. The bottom panel shows the data from the*
1535 *top panel minus the seasonal average from 1991-1993; data values above the origin indicate increases relative to the 1991-93*
1536 *period and below indicate decreases.*
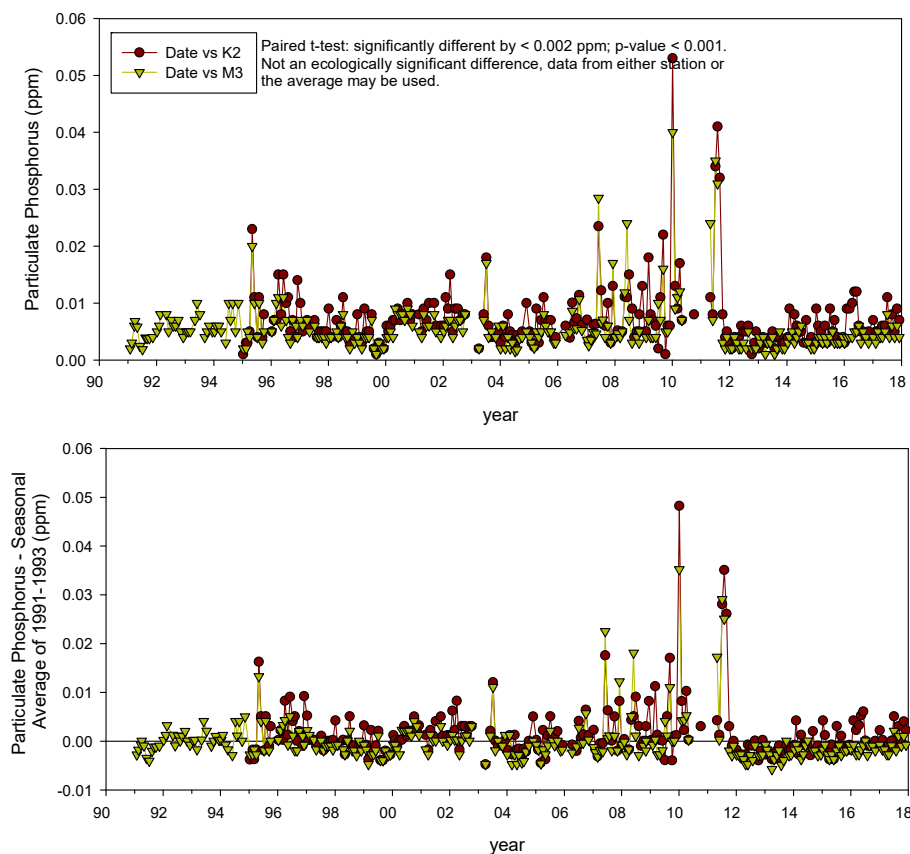
1537
1538 *Figure 50: Particulate Phosphorus, Niantic Bay Boundary Conditions.*
1539 *The top panel shows the available data from stations M3 and K2 of the CTDEEP Long Island Sound sampling program (see Figure*
1540 *24, page 53 for a map of station locations). Data were compared by date using a Paired t-test and when the assumption of*
1541 *normality was not met, a Signed Rank test; results are shown in the in-figure caption. The bottom panel shows the data from the*
1542 *top panel minus the seasonal average from 1991-1993; data values above the origin indicate increases relative to the 1991-93*
1543 *period and below indicate decreases.*
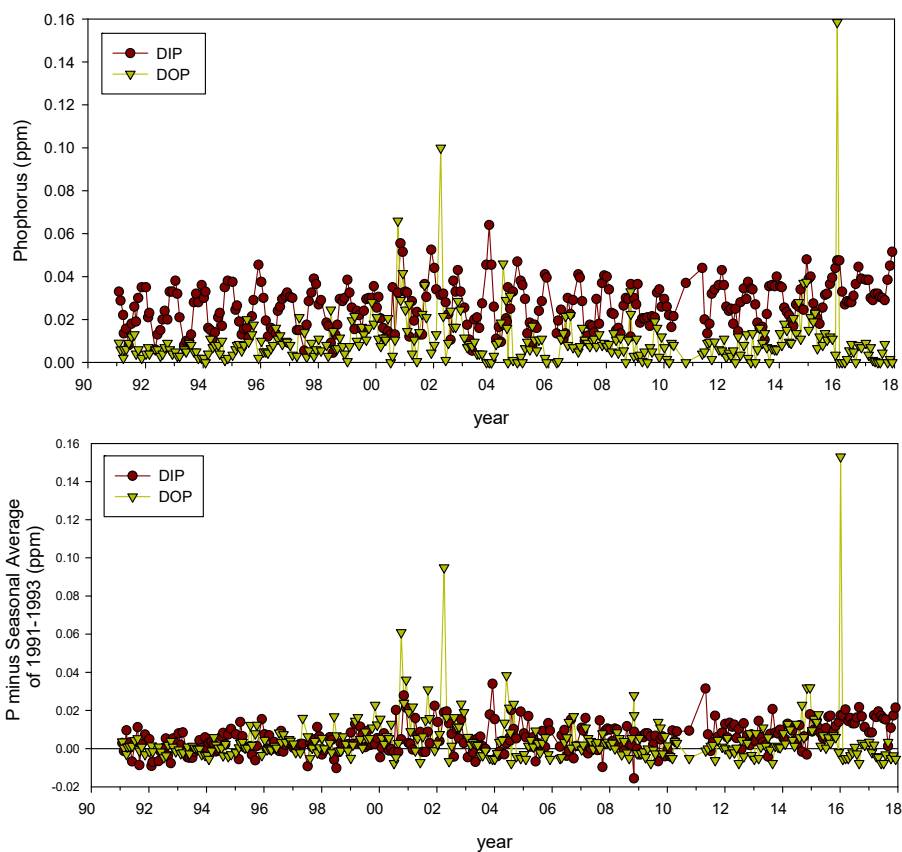
1545   *Figure 51: Dissolved Inorganic Phosphorus and Dissolved Organic Phosphorus, Niantic Bay Boundary Conditions.*
1546   *Data averaged from stations M3 and K2 of the CTDEEP Long Island Sound sampling program (see Figure 24, page 53 for a map*
1547   *of station locations). DOP is only calculated when DIP and TDP were both available. The bottom panel shows the data from the*
1548   *top panel minus the seasonal average from 1991-1993; data values above the origin indicate increases relative to the 1991-93*
1549   *period and below indicate decreases.*

1550
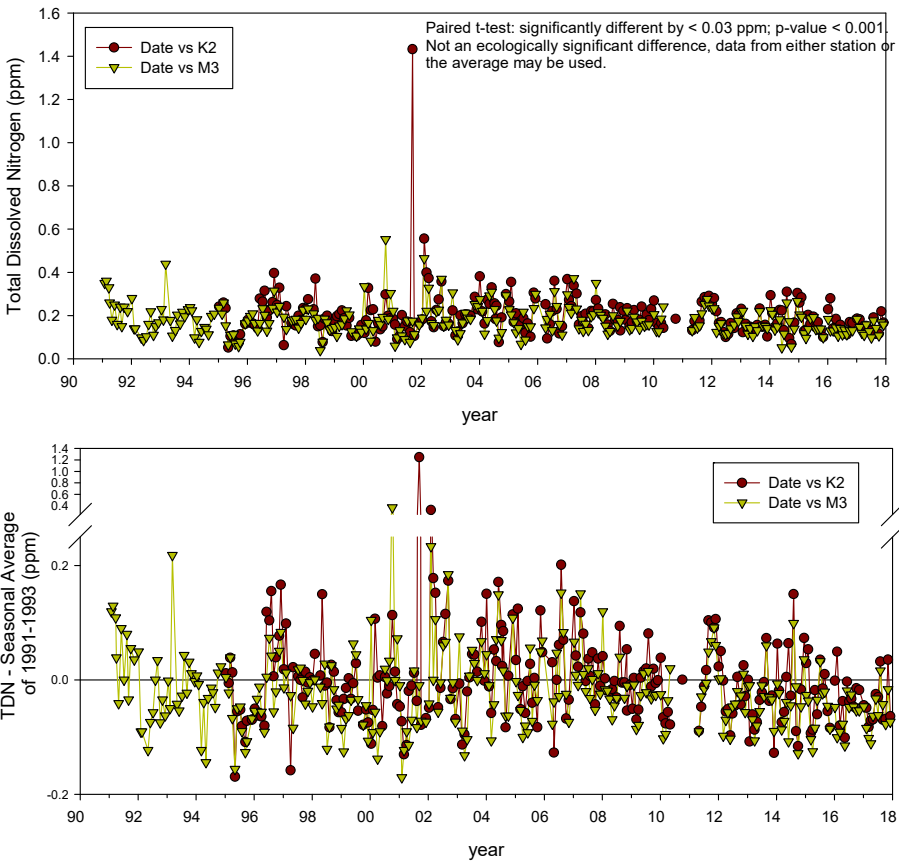
1551
1552 *Figure 52: Total Dissolved Nitrogen (TDN), Niantic Bay Boundary Conditions.*
1553 *The top panel shows the available data from stations M3 and K2 of the CTDEEP Long Island Sound sampling program (see Figure*
1554 *24, page 53 for a map of station locations). Data were compared by date using a Paired t-test and when the assumption of*
1555 *normality was not met, a Signed Rank test; results are shown in the in-figure caption. The bottom panel shows the data from the*
1556 *top panel minus the seasonal average from 1991-1993; data values above the origin indicate increases relative to the 1991-93*
1557 *period and below indicate decreases.*
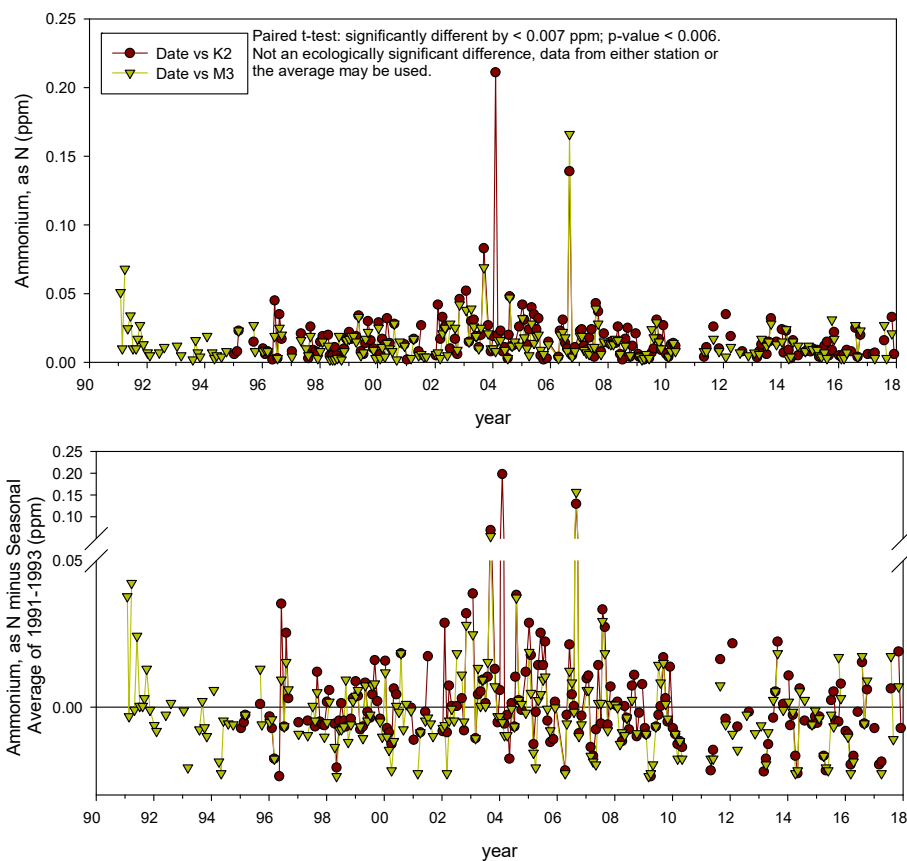
1558
1559 *Figure 53: Dissolved Ammonium, Niantic Bay Boundary Conditions.*
1560 *The top panel shows the available data from stations M3 and K2 of the CTDEEP Long Island Sound sampling program (see Figure*
1561 *24, page 53 for a map of station locations). Data were compared by date using a Paired t-test and when the assumption of*
1562 *normality was not met, a Signed Rank test; results are shown in the in-figure caption. The bottom panel shows the data from the*
1563 *top panel minus the seasonal average from 1991-1993; data values above the origin indicate increases relative to the 1991-93*
1564 *period and below indicate decreases.*
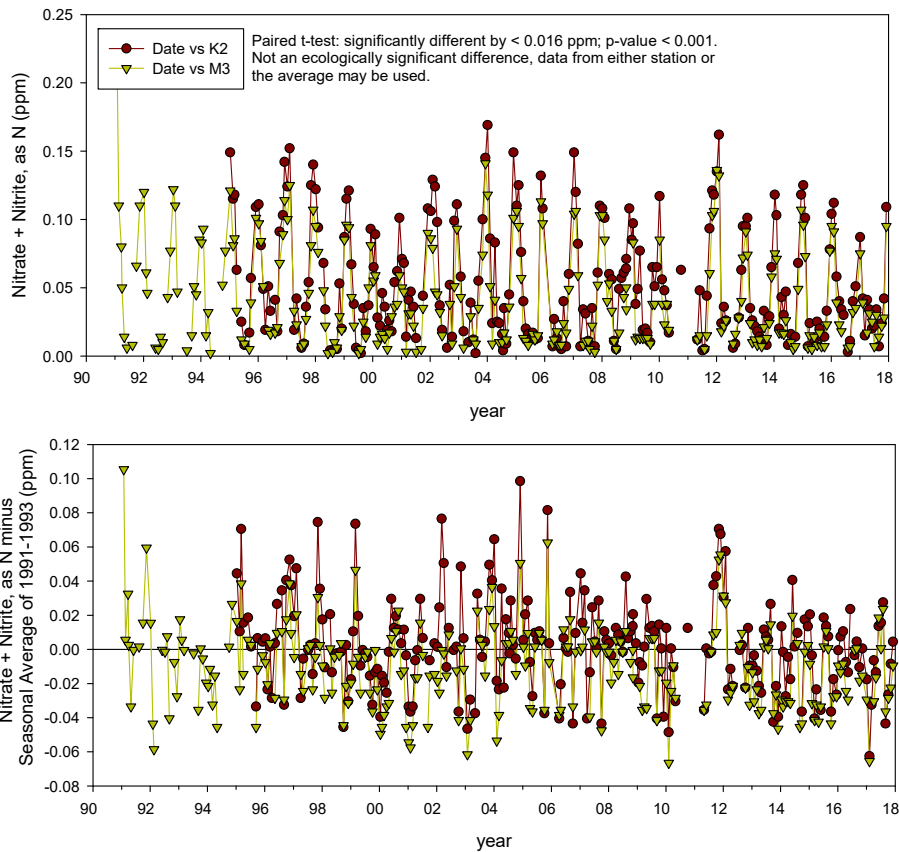
Figure 54: Dissolved Nitrate + Nitrite, Niantic Bay Boundary Conditions.
The top panel shows the available data from stations M3 and K2 of the CTDEEP Long Island Sound sampling program (see Figure 24, page 53 for a map of station locations). Data were compared by date using a Paired t-test and when the assumption of normality was not met, a Signed Rank test; results are shown in the in-figure caption. The bottom panel shows the data from the top panel minus the seasonal average from 1991-1993; data values above the origin indicate increases relative to the 1991-93 period and below indicate decreases.
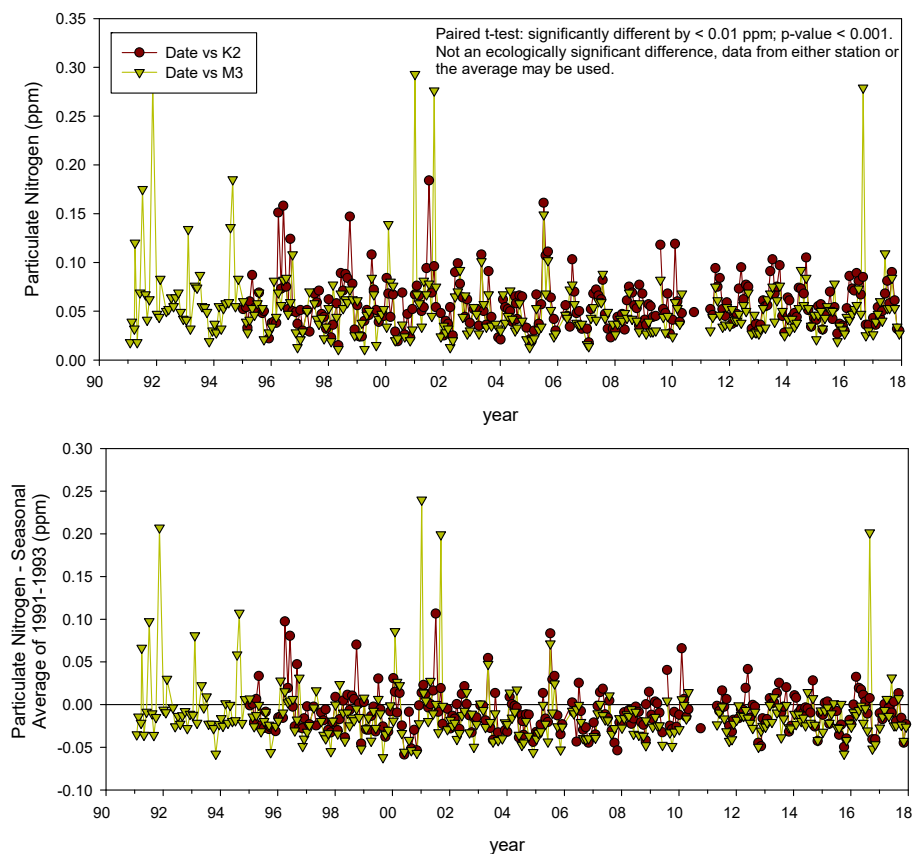
1572
1573   *Figure 55: Particulate Nitrogen, Niantic Bay Boundary Conditions.*
1574   *The top panel shows the available data from stations M3 and K2 of the CTDEEP Long Island Sound sampling program (see Figure*
1575   *24, page 53 for a map of station locations). Data were compared by date using a Paired t-test and when the assumption of*
1576   *normality was not met, a Signed Rank test; results are shown in the in-figure caption. The bottom panel shows the data from the*
1577   *top panel minus the seasonal average from 1991-1993; data values above the origin indicate increases relative to the 1991-93*
1578   *period and below indicate decreases.*
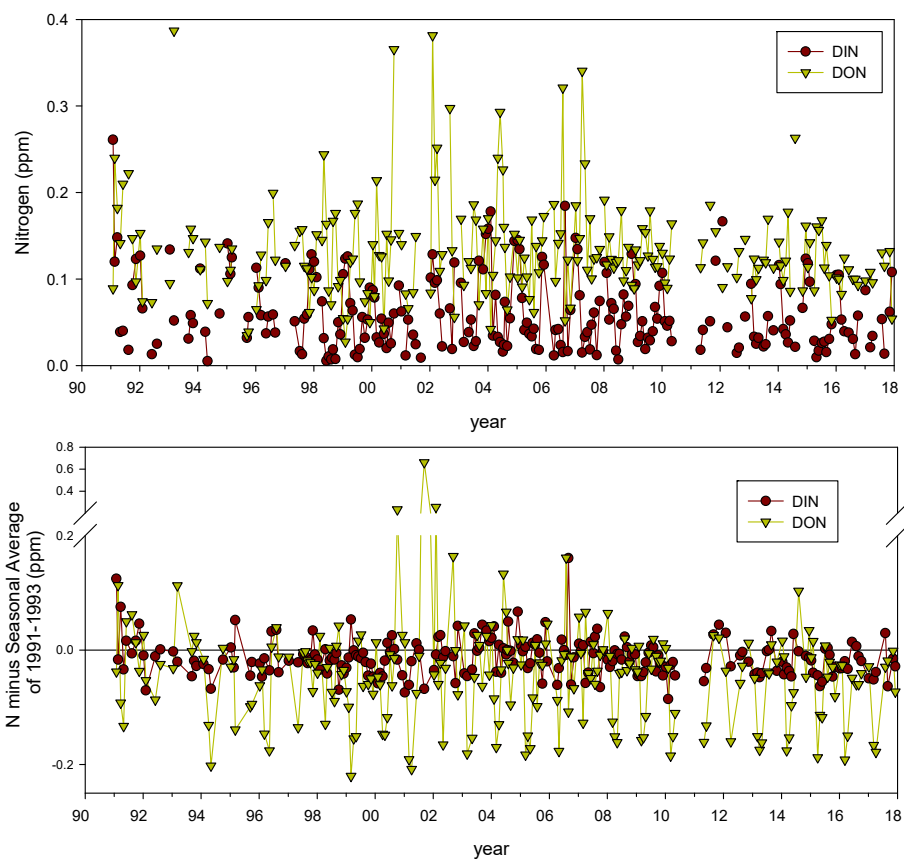
1579
1580 *Figure 56: Dissolved Inorganic Nitrogen and Dissolved Organic Nitrogen, Niantic Bay Boundary Conditions.*
1581 *Data averaged from stations M3 and K2 of the CTDEEP Long Island Sound sampling program (see Figure 24, page 53 for a map*
1582 *of station locations). DIN is only calculated for dates when ammonium and nitrate + nitrite were both available. DON is only*
1583 *calculated when DIN and TDN were both available. The bottom panel shows the data from the top panel minus the seasonal*
1584 *average from 1991-1993; data values above the origin indicate increases relative to the 1991-93 period and below indicate*
1585 *decreases.*

1586

11 Appendix C – Data Tables

11.1 C:N molar ratios for macrophytes, by ordinal date

calendar date	ordinal date	*Agardhiella* C:N molar ratio	*Ulva* sp., blade form C:N molar ratio	*Zostera marina* C:N molar ratio
1/1	1	8.30	8.60	18.63
1/2	2	8.30	8.60	18.63
1/3	3	8.30	8.60	18.63
1/4	4	8.30	8.60	18.63
1/5	5	8.30	8.60	18.63
1/6	6	8.30	8.60	18.63
1/7	7	8.30	8.60	18.63
1/8	8	8.30	8.60	18.63
1/9	9	8.30	8.60	18.63
1/10	10	8.30	8.60	18.63
1/11	11	8.30	8.60	18.63
1/12	12	8.30	8.60	18.63
1/13	13	8.30	8.60	18.63
1/14	14	8.30	8.60	18.63
1/15	15	8.30	8.60	18.63
1/16	16	8.30	8.60	18.63
1/17	17	8.30	8.60	18.63
1/18	18	8.30	8.60	18.63
1/19	19	8.30	8.60	18.63
1/20	20	8.30	8.60	18.63
1/21	21	8.30	8.60	18.63
1/22	22	8.30	8.60	18.63
1/23	23	8.30	8.60	18.63
1/24	24	8.30	8.60	18.63
1/25	25	8.30	8.60	18.63
1/26	26	8.30	8.60	18.63
1/27	27	8.30	8.60	18.63
1/28	28	8.30	8.60	18.63
1/29	29	8.30	8.60	18.63
1/30	30	8.30	8.60	18.63
1/31	31	8.30	8.60	18.63
2/1	32	8.30	8.60	18.63
2/2	33	8.30	8.60	18.63
2/3	34	8.30	8.60	18.63
2/4	35	8.30	8.60	18.63
2/5	36	8.30	8.60	18.63
2/6	37	8.30	8.60	18.63

calendar date	ordinal date	*Agardhiella* C:N molar ratio	*Ulva* sp., blade form C:N molar ratio	*Zostera marina* C:N molar ratio
2/7	38	8.30	8.60	18.63
2/8	39	8.30	8.60	18.63
2/9	40	8.30	8.60	18.63
2/10	41	8.30	8.60	18.63
2/11	42	8.30	8.60	18.63
2/12	43	8.30	8.60	18.63
2/13	44	8.30	8.60	18.63
2/14	45	8.30	8.60	18.63
2/15	46	8.30	8.60	18.63
2/16	47	8.30	8.60	18.63
2/17	48	8.30	8.60	18.63
2/18	49	8.30	13.31	18.63
2/19	50	8.30	13.58	18.63
2/20	51	8.30	13.85	18.63
2/21	52	8.30	14.12	18.63
2/22	53	8.30	14.38	18.63
2/23	54	8.30	14.64	18.63
2/24	55	8.30	14.90	18.63
2/25	56	8.30	15.15	18.63
2/26	57	8.30	15.40	18.63
2/27	58	8.30	15.65	18.63
2/28	59	8.30	15.90	18.63
2/29	60	8.30	16.14	18.63
3/1	61	8.30	16.38	18.63
3/2	62	8.30	16.62	18.63
3/3	63	8.30	16.85	18.63
3/4	64	8.30	17.09	18.63
3/5	65	8.30	17.31	18.63
3/6	66	8.30	17.54	18.63
3/7	67	8.30	17.76	18.63
3/8	68	8.30	17.98	18.63
3/9	69	8.30	18.20	18.63
3/10	70	8.30	18.42	18.63
3/11	71	8.30	18.63	18.63
3/12	72	8.30	18.84	18.63
3/13	73	8.30	19.05	18.63
3/14	74	8.30	19.25	18.63
3/15	75	8.30	19.45	18.63
3/16	76	8.30	19.65	18.63
3/17	77	8.30	19.85	18.63
3/18	78	8.30	20.04	18.63

calendar date	ordinal date	*Agardhiella* C:N molar ratio	*Ulva* sp., blade form C:N molar ratio	*Zostera marina* C:N molar ratio
3/19	79	8.30	20.23	18.63
3/20	80	8.30	20.42	18.63
3/21	81	8.30	20.60	18.63
3/22	82	8.30	20.79	18.63
3/23	83	8.30	20.97	18.63
3/24	84	8.30	21.15	18.63
3/25	85	8.30	21.32	18.63
3/26	86	8.30	21.49	18.63
3/27	87	8.30	21.66	18.63
3/28	88	8.30	21.83	18.63
3/29	89	8.30	22.00	18.63
3/30	90	8.30	22.16	18.63
3/31	91	8.30	22.32	18.63
4/1	92	8.30	22.48	18.63
4/2	93	8.30	22.63	18.63
4/3	94	8.30	22.78	18.63
4/4	95	8.30	22.93	18.63
4/5	96	8.30	23.08	18.63
4/6	97	8.30	23.23	18.63
4/7	98	8.30	23.37	18.63
4/8	99	8.30	23.51	18.63
4/9	100	8.30	23.65	18.63
4/10	101	8.30	23.78	18.63
4/11	102	8.30	23.92	18.63
4/12	103	8.30	24.05	18.63
4/13	104	8.30	24.18	18.63
4/14	105	8.30	24.30	18.63
4/15	106	8.30	24.43	18.63
4/16	107	8.30	24.55	18.63
4/17	108	8.30	24.67	18.63
4/18	109	8.30	24.79	18.63
4/19	110	8.30	24.90	18.63
4/20	111	8.33	25.01	18.63
4/21	112	8.38	25.13	18.63
4/22	113	8.43	25.23	18.63
4/23	114	8.48	25.34	18.63
4/24	115	8.52	25.44	18.63
4/25	116	8.57	25.55	18.63
4/26	117	8.62	25.64	18.63
4/27	118	8.66	25.74	18.63
4/28	119	8.71	25.84	18.63

calendar date	ordinal date	*Agardhiella* C:N molar ratio	*Ulva* sp., blade form C:N molar ratio	*Zostera marina* C:N molar ratio
4/29	120	8.75	25.93	18.63
4/30	121	8.80	26.02	18.63
5/1	122	8.84	26.11	18.63
5/2	123	8.89	26.20	18.63
5/3	124	8.93	26.28	18.63
5/4	125	8.98	26.36	18.63
5/5	126	9.02	26.44	18.63
5/6	127	9.06	26.52	18.63
5/7	128	9.11	26.60	18.63
5/8	129	9.15	26.67	18.63
5/9	130	9.19	26.75	18.63
5/10	131	9.23	26.82	18.63
5/11	132	9.28	26.88	18.63
5/12	133	9.32	26.95	18.63
5/13	134	9.36	27.01	18.63
5/14	135	9.40	27.08	18.63
5/15	136	9.44	27.14	18.63
5/16	137	9.48	27.20	18.63
5/17	138	9.52	27.25	18.63
5/18	139	9.56	27.31	18.63
5/19	140	9.60	27.36	18.63
5/20	141	9.64	27.41	18.63
5/21	142	9.68	27.46	18.63
5/22	143	9.72	27.51	18.63
5/23	144	9.76	27.55	18.63
5/24	145	9.79	27.60	18.63
5/25	146	9.83	27.64	18.63
5/26	147	9.87	27.68	18.63
5/27	148	9.91	27.72	18.63
5/28	149	9.94	27.75	18.63
5/29	150	9.98	27.79	18.63
5/30	151	10.01	27.82	18.63
5/31	152	10.05	27.85	18.63
6/1	153	10.09	27.88	18.63
6/2	154	10.12	27.91	18.63
6/3	155	10.15	27.93	18.63
6/4	156	10.19	27.96	18.63
6/5	157	10.22	27.98	18.63
6/6	158	10.26	28.00	18.74
6/7	159	10.29	28.02	19.54
6/8	160	10.32	28.04	20.32

calendar date	ordinal date	*Agardhiella* C:N molar ratio	*Ulva* sp., blade form C:N molar ratio	*Zostera marina* C:N molar ratio
6/9	161	10.35	28.05	21.08
6/10	162	10.39	28.07	21.83
6/11	163	10.42	28.08	22.56
6/12	164	10.45	28.09	23.27
6/13	165	10.48	28.10	23.97
6/14	166	10.51	28.11	24.64
6/15	167	10.54	28.11	25.30
6/16	168	10.57	28.12	25.95
6/17	169	10.60	28.12	26.57
6/18	170	10.63	28.12	27.18
6/19	171	10.65	28.12	27.77
6/20	172	10.68	28.12	28.35
6/21	173	10.71	28.12	28.91
6/22	174	10.74	28.12	29.45
6/23	175	10.76	28.11	29.98
6/24	176	10.79	28.10	30.49
6/25	177	10.82	28.09	30.99
6/26	178	10.84	28.08	31.47
6/27	179	10.87	28.07	31.94
6/28	180	10.89	28.06	32.39
6/29	181	10.91	28.05	32.82
6/30	182	10.94	28.03	33.25
7/1	183	10.96	28.01	33.65
7/2	184	10.98	27.99	34.04
7/3	185	11.01	27.97	34.42
7/4	186	11.03	27.95	34.78
7/5	187	11.05	27.93	35.13
7/6	188	11.07	27.91	35.47
7/7	189	11.09	27.88	35.79
7/8	190	11.11	27.86	36.10
7/9	191	11.13	27.83	36.39
7/10	192	11.15	27.80	36.67
7/11	193	11.17	27.77	36.94
7/12	194	11.19	27.74	37.20
7/13	195	11.20	27.71	37.44
7/14	196	11.22	27.67	37.67
7/15	197	11.24	27.64	37.89
7/16	198	11.25	27.60	38.09
7/17	199	11.27	27.56	38.29
7/18	200	11.29	27.53	38.47
7/19	201	11.30	27.49	38.64

calendar date	ordinal date	*Agardhiella* C:N molar ratio	*Ulva* sp., blade form C:N molar ratio	*Zostera marina* C:N molar ratio
7/20	202	11.31	27.45	38.79
7/21	203	11.33	27.40	38.94
7/22	204	11.34	27.36	39.07
7/23	205	11.35	27.32	39.19
7/24	206	11.37	27.27	39.31
7/25	207	11.38	27.23	39.41
7/26	208	11.39	27.18	39.50
7/27	209	11.40	27.13	39.58
7/28	210	11.41	27.08	39.65
7/29	211	11.42	27.03	39.70
7/30	212	11.43	26.98	39.75
7/31	213	11.44	26.93	39.79
8/1	214	11.45	26.87	39.82
8/2	215	11.45	26.82	39.84
8/3	216	11.46	26.76	39.85
8/4	217	11.47	26.71	39.85
8/5	218	11.47	26.65	39.84
8/6	219	11.48	26.59	39.82
8/7	220	11.48	26.53	39.79
8/8	221	11.49	26.47	39.75
8/9	222	11.49	26.41	39.71
8/10	223	11.50	26.35	39.66
8/11	224	11.50	26.29	39.59
8/12	225	11.50	26.23	39.52
8/13	226	11.50	26.16	39.45
8/14	227	11.50	26.10	39.36
8/15	228	11.51	26.03	39.27
8/16	229	11.51	25.96	39.17
8/17	230	11.50	25.90	39.06
8/18	231	11.50	25.83	38.94
8/19	232	11.50	25.76	38.82
8/20	233	11.50	25.69	38.69
8/21	234	11.50	25.62	38.55
8/22	235	11.49	25.55	38.41
8/23	236	11.49	25.48	38.26
8/24	237	11.48	25.40	38.10
8/25	238	11.48	25.33	37.94
8/26	239	11.47	25.26	37.77
8/27	240	11.47	25.18	37.60
8/28	241	11.46	25.11	37.42
8/29	242	11.45	25.03	37.23

calendar date	ordinal date	*Agardhiella* C:N molar ratio	*Ulva* sp., blade form C:N molar ratio	*Zostera marina* C:N molar ratio
8/30	243	11.44	24.95	37.04
8/31	244	11.44	24.88	36.85
9/1	245	11.43	24.80	36.65
9/2	246	11.42	24.72	36.44
9/3	247	11.41	24.64	36.23
9/4	248	11.39	24.56	36.01
9/5	249	11.38	24.48	35.79
9/6	250	11.37	24.40	35.57
9/7	251	11.36	24.32	35.34
9/8	252	11.34	24.24	35.11
9/9	253	11.33	24.16	34.87
9/10	254	11.31	24.07	34.63
9/11	255	11.30	23.99	34.39
9/12	256	11.28	23.91	34.14
9/13	257	11.26	23.82	33.89
9/14	258	11.25	23.74	33.64
9/15	259	11.23	23.65	33.38
9/16	260	11.21	23.57	33.12
9/17	261	11.19	23.48	32.86
9/18	262	11.17	23.40	32.60
9/19	263	11.15	23.31	32.33
9/20	264	11.13	23.22	32.07
9/21	265	11.10	23.13	31.80
9/22	266	11.08	23.05	31.52
9/23	267	11.06	22.96	31.25
9/24	268	11.03	22.87	30.97
9/25	269	11.01	22.78	30.70
9/26	270	10.98	22.69	30.42
9/27	271	10.96	22.60	30.14
9/28	272	10.93	22.51	29.86
9/29	273	10.90	22.42	29.58
9/30	274	10.87	22.33	29.30
10/1	275	10.85	22.24	29.02
10/2	276	10.82	22.15	28.74
10/3	277	10.78	22.06	28.45
10/4	278	10.75	21.97	28.17
10/5	279	10.72	21.88	27.89
10/6	280	10.69	21.79	27.61
10/7	281	10.66	21.70	27.33
10/8	282	10.62	21.61	27.05
10/9	283	10.59	21.52	26.77

calendar date	ordinal date	*Agardhiella* C:N molar ratio	*Ulva* sp., blade form C:N molar ratio	*Zostera marina* C:N molar ratio
10/10	284	10.55	21.42	26.49
10/11	285	10.52	21.33	26.21
10/12	286	10.48	21.24	25.93
10/13	287	10.44	21.15	25.66
10/14	288	10.40	21.06	25.39
10/15	289	10.36	20.96	25.11
10/16	290	10.32	20.87	24.84
10/17	291	10.28	20.78	24.58
10/18	292	10.24	20.69	24.31
10/19	293	10.20	20.59	24.05
10/20	294	10.16	20.50	23.79
10/21	295	10.11	20.41	23.53
10/22	296	10.07	20.32	23.27
10/23	297	10.03	20.22	23.02
10/24	298	9.98	20.13	22.77
10/25	299	9.93	20.04	22.53
10/26	300	9.89	19.95	22.28
10/27	301	9.84	19.85	22.04
10/28	302	9.79	19.76	21.81
10/29	303	9.74	19.67	21.58
10/30	304	9.69	19.58	21.35
10/31	305	9.64	19.49	21.13
11/1	306	9.59	19.40	20.91
11/2	307	9.53	19.30	20.69
11/3	308	9.48	19.21	20.48
11/4	309	9.43	19.12	20.28
11/5	310	9.37	19.03	20.08
11/6	311	9.31	18.94	19.89
11/7	312	9.26	18.85	19.70
11/8	313	9.20	18.76	19.51
11/9	314	9.14	18.67	19.33
11/10	315	9.08	18.58	19.16
11/11	316	9.02	18.49	18.99
11/12	317	8.96	18.40	18.83
11/13	318	8.90	18.31	18.68
11/14	319	8.84	18.22	18.63
11/15	320	8.78	18.14	18.63
11/16	321	8.71	18.05	18.63
11/17	322	8.65	17.96	18.63
11/18	323	8.58	17.87	18.63
11/19	324	8.52	17.79	18.63

calendar date	ordinal date	*Agardhiella* C:N molar ratio	*Ulva* sp., blade form C:N molar ratio	*Zostera marina* C:N molar ratio
11/20	325	8.45	17.70	18.63
11/21	326	8.38	17.61	18.63
11/22	327	8.31	17.53	18.63
11/23	328	8.30	17.44	18.63
11/24	329	8.30	17.36	18.63
11/25	330	8.30	17.27	18.63
11/26	331	8.30	17.19	18.63
11/27	332	8.30	17.11	18.63
11/28	333	8.30	8.60	18.63
11/29	334	8.30	8.60	18.63
11/30	335	8.30	8.60	18.63
12/1	336	8.30	8.60	18.63
12/2	337	8.30	8.60	18.63
12/3	338	8.30	8.60	18.63
12/4	339	8.30	8.60	18.63
12/5	340	8.30	8.60	18.63
12/6	341	8.30	8.60	18.63
12/7	342	8.30	8.60	18.63
12/8	343	8.30	8.60	18.63
12/9	344	8.30	8.60	18.63
12/10	345	8.30	8.60	18.63
12/11	346	8.30	8.60	18.63
12/12	347	8.30	8.60	18.63
12/13	348	8.30	8.60	18.63
12/14	349	8.30	8.60	18.63
12/15	350	8.30	8.60	18.63
12/16	351	8.30	8.60	18.63
12/17	352	8.30	8.60	18.63
12/18	353	8.30	8.60	18.63
12/19	354	8.30	8.60	18.63
12/20	355	8.30	8.60	18.63
12/21	356	8.30	8.60	18.63
12/22	357	8.30	8.60	18.63
12/23	358	8.30	8.60	18.63
12/24	359	8.30	8.60	18.63
12/25	360	8.30	8.60	18.63
12/26	361	8.30	8.60	18.63
12/27	362	8.30	8.60	18.63
12/28	363	8.30	8.60	18.63
12/29	364	8.30	8.60	18.63
12/30	365	8.30	8.60	18.63

calendar date 12/31	ordinal date 366	*Agardhiella* C:N molar ratio 8.30	*Ulva* sp., blade form C:N molar ratio 8.60	*Zostera marina* C:N molar ratio

12 Appendix D – Statistical Results

12.1 *Agardhiella subulata* non-winter C:N molar ratio

Note: X is ordinal date.

Nonlinear Regression   **Sunday, June 04, 2017, 4:55:03 PM**

Data Source: Data 2 in MacrophyteCN.JNB
Equation: Polynomial, Cubic
$f = y_0 + a*x + b*x^2 + c*x^3$

R	**Rsqr**	**Adj Rsqr**	**Standard Error of Estimate**
0.5790	0.3352	0.3036	1.7794

	Coefficient	**Std. Error**	**t**	**P**
y0	2.1855	6.3945	0.3418	0.7337
a	0.0575	0.1069	0.5379	0.5926
b	3.2202E-005	0.0005	0.0589	0.9532
c	-4.6103E-007	8.6619E-007	-0.5322	0.5964

Analysis of Variance:

Analysis of Variance:

	DF	**SS**	**MS**		
Regression	4	7456.1860	1864.0465		
Residual	63	199.4844	3.1664		
Total	67	7655.6704	114.2637		

Corrected for the mean of the observations:

	DF	**SS**	**MS**	**F**	**P**
Regression	3	100.5877	33.5292	10.5890	<0.0001
Residual	63	199.4844	3.1664		
Total	66	300.0721	4.5465		

Statistical Tests:

Normality Test (Shapiro-Wilk)   Failed   (P = 0.0448)

W Statistic= 0.9632   Significance Level = 0.0500

Constant Variance Test   Passed   (P = 0.3797)

1633 **Fit Equation Description:**
1634 [Variables]
1635 x = col(9)
1636 y = col(7)
1637 reciprocal_y = 1/abs(y)
1638 reciprocal_ysquare = 1/y^2
1639 'Automatic Initial Parameter Estimate Functions
1640 F(q)=ape(x,y,3,0,1)
1641 [Parameters]
1642 y0 = F(0)[1] "Auto [[previous: 2.18554]]
1643 a = F(0)[2] "Auto [[previous: 0.0575006]]
1644 b = F(0)[3] "Auto [[previous: 3.22019e-005]]
1645 c = F(0)[4] "Auto [[previous: -4.61028e-007]]
1646 [Equation]
1647 f=y0+a*x+b*x^2+c*x^3
1648 fit f to y
1649 "fit f to y with weight reciprocal_y
1650 "fit f to y with weight reciprocal_ysquare
1651 [Constraints]
1652 [Options]
1653 tolerance=1e-10
1654 stepsize=1
1655 iterations=200
1656
1657 Number of Iterations Performed = 1
1658

1659 ## 12.2 *Ulva* sp., blade form non-winter C:N molar ratio

1660 *Note: X is ordinal date.*

1661 **Nonlinear Regression**   **Sunday, June 04, 2017, 4:51:37 PM**
1662
1663 **Data Source: Copy of Data 2 in MacrophyteCN.JNB**
1664 **Equation: Polynomial, Cubic**
1665 f=y0+a*x+b*x^2+c*x^3
1666
1667
1668 **R   Rsqr   Adj Rsqr   Standard Error of Estimate**
1669
1670 0.5090   0.2591   0.2443   6.6434
1671

	Coefficient	Std. Error	t	P
y0	-3.9563	6.6285	-0.5969	0.5515
a	0.4356	0.1305	3.3375	0.0011
b	-0.0018	0.0008	-2.3526	0.0199
c	2.0453E-006	1.3748E-006	1.4877	0.1389

1678
1679 **Analysis of Variance:**
1680
1681 Analysis of Variance:

	DF	SS	MS

Regression	4	91323.8632	22830.9658		
Residual	150	6620.2800	44.1352		
Total	154	97944.1431	636.0009		

Corrected for the mean of the observations:

	DF	SS	MS	F	P
Regression	3	2315.0402	771.6801	17.4845	<0.0001
Residual	150	6620.2800	44.1352		
Total	153	8935.3202	58.4008		

Statistical Tests:

Normality Test (Shapiro-Wilk)   Failed   (P = 0.0331)

W Statistic= 0.9811   Significance Level = 0.0500

Constant Variance Test   Passed   (P = 0.2539)

Fit Equation Description:
[Variables]
x = col(9)
y = col(7)
reciprocal_y = 1/abs(y)
reciprocal_ysquare = 1/y^2
'Automatic Initial Parameter Estimate Functions
F(q)=ape(x,y,3,0,1)
[Parameters]
y0 = F(0)[1] "Auto [[previous: -3.95632]]
a = F(0)[2] "Auto [[previous: 0.4356]]
b = F(0)[3] "Auto [[previous: -0.00181005]]
c = F(0)[4] "Auto [[previous: 2.04529e-006]]
[Equation]
f=y0+a*x+b*x^2+c*x^3
fit f to y
"fit f to y with weight reciprocal_y
"fit f to y with weight reciprocal_ysquare
[Constraints]
[Options]
tolerance=1e-10
stepsize=1
iterations=200

Number of Iterations Performed = 1

12.3 *Zostera marina* non-winter C:N molar ratio

Nonlinear Regression   **Sunday, February 25, 2018, 9:13:28 AM**

Data Source: Copy of Copy of Data 2 in MacrophyteCN.JNB
Equation: Polynomial, Cubic
f=y0+a*x+b*x^2+c*x^3

1734	R	Rsqr	Adj Rsqr	Standard Error of Estimate
1735				
1736	0.7009	0.4913	0.4747	5.9015

1737		Coefficient	Std. Error	t	P
1738					
1739					
1740	y0	-440.2775	129.8478	-3.3907	0.0010
1741	a	5.6432	1.8002	3.1347	0.0023
1742	b	-0.0214	0.0082	-2.6162	0.0104
1743	c	2.5763E-005	1.2235E-005	2.1057	0.0380

1744
1745 **Analysis of Variance:**
1746
1747 Analysis of Variance:

1748		DF	SS	MS		
1749	Regression	4	109541.3522	27385.3380		
1750	Residual	92	3204.1499	34.8277		
1751	Total	96	112745.5021	1174.4323		

1752
1753 Corrected for the mean of the observations:

1754		DF	SS	MS	F	P
1755	Regression	3	3094.7100	1031.5700	29.6192	<0.0001
1756	Residual	92	3204.1499	34.8277		
1757	Total	95	6298.8599	66.3038		

1758
1759 **Statistical Tests:**
1760
1761 **Normality Test (Shapiro-Wilk)** Passed (P = 0.9494)
1762
1763 W Statistic= 0.9940 Significance Level = 0.0500
1764
1765 **Constant Variance Test** Failed (P = 0.0077)
1766
1767 **Fit Equation Description:**
1768 [Variables]
1769 x = col(9)
1770 y = col(7)
1771 reciprocal_y = 1/abs(y)
1772 reciprocal_ysquare = 1/y^2
1773 'Automatic Initial Parameter Estimate Functions
1774 F(q)=ape(x,y,3,0,1)
1775 [Parameters]
1776 y0 = F(0)[1] "Auto [[previous: -440.278]]
1777 a = F(0)[2] "Auto [[previous: 5.64317]]
1778 b = F(0)[3] "Auto [[previous: -0.0214138]]
1779 c = F(0)[4] "Auto [[previous: 2.5763e-005]]
1780 [Equation]
1781 f=y0+a*x+b*x^2+c*x^3
1782 fit f to y
1783 "fit f to y with weight reciprocal_y
1784 "fit f to y with weight reciprocal_ysquare
1785 [Constraints]
1786 [Options]
1787 tolerance=1e-10

1788   stepsize=1
1789   iterations=200
1790   Number of Iterations Performed = 1
1791

13 Appendix E – Model Box Hypsography Calculations

1792

1793 Following are output from the program Surfer, from which the volume and area at various box depths
1794 were calculated for model boxes. The volume is listed as the "Positive Volume [Cut]". Area is listed as
1795 the "Positive Planar Area".

1796 VOLUME COMPUTATIONS
1797
1798 UPPER SURFACE
1799   Grid File: C:\Users\Vaudrey\Dropbox\bathymetry\Niantic\NRE model
1800 2018\NRbathCCmean_out_UPPER_2018.grd
1801   Grid size as read: 100 cols by 285 rows
1802   Delta X: 17.5590585859
1803   Delta Y: 17.2143333451
1804   X-Range: 229335.0473 to 231073.3941
1805   Y-Range: 54701.06707 to 59589.93774
1806   Z-Range: -0.106743097696 to 7.11382401109
1807
1808 LOWER SURFACE
1809   Level Surface defined by Z = 0
1810
1811 VOLUMES
1812   Approximated Volume by
1813   Trapezoidal Rule: 1946086.13002
1814   Simpson's Rule: 1944194.88825
1815   Simpson's 3/8 Rule: 1946227.0003
1816
1817 CUT & FILL VOLUMES
1818   Positive Volume [Cut]:   1946110.50655
1819   Negative Volume [Fill]:   24.3765256193
1820   Cut minus Fill: 1946086.13002
1821
1822 AREAS
1823   Positive Planar Area
1824   (Upper above Lower):   608589.825729
1825   Negative Planar Area
1826   (Lower above Upper):   25.7608001781
1827   Blanked Planar Area: 7889937.09828
1828   Total Planar Area: 8498552.68481
1829
1830   Positive Surface Area
1831   (Upper above Lower):   609233.011375

1832   Negative Surface Area
1833   (Lower above Upper):   25.8395440627
1834
1835   VOLUME COMPUTATIONS
1836
1837   UPPER SURFACE
1838   Grid File: C:\Users\Vaudrey\Dropbox\bathymetry\Niantic\NRE model
1839   2018\NRbathCCmean_out_UPPER_2018.grd
1840   Grid size as read: 100 cols by 285 rows
1841   Delta X: 17.5590585859
1842   Delta Y: 17.2143333451
1843   X-Range: 229335.0473 to 231073.3941
1844   Y-Range: 54701.06707 to 59589.93774
1845   Z-Range: -0.106743097696 to 7.11382401109
1846
1847   LOWER SURFACE
1848   Level Surface defined by Z = 0.5
1849
1850   VOLUMES
1851   Approximated Volume by
1852   Trapezoidal Rule: 1615405.49845
1853   Simpson's Rule: 1613379.91558
1854   Simpson's 3/8 Rule: 1616382.32725
1855
1856   CUT & FILL VOLUMES
1857   Positive Volume [Cut]:   1626654.01474
1858   Negative Volume [Fill]: 11248.5162899
1859   Cut minus Fill: 1615405.49845
1860
1861   AREAS
1862   Positive Planar Area
1863   (Upper above Lower):   587671.140076
1864   Negative Planar Area
1865   (Lower above Upper):   20944.4464531
1866   Blanked Planar Area: 7889937.09828
1867   Total Planar Area: 8498552.68481
1868
1869   Positive Surface Area
1870   (Upper above Lower):   588300.574776
1871   Negative Surface Area
1872   (Lower above Upper):   20958.2761436
1873
1874   VOLUME COMPUTATIONS
1875
1876   UPPER SURFACE
1877   Grid File: C:\Users\Vaudrey\Dropbox\bathymetry\Niantic\NRE model
1878   2018\NRbathCCmean_out_UPPER_2018.grd

1879   Grid size as read: 100 cols by 285 rows
1880   Delta X: 17.5590585859
1881   Delta Y: 17.2143333451
1882   X-Range: 229335.0473 to 231073.3941
1883   Y-Range: 54701.06707 to 59589.93774
1884   Z-Range: -0.106743097696 to 7.11382401109
1885
1886   LOWER SURFACE
1887   Level Surface defined by Z = 1
1888
1889   VOLUMES
1890   Approximated Volume by
1891   Trapezoidal Rule: 1284724.86689
1892   Simpson's Rule: 1282564.9429
1893   Simpson's 3/8 Rule: 1286537.6542
1894
1895   CUT & FILL VOLUMES
1896   Positive Volume [Cut]: 1330928.87615
1897   Negative Volume [Fill]: 46204.0092697
1898   Cut minus Fill: 1284724.86689
1899
1900   AREAS
1901   Positive Planar Area
1902   (Upper above Lower):   549434.038268
1903   Negative Planar Area
1904   (Lower above Upper):   59181.5482614
1905   Blanked Planar Area: 7889937.09828
1906   Total Planar Area: 8498552.68481
1907
1908   Positive Surface Area
1909   (Upper above Lower):   550014.718271
1910   Negative Surface Area
1911   (Lower above Upper):   59244.1326481
1912
1913   VOLUME COMPUTATIONS
1914
1915   UPPER SURFACE
1916   Grid File: C:\Users\Vaudrey\Dropbox\bathymetry\Niantic\NRE model
1917   2018\NRbathCCmean_out_UPPER_2018.grd
1918   Grid size as read: 100 cols by 285 rows
1919   Delta X: 17.5590585859
1920   Delta Y: 17.2143333451
1921   X-Range: 229335.0473 to 231073.3941
1922   Y-Range: 54701.06707 to 59589.93774
1923   Z-Range: -0.106743097696 to 7.11382401109
1924
1925   LOWER SURFACE

1926	Level Surface defined by Z = 1.5
1927	
1928	VOLUMES
1929	Approximated Volume by
1930	Trapezoidal Rule: 954044.235317
1931	Simpson's Rule: 951749.970228
1932	Simpson's 3/8 Rule: 956692.981152
1933	
1934	CUT & FILL VOLUMES
1935	Positive Volume [Cut]: 1066972.97662
1936	Negative Volume [Fill]: 112928.741301
1937	Cut minus Fill: 954044.235317
1938	
1939	AREAS
1940	Positive Planar Area
1941	(Upper above Lower): 485076.506607
1942	Negative Planar Area
1943	(Lower above Upper): 123539.079922
1944	Blanked Planar Area: 7889937.09828
1945	Total Planar Area: 8498552.68481
1946	
1947	Positive Surface Area
1948	(Upper above Lower): 485587.75343
1949	Negative Surface Area
1950	(Lower above Upper): 123671.097489
1951	
1952	VOLUME COMPUTATIONS
1953	
1954	UPPER SURFACE
1955	Grid File: C:\Users\Vaudrey\Dropbox\bathymetry\Niantic\NRE model
1956	2018\NRbathCCmean_out_UPPER_2018.grd
1957	Grid size as read: 100 cols by 285 rows
1958	Delta X: 17.5590585859
1959	Delta Y: 17.2143333451
1960	X-Range: 229335.0473 to 231073.3941
1961	Y-Range: 54701.06707 to 59589.93774
1962	Z-Range: -0.106743097696 to 7.11382401109
1963	
1964	LOWER SURFACE
1965	Level Surface defined by Z = 2
1966	
1967	VOLUMES
1968	Approximated Volume by
1969	Trapezoidal Rule: 623363.603748
1970	Simpson's Rule: 620934.997554
1971	Simpson's 3/8 Rule: 626848.308105
1972	

```
1973   CUT & FILL VOLUMES
1974          Positive Volume [Cut]:  832014.371205
1975          Negative Volume [Fill]:  208650.767457
1976          Cut minus Fill:  623363.603748
1977
1978   AREAS
1979          Positive Planar Area
1980          (Upper above Lower):  437586.029887
1981          Negative Planar Area
1982          (Lower above Upper):  171029.556642
1983          Blanked Planar Area:  7889937.09828
1984          Total Planar Area:  8498552.68481
1985
1986          Positive Surface Area
1987          (Upper above Lower):  438017.511006
1988          Negative Surface Area
1989          (Lower above Upper):  171241.339913
1990
1991   VOLUME COMPUTATIONS
1992
1993   UPPER SURFACE
1994          Grid File:        C:\Users\Vaudrey\Dropbox\bathymetry\Niantic\NRE model
1995   2018\NRbathCCmean_out_UPPER_2018.grd
1996          Grid size as read:        100 cols by 285 rows
1997          Delta X: 17.5590585859
1998          Delta Y: 17.2143333451
1999          X-Range:        229335.0473 to 231073.3941
2000          Y-Range:        54701.06707 to 59589.93774
2001          Z-Range:        -0.106743097696 to 7.11382401109
2002
2003   LOWER SURFACE
2004          Level Surface defined by Z = 2.5
2005
2006   VOLUMES
2007          Approximated Volume by
2008          Trapezoidal Rule:        292682.97218
2009          Simpson's Rule: 290120.02488
2010          Simpson's 3/8 Rule:        297003.635057
2011
2012   CUT & FILL VOLUMES
2013          Positive Volume [Cut]:  623525.159625
2014          Negative Volume [Fill]:  330842.187446
2015          Cut minus Fill:  292682.97218
2016
2017   AREAS
2018          Positive Planar Area
2019          (Upper above Lower):  384399.547469
```

2020   Negative Planar Area

2021   (Lower above Upper):   224216.03906

2022   Blanked Planar Area: 7889937.09828

2023   Total Planar Area: 8498552.68481

2024

2025   Positive Surface Area

2026   (Upper above Lower):   384748.73674

2027   Negative Surface Area

2028   (Lower above Upper):   224510.11418

2029

2030   VOLUME COMPUTATIONS

2031

2032   UPPER SURFACE

2033   Grid File: C:\Users\Vaudrey\Dropbox\bathymetry\Niantic\NRE model

2034   2018\NRbathCCmean_out_UPPER_2018.grd

2035   Grid size as read: 100 cols by 285 rows

2036   Delta X:17.5590585859

2037   Delta Y:17.2143333451

2038   X-Range: 229335.0473 to 231073.3941

2039   Y-Range: 54701.06707 to 59589.93774

2040   Z-Range: -0.106743097696 to 7.11382401109

2041

2042   LOWER SURFACE

2043   Level Surface defined by Z = 3

2044

2045   VOLUMES

2046   Approximated Volume by

2047   Trapezoidal Rule: -37997.6593889

2048   Simpson's Rule: -40694.9477943

2049   Simpson's 3/8 Rule: -32841.0379911

2050

2051   CUT & FILL VOLUMES

2052   Positive Volume [Cut]: 447810.592183

2053   Negative Volume [Fill]: 485808.251572

2054   Cut minus Fill: -37997.6593889

2055

2056   AREAS

2057   Positive Planar Area

2058   (Upper above Lower):   309019.769831

2059   Negative Planar Area

2060   (Lower above Upper):   299595.816698

2061   Blanked Planar Area: 7889937.09828

2062   Total Planar Area: 8498552.68481

2063

2064   Positive Surface Area

2065   (Upper above Lower):   309291.81243

2066   Negative Surface Area

```
2067            (Lower above Upper):    299967.038489
2068
2069    VOLUME COMPUTATIONS
2070
2071    UPPER SURFACE
2072            Grid File:          C:\Users\Vaudrey\Dropbox\bathymetry\Niantic\NRE model
2073    2018\NRbathCCmean_out_UPPER_2018.grd
2074            Grid size as read:          100 cols by 285 rows
2075            Delta X: 17.5590585859
2076            Delta Y: 17.2143333451
2077            X-Range:          229335.0473 to 231073.3941
2078            Y-Range:          54701.06707 to 59589.93774
2079            Z-Range:          -0.106743097696 to 7.11382401109
2080
2081    LOWER SURFACE
2082            Level Surface defined by Z = 3.5
2083
2084    VOLUMES
2085            Approximated Volume by
2086            Trapezoidal Rule:       -368678.290957
2087            Simpson's Rule: -371509.920468
2088            Simpson's 3/8 Rule:       -362685.711039
2089
2090    CUT & FILL VOLUMES
2091            Positive Volume [Cut]:   305880.973592
2092            Negative Volume [Fill]:  674559.264549
2093            Cut minus Fill:   -368678.290957
2094
2095    AREAS
2096            Positive Planar Area
2097            (Upper above Lower):    253258.222302
2098            Negative Planar Area
2099            (Lower above Upper):    355357.364227
2100            Blanked Planar Area:     7889937.09828
2101            Total Planar Area:       8498552.68481
2102
2103            Positive Surface Area
2104            (Upper above Lower):    253461.424742
2105            Negative Surface Area
2106            (Lower above Upper):    355797.426178
2107
2108    VOLUME COMPUTATIONS
2109
2110    UPPER SURFACE
2111            Grid File:          C:\Users\Vaudrey\Dropbox\bathymetry\Niantic\NRE model
2112    2018\NRbathCCmean_out_UPPER_2018.grd
2113            Grid size as read:          100 cols by 285 rows
```

2114	Delta X: 17.5590585859
2115	Delta Y: 17.2143333451
2116	X-Range:	229335.0473 to 231073.3941
2117	Y-Range:	54701.06707 to 59589.93774
2118	Z-Range:	-0.106743097696 to 7.11382401109
2119	
2120	LOWER SURFACE
2121	Level Surface defined by Z = 4
2122	
2123	VOLUMES
2124	Approximated Volume by
2125	Trapezoidal Rule:	-699358.922526
2126	Simpson's Rule: -702324.893143
2127	Simpson's 3/8 Rule:	-692530.384087
2128	
2129	CUT & FILL VOLUMES
2130	Positive Volume [Cut]:	189516.305145
2131	Negative Volume [Fill]:	888875.227671
2132	Cut minus Fill:	-699358.922526
2133	
2134	AREAS
2135	Positive Planar Area
2136	(Upper above Lower):	206388.339232
2137	Negative Planar Area
2138	(Lower above Upper):	402227.247297
2139	Blanked Planar Area:	7889937.09828
2140	Total Planar Area:	8498552.68481
2141	
2142	Positive Surface Area
2143	(Upper above Lower):	206528.7256
2144	Negative Surface Area
2145	(Lower above Upper):	402730.125319
2146	
2147	VOLUME COMPUTATIONS
2148	
2149	UPPER SURFACE
2150	Grid File:	C:\Users\Vaudrey\Dropbox\bathymetry\Niantic\NRE model
2151	2018\NRbathCCmean_out_UPPER_2018.grd
2152	Grid size as read:	100 cols by 285 rows
2153	Delta X: 17.5590585859
2154	Delta Y: 17.2143333451
2155	X-Range:	229335.0473 to 231073.3941
2156	Y-Range:	54701.06707 to 59589.93774
2157	Z-Range:	-0.106743097696 to 7.11382401109
2158	
2159	LOWER SURFACE
2160	Level Surface defined by Z = 4.5

2161
2162   VOLUMES
2163   Approximated Volume by
2164   Trapezoidal Rule: -1030039.55409
2165   Simpson's Rule: -1033139.86582
2166   Simpson's 3/8 Rule: -1022375.05713
2167
2168   CUT & FILL VOLUMES
2169   Positive Volume [Cut]:   95713.0994418
2170   Negative Volume [Fill]: 1125752.65354
2171   Cut minus Fill: -1030039.55409
2172
2173   AREAS
2174   Positive Planar Area
2175   (Upper above Lower):   161880.90723
2176   Negative Planar Area
2177   (Lower above Upper):   446734.679299
2178   Blanked Planar Area: 7889937.09828
2179   Total Planar Area: 8498552.68481
2180
2181   Positive Surface Area
2182   (Upper above Lower):   161967.161141
2183   Negative Surface Area
2184   (Lower above Upper):   447291.689778
2185
2186   VOLUME COMPUTATIONS
2187
2188   UPPER SURFACE
2189   Grid File: C:\Users\Vaudrey\Dropbox\bathymetry\Niantic\NRE model
2190   2018\NRbathCCmean_out_UPPER_2018.grd
2191   Grid size as read: 100 cols by 285 rows
2192   Delta X: 17.5590585859
2193   Delta Y: 17.2143333451
2194   X-Range: 229335.0473 to 231073.3941
2195   Y-Range: 54701.06707 to 59589.93774
2196   Z-Range: -0.106743097696 to 7.11382401109
2197
2198   LOWER SURFACE
2199   Level Surface defined by Z = 5
2200
2201   VOLUMES
2202   Approximated Volume by
2203   Trapezoidal Rule: -1360720.18566
2204   Simpson's Rule: -1363954.83849
2205   Simpson's 3/8 Rule: -1352219.73018
2206
2207   CUT & FILL VOLUMES

2208		Positive Volume [Cut]:	29683.7191839
2209		Negative Volume [Fill]:	1390403.90485
2210		Cut minus Fill:	-1360720.18566
2211			
2212	AREAS		
2213		Positive Planar Area	
2214		(Upper above Lower):	92279.1236833
2215		Negative Planar Area	
2216		(Lower above Upper):	516336.462846
2217		Blanked Planar Area:	7889937.09828
2218		Total Planar Area:	8498552.68481
2219			
2220		Positive Surface Area	
2221		(Upper above Lower):	92323.7727569
2222		Negative Surface Area	
2223		(Lower above Upper):	516935.078163
2224			
2225	VOLUME COMPUTATIONS		
2226			
2227	UPPER SURFACE		
2228		Grid File:	C:\Users\Vaudrey\Dropbox\bathymetry\Niantic\NRE model
2229	2018\NRbathCCmean_out_UPPER_2018.grd		
2230		Grid size as read:	100 cols by 285 rows
2231		Delta X: 17.5590585859	
2232		Delta Y: 17.2143333451	
2233		X-Range:	229335.0473 to 231073.3941
2234		Y-Range:	54701.06707 to 59589.93774
2235		Z-Range:	-0.106743097696 to 7.11382401109
2236			
2237	LOWER SURFACE		
2238		Level Surface defined by Z = 5.5	
2239			
2240	VOLUMES		
2241		Approximated Volume by	
2242		Trapezoidal Rule:	-1691400.81723
2243		Simpson's Rule: -1694769.81117	
2244		Simpson's 3/8 Rule:	-1682064.40323
2245			
2246	CUT & FILL VOLUMES		
2247		Positive Volume [Cut]:	5864.13679473
2248		Negative Volume [Fill]:	1697264.95403
2249		Cut minus Fill:	-1691400.81723
2250			
2251	AREAS		
2252		Positive Planar Area	
2253		(Upper above Lower):	17472.2188078
2254		Negative Planar Area	

2255	(Lower above Upper):	591143.367722
2256	Blanked Planar Area:	7889937.09828
2257	Total Planar Area:	8498552.68481
2258		
2259	Positive Surface Area	
2260	(Upper above Lower):	17490.3829213
2261	Negative Surface Area	
2262	(Lower above Upper):	591768.467998
2263		
2264	VOLUME COMPUTATIONS	
2265		
2266	UPPER SURFACE	
2267	Grid File:	C:\Users\Vaudrey\Dropbox\bathymetry\Niantic\NRE model
2268	2018\NRbathCCmean_out_UPPER_2018.grd	
2269	Grid size as read:	100 cols by 285 rows
2270	Delta X: 17.5590585859	
2271	Delta Y: 17.2143333451	
2272	X-Range:	229335.0473 to 231073.3941
2273	Y-Range:	54701.06707 to 59589.93774
2274	Z-Range:	-0.106743097696 to 7.11382401109
2275		
2276	LOWER SURFACE	
2277	Level Surface defined by Z = 6	
2278		
2279	VOLUMES	
2280	Approximated Volume by	
2281	Trapezoidal Rule:	-2022081.4488
2282	Simpson's Rule: -2025584.78384	
2283	Simpson's 3/8 Rule:	-2011909.07628
2284		
2285	CUT & FILL VOLUMES	
2286	Positive Volume [Cut]:	1233.98848933
2287	Negative Volume [Fill]:	2023315.43729
2288	Cut minus Fill: -2022081.4488	
2289		
2290	AREAS	
2291	Positive Planar Area	
2292	(Upper above Lower):	3501.76497884
2293	Negative Planar Area	
2294	(Lower above Upper):	605113.821551
2295	Blanked Planar Area:	7889937.09828
2296	Total Planar Area:	8498552.68481
2297		
2298	Positive Surface Area	
2299	(Upper above Lower):	3508.44204028
2300	Negative Surface Area	

2301	(Lower above Upper): 605750.408879
2302	
2303	
2304	VOLUME COMPUTATIONS
2305	
2306	UPPER SURFACE
2307	Grid File: C:\Users\Vaudrey\Dropbox\bathymetry\Niantic\NRE model
2308	2018\NRbathCCmean_out_MID_2018.grd
2309	Grid size as read: 100 cols by 285 rows
2310	Delta X: 17.5590585859
2311	Delta Y: 17.2143333451
2312	X-Range: 229335.0473 to 231073.3941
2313	Y-Range: 54701.06707 to 59589.93774
2314	Z-Range: -0.0566458832731 to 6.710455571
2315	
2316	LOWER SURFACE
2317	Level Surface defined by Z = 0
2318	
2319	VOLUMES
2320	Approximated Volume by
2321	Trapezoidal Rule: 2880061.05517
2322	Simpson's Rule: 2879341.25147
2323	Simpson's 3/8 Rule: 2880165.85919
2324	
2325	CUT & FILL VOLUMES
2326	Positive Volume [Cut]: 2880127.32452
2327	Negative Volume [Fill]: 66.2693513709
2328	Cut minus Fill: 2880061.05517
2329	
2330	AREAS
2331	Positive Planar Area
2332	(Upper above Lower): 917857.378046
2333	Negative Planar Area
2334	(Lower above Upper): 4965.26197137
2335	Blanked Planar Area: 7575730.04479
2336	Total Planar Area: 8498552.68481
2337	
2338	Positive Surface Area
2339	(Upper above Lower): 918237.092028
2340	Negative Surface Area
2341	(Lower above Upper): 4965.31459899
2342	
2343	VOLUME COMPUTATIONS
2344	
2345	UPPER SURFACE

2346   Grid File: C:\Users\Vaudrey\Dropbox\bathymetry\Niantic\NRE model
2347   2018\NRbathCCmean_out_MID_2018.grd
2348   Grid size as read: 100 cols by 285 rows
2349   Delta X: 17.5590585859
2350   Delta Y: 17.2143333451
2351   X-Range: 229335.0473 to 231073.3941
2352   Y-Range: 54701.06707 to 59589.93774
2353   Z-Range: -0.0566458832731 to 6.710455571
2354
2355   LOWER SURFACE
2356   Level Surface defined by Z = 0.5
2357
2358   VOLUMES
2359   Approximated Volume by
2360   Trapezoidal Rule: 2391899.0625
2361   Simpson's Rule: 2390843.40603
2362   Simpson's 3/8 Rule: 2391597.69459
2363
2364   CUT & FILL VOLUMES
2365   Positive Volume [Cut]:   2408044.56755
2366   Negative Volume [Fill]:   16145.5050508
2367   Cut minus Fill: 2391899.0625
2368
2369   AREAS
2370   Positive Planar Area
2371   (Upper above Lower):   897495.838806
2372   Negative Planar Area
2373   (Lower above Upper):   25326.8012111
2374   Blanked Planar Area: 7575730.04479
2375   Total Planar Area: 8498552.68481
2376
2377   Positive Surface Area
2378   (Upper above Lower):   897864.274056
2379   Negative Surface Area
2380   (Lower above Upper):   25338.1325713
2381
2382   VOLUME COMPUTATIONS
2383
2384   UPPER SURFACE
2385   Grid File: C:\Users\Vaudrey\Dropbox\bathymetry\Niantic\NRE model
2386   2018\NRbathCCmean_out_MID_2018.grd
2387   Grid size as read: 100 cols by 285 rows
2388   Delta X: 17.5590585859
2389   Delta Y: 17.2143333451
2390   X-Range: 229335.0473 to 231073.3941
2391   Y-Range: 54701.06707 to 59589.93774
2392   Z-Range: -0.0566458832731 to 6.710455571

2393
2394   LOWER SURFACE
2395   Level Surface defined by Z = 1
2396
2397   VOLUMES
2398   Approximated Volume by
2399   Trapezoidal Rule: 1903737.06983
2400   Simpson's Rule: 1902345.56059
2401   Simpson's 3/8 Rule: 1903029.52998
2402
2403   CUT & FILL VOLUMES
2404   Positive Volume [Cut]:   1955424.41304
2405   Negative Volume [Fill]: 51687.343217
2406   Cut minus Fill: 1903737.06983
2407
2408   AREAS
2409   Positive Planar Area
2410   (Upper above Lower):   865215.118635
2411   Negative Planar Area
2412   (Lower above Upper):   57607.5213819
2413   Blanked Planar Area: 7575730.04479
2414   Total Planar Area: 8498552.68481
2415
2416   Positive Surface Area
2417   (Upper above Lower):   865548.907176
2418   Negative Surface Area
2419   (Lower above Upper):   57653.4994507
2420
2421   VOLUME COMPUTATIONS
2422
2423   UPPER SURFACE
2424   Grid File: C:\Users\Vaudrey\Dropbox\bathymetry\Niantic\NRE model
2425   2018\NRbathCCmean_out_MID_2018.grd
2426   Grid size as read: 100 cols by 285 rows
2427   Delta X: 17.5590585859
2428   Delta Y: 17.2143333451
2429   X-Range: 229335.0473 to 231073.3941
2430   Y-Range: 54701.06707 to 59589.93774
2431   Z-Range: -0.0566458832731 to 6.710455571
2432
2433   LOWER SURFACE
2434   Level Surface defined by Z = 1.5
2435
2436   VOLUMES
2437   Approximated Volume by
2438   Trapezoidal Rule: 1415575.07716
2439   Simpson's Rule: 1413847.71516

2440   Simpson's 3/8 Rule: 1414461.36537
2441
2442   CUT & FILL VOLUMES
2443   Positive Volume [Cut]: 1525704.21346
2444   Negative Volume [Fill]: 110129.136299
2445   Cut minus Fill: 1415575.07716
2446
2447   AREAS
2448   Positive Planar Area
2449   (Upper above Lower): 822835.421387
2450   Negative Planar Area
2451   (Lower above Upper): 99987.2186296
2452   Blanked Planar Area: 7575730.04479
2453   Total Planar Area: 8498552.68481
2454
2455   Positive Surface Area
2456   (Upper above Lower): 823117.143809
2457   Negative Surface Area
2458   (Lower above Upper): 100085.262818
2459
2460   VOLUME COMPUTATIONS
2461
2462   UPPER SURFACE
2463   Grid File: C:\Users\Vaudrey\Dropbox\bathymetry\Niantic\NRE model
2464   2018\NRbathCCmean_out_MID_2018.grd
2465   Grid size as read: 100 cols by 285 rows
2466   Delta X: 17.5590585859
2467   Delta Y: 17.2143333451
2468   X-Range: 229335.0473 to 231073.3941
2469   Y-Range: 54701.06707 to 59589.93774
2470   Z-Range: -0.0566458832731 to 6.710455571
2471
2472   LOWER SURFACE
2473   Level Surface defined by Z = 2
2474
2475   VOLUMES
2476   Approximated Volume by
2477   Trapezoidal Rule: 927413.084484
2478   Simpson's Rule: 925349.869722
2479   Simpson's 3/8 Rule: 925893.20076
2480
2481   CUT & FILL VOLUMES
2482   Positive Volume [Cut]: 1122121.61887
2483   Negative Volume [Fill]: 194708.534382
2484   Cut minus Fill: 927413.084484
2485
2486   AREAS

2487	Positive Planar Area	
2488	(Upper above Lower):	762942.291929
2489	Negative Planar Area	
2490	(Lower above Upper):	159880.348088
2491	Blanked Planar Area:	7575730.04479
2492	Total Planar Area:	8498552.68481
2493		
2494	Positive Surface Area	
2495	(Upper above Lower):	763164.09629
2496	Negative Surface Area	
2497	(Lower above Upper):	160038.310337
2498		
2499	VOLUME COMPUTATIONS	
2500		
2501	UPPER SURFACE	
2502	Grid File:	C:\Users\Vaudrey\Dropbox\bathymetry\Niantic\NRE model
2503	2018\NRbathCCmean_out_MID_2018.grd	
2504	Grid size as read:	100 cols by 285 rows
2505	Delta X: 17.5590585859	
2506	Delta Y: 17.2143333451	
2507	X-Range:	229335.0473 to 231073.3941
2508	Y-Range:	54701.06707 to 59589.93774
2509	Z-Range:	-0.0566458832731 to 6.710455571
2510		
2511	LOWER SURFACE	
2512	Level Surface defined by Z = 2.5	
2513		
2514	VOLUMES	
2515	Approximated Volume by	
2516	Trapezoidal Rule:	439251.091812
2517	Simpson's Rule: 436852.024286	
2518	Simpson's 3/8 Rule:	437325.036152
2519		
2520	CUT & FILL VOLUMES	
2521	Positive Volume [Cut]:	759604.858315
2522	Negative Volume [Fill]:	320353.766503
2523	Cut minus Fill:	439251.091812
2524		
2525	AREAS	
2526	Positive Planar Area	
2527	(Upper above Lower):	672668.084765
2528	Negative Planar Area	
2529	(Lower above Upper):	250154.555252
2530	Blanked Planar Area:	7575730.04479
2531	Total Planar Area:	8498552.68481
2532		
2533	Positive Surface Area	

2534	(Upper above Lower): 672831.974334
2535	Negative Surface Area
2536	(Lower above Upper): 250370.432293
2537	
2538	VOLUME COMPUTATIONS
2539	
2540	UPPER SURFACE
2541	Grid File: C:\Users\Vaudrey\Dropbox\bathymetry\Niantic\NRE model
2542	2018\NRbathCCmean_out_MID_2018.grd
2543	Grid size as read: 100 cols by 285 rows
2544	Delta X: 17.5590585859
2545	Delta Y: 17.2143333451
2546	X-Range: 229335.0473 to 231073.3941
2547	Y-Range: 54701.06707 to 59589.93774
2548	Z-Range: -0.0566458832731 to 6.710455571
2549	
2550	LOWER SURFACE
2551	Level Surface defined by Z = 3
2552	
2553	VOLUMES
2554	Approximated Volume by
2555	Trapezoidal Rule: -48910.90086
2556	Simpson's Rule: -51645.8211502
2557	Simpson's 3/8 Rule: -51243.1284568
2558	
2559	CUT & FILL VOLUMES
2560	Positive Volume [Cut]: 447847.123755
2561	Negative Volume [Fill]: 496758.024615
2562	Cut minus Fill: -48910.90086
2563	
2564	AREAS
2565	Positive Planar Area
2566	(Upper above Lower): 551960.430792
2567	Negative Planar Area
2568	(Lower above Upper): 370862.209225
2569	Blanked Planar Area: 7575730.04479
2570	Total Planar Area: 8498552.68481
2571	
2572	Positive Surface Area
2573	(Upper above Lower): 552074.55412
2574	Negative Surface Area
2575	(Lower above Upper): 371127.852508
2576	
2577	VOLUME COMPUTATIONS
2578	
2579	UPPER SURFACE

2580   Grid File: C:\Users\Vaudrey\Dropbox\bathymetry\Niantic\NRE model
2581   2018\NRbathCCmean_out_MID_2018.grd
2582   Grid size as read: 100 cols by 285 rows
2583   Delta X: 17.5590585859
2584   Delta Y: 17.2143333451
2585   X-Range: 229335.0473 to 231073.3941
2586   Y-Range: 54701.06707 to 59589.93774
2587   Z-Range: -0.0566458832731 to 6.710455571
2588
2589   LOWER SURFACE
2590   Level Surface defined by Z = 3.5
2591
2592   VOLUMES
2593   Approximated Volume by
2594   Trapezoidal Rule: -537072.893532
2595   Simpson's Rule: -540143.666586
2596   Simpson's 3/8 Rule: -539811.293065
2597
2598   CUT & FILL VOLUMES
2599   Positive Volume [Cut]:   220657.658516
2600   Negative Volume [Fill]: 757730.552048
2601   Cut minus Fill: -537072.893532
2602
2603   AREAS
2604   Positive Planar Area
2605   (Upper above Lower): 355274.393694
2606   Negative Planar Area
2607   (Lower above Upper): 567548.246323
2608   Blanked Planar Area: 7575730.04479
2609   Total Planar Area: 8498552.68481
2610
2611   Positive Surface Area
2612   (Upper above Lower): 355348.867051
2613   Negative Surface Area
2614   (Lower above Upper): 567853.539576
2615
2616   VOLUME COMPUTATIONS
2617
2618   UPPER SURFACE
2619   Grid File: C:\Users\Vaudrey\Dropbox\bathymetry\Niantic\NRE model
2620   2018\NRbathCCmean_out_MID_2018.grd
2621   Grid size as read: 100 cols by 285 rows
2622   Delta X: 17.5590585859
2623   Delta Y: 17.2143333451
2624   X-Range: 229335.0473 to 231073.3941
2625   Y-Range: 54701.06707 to 59589.93774
2626   Z-Range: -0.0566458832731 to 6.710455571

2627
2628   LOWER SURFACE
2629   Level Surface defined by Z = 4
2630
2631   VOLUMES
2632   Approximated Volume by
2633   Trapezoidal Rule: -1025234.8862
2634   Simpson's Rule: -1028641.51202
2635   Simpson's 3/8 Rule: -1028379.45767
2636
2637   CUT & FILL VOLUMES
2638   Positive Volume [Cut]:   95989.9780408
2639   Negative Volume [Fill]:   1121224.86424
2640   Cut minus Fill: -1025234.8862
2641
2642   AREAS
2643   Positive Planar Area
2644   (Upper above Lower):   152547.292398
2645   Negative Planar Area
2646   (Lower above Upper):   770275.347619
2647   Blanked Planar Area: 7575730.04479
2648   Total Planar Area: 8498552.68481
2649
2650   Positive Surface Area
2651   (Upper above Lower):   152592.475451
2652   Negative Surface Area
2653   (Lower above Upper):   770609.931176
2654
2655   VOLUME COMPUTATIONS
2656
2657   UPPER SURFACE
2658   Grid File: C:\Users\Vaudrey\Dropbox\bathymetry\Niantic\NRE model
2659   2018\NRbathCCmean_out_MID_2018.grd
2660   Grid size as read: 100 cols by 285 rows
2661   Delta X: 17.5590585859
2662   Delta Y: 17.2143333451
2663   X-Range: 229335.0473 to 231073.3941
2664   Y-Range: 54701.06707 to 59589.93774
2665   Z-Range: -0.0566458832731 to 6.710455571
2666
2667   LOWER SURFACE
2668   Level Surface defined by Z = 4.5
2669
2670   VOLUMES
2671   Approximated Volume by
2672   Trapezoidal Rule: -1513396.87888
2673   Simpson's Rule: -1517139.35746

| 2674 | Simpson's 3/8 Rule: | -1516947.62228 |

2675

2676 CUT & FILL VOLUMES
2677   Positive Volume [Cut]: 43340.2501048
2678   Negative Volume [Fill]: 1556737.12898
2679   Cut minus Fill: -1513396.87888

2680

2681 AREAS
2682   Positive Planar Area
2683   (Upper above Lower): 67672.9035464
2684   Negative Planar Area
2685   (Lower above Upper): 855149.736471
2686   Blanked Planar Area: 7575730.04479
2687   Total Planar Area: 8498552.68481

2688

2689   Positive Surface Area
2690   (Upper above Lower): 67700.4865589
2691   Negative Surface Area
2692   (Lower above Upper): 855501.920068

2693

2694 VOLUME COMPUTATIONS

2695

2696 UPPER SURFACE
2697   Grid File: C:\Users\Vaudrey\Dropbox\bathymetry\Niantic\NRE model
2698 2018\NRbathCCmean_out_MID_2018.grd
2699   Grid size as read: 100 cols by 285 rows
2700   Delta X: 17.5590585859
2701   Delta Y: 17.2143333451
2702   X-Range: 229335.0473 to 231073.3941
2703   Y-Range: 54701.06707 to 59589.93774
2704   Z-Range: -0.0566458832731 to 6.710455571

2705

2706 LOWER SURFACE
2707   Level Surface defined by Z = 5

2708

2709 VOLUMES
2710   Approximated Volume by
2711   Trapezoidal Rule: -2001558.87155
2712   Simpson's Rule: -2005637.20289
2713   Simpson's 3/8 Rule: -2005515.78689

2714

2715 CUT & FILL VOLUMES
2716   Positive Volume [Cut]: 16585.6928057
2717   Negative Volume [Fill]: 2018144.56435
2718   Cut minus Fill: -2001558.87155

2719

2720 AREAS

2721	Positive Planar Area	
2722	(Upper above Lower):	37935.7566796
2723	Negative Planar Area	
2724	(Lower above Upper):	884886.883338
2725	Blanked Planar Area:	7575730.04479
2726	Total Planar Area:	8498552.68481
2727		
2728	Positive Surface Area	
2729	(Upper above Lower):	37950.7750565
2730	Negative Surface Area	
2731	(Lower above Upper):	885251.631571
2732		
2733	VOLUME COMPUTATIONS	
2734		
2735	UPPER SURFACE	
2736	Grid File:	C:\Users\Vaudrey\Dropbox\bathymetry\Niantic\NRE model
2737	2018\NRbathCCmean_out_MID_2018.grd	
2738	Grid size as read:	100 cols by 285 rows
2739	Delta X: 17.5590585859	
2740	Delta Y: 17.2143333451	
2741	X-Range:	229335.0473 to 231073.3941
2742	Y-Range:	54701.06707 to 59589.93774
2743	Z-Range:	-0.0566458832731 to 6.710455571
2744		
2745	LOWER SURFACE	
2746	Level Surface defined by Z = 5.5	
2747		
2748	VOLUMES	
2749	Approximated Volume by	
2750	Trapezoidal Rule:	-2489720.86422
2751	Simpson's Rule: -2494135.04833	
2752	Simpson's 3/8 Rule:	-2494083.9515
2753		
2754	CUT & FILL VOLUMES	
2755	Positive Volume [Cut]:	3885.94312719
2756	Negative Volume [Fill]:	2493606.80735
2757	Cut minus Fill:	-2489720.86422
2758		
2759	AREAS	
2760	Positive Planar Area	
2761	(Upper above Lower):	12727.1708714
2762	Negative Planar Area	
2763	(Lower above Upper):	910095.469146
2764	Blanked Planar Area:	7575730.04479
2765	Total Planar Area:	8498552.68481
2766		
2767	Positive Surface Area	

2768   (Upper above Lower):   12733.8573727
2769   Negative Surface Area
2770   (Lower above Upper):   910468.549254
2771
2772 VOLUME COMPUTATIONS
2773
2774 UPPER SURFACE
2775   Grid File: C:\Users\Vaudrey\Dropbox\bathymetry\Niantic\NRE model
2776 2018\NRbathCCmean_out_MID_2018.grd
2777   Grid size as read: 100 cols by 285 rows
2778   Delta X: 17.5590585859
2779   Delta Y: 17.2143333451
2780   X-Range: 229335.0473 to 231073.3941
2781   Y-Range: 54701.06707 to 59589.93774
2782   Z-Range: -0.0566458832731 to 6.710455571
2783
2784 LOWER SURFACE
2785   Level Surface defined by Z = 6
2786
2787 VOLUMES
2788   Approximated Volume by
2789   Trapezoidal Rule: -2977882.85689
2790   Simpson's Rule: -2982632.89377
2791   Simpson's 3/8 Rule: -2982652.11611
2792
2793 CUT & FILL VOLUMES
2794   Positive Volume [Cut]:   418.474738025
2795   Negative Volume [Fill]: 2978301.33163
2796   Cut minus Fill: -2977882.85689
2797
2798 AREAS
2799   Positive Planar Area
2800   (Upper above Lower):   2204.75259987
2801   Negative Planar Area
2802   (Lower above Upper):   920617.887417
2803   Blanked Planar Area: 7575730.04479
2804   Total Planar Area: 8498552.68481
2805
2806   Positive Surface Area
2807   (Upper above Lower):   2207.01150309
2808   Negative Surface Area
2809   (Lower above Upper):   920995.395124
2810
2811
2812 VOLUME COMPUTATIONS
2813

```
2814   UPPER SURFACE
2815        Grid File:        C:\Users\Vaudrey\Dropbox\bathymetry\Niantic\NRE model
2816   2018\NRbathCCmean_out_LOWER_2018.grd
2817        Grid size as read:        100 cols by 285 rows
2818        Delta X: 17.5590585859
2819        Delta Y: 17.2143333451
2820        X-Range:        229335.0473 to 231073.3941
2821        Y-Range:        54701.06707 to 59589.93774
2822        Z-Range:        -0.119693311644 to 4.16498545386
2823
2824   LOWER SURFACE
2825        Level Surface defined by Z = 0
2826
2827   VOLUMES
2828        Approximated Volume by
2829        Trapezoidal Rule:        2131303.13199
2830        Simpson's Rule: 2131870.03508
2831        Simpson's 3/8 Rule:        2129842.19271
2832
2833   CUT & FILL VOLUMES
2834        Positive Volume [Cut]:  2131341.0067
2835        Negative Volume [Fill]:  37.8747111329
2836        Cut minus Fill:   2131303.13199
2837
2838   AREAS
2839        Positive Planar Area
2840        (Upper above Lower):  1403335.9004
2841        Negative Planar Area
2842        (Lower above Upper):  243.178838157
2843        Blanked Planar Area:  7094973.60557
2844        Total Planar Area:  8498552.68481
2845
2846        Positive Surface Area
2847        (Upper above Lower):  1403711.84297
2848        Negative Surface Area
2849        (Lower above Upper):  243.2028634
2850
2851   VOLUME COMPUTATIONS
2852
2853   UPPER SURFACE
2854        Grid File:        C:\Users\Vaudrey\Dropbox\bathymetry\Niantic\NRE model
2855   2018\NRbathCCmean_out_LOWER_2018.grd
2856        Grid size as read:        100 cols by 285 rows
2857        Delta X: 17.5590585859
2858        Delta Y: 17.2143333451
2859        X-Range:        229335.0473 to 231073.3941
2860        Y-Range:        54701.06707 to 59589.93774
```

2861   Z-Range: -0.119693311644 to 4.16498545386
2862
2863 LOWER SURFACE
2864   Level Surface defined by Z = 0.5
2865
2866 VOLUMES
2867   Approximated Volume by
2868   Trapezoidal Rule: 1393014.79323
2869   Simpson's Rule: 1393161.88036
2870   Simpson's 3/8 Rule: 1391612.89056
2871
2872 CUT & FILL VOLUMES
2873   Positive Volume [Cut]: 1423642.70029
2874   Negative Volume [Fill]: 30627.9070607
2875   Cut minus Fill: 1393014.79323
2876
2877 AREAS
2878   Positive Planar Area
2879   (Upper above Lower): 1327996.3562
2880   Negative Planar Area
2881   (Lower above Upper): 75582.7230357
2882   Blanked Planar Area: 7094973.60557
2883   Total Planar Area: 8498552.68481
2884
2885   Positive Surface Area
2886   (Upper above Lower): 1328356.29255
2887   Negative Surface Area
2888   (Lower above Upper): 75598.7532807
2889
2890 VOLUME COMPUTATIONS
2891
2892 UPPER SURFACE
2893   Grid File: C:\Users\Vaudrey\Dropbox\bathymetry\Niantic\NRE model
2894 2018\NRbathCCmean_out_LOWER_2018.grd
2895   Grid size as read: 100 cols by 285 rows
2896   Delta X: 17.5590585859
2897   Delta Y: 17.2143333451
2898   X-Range: 229335.0473 to 231073.3941
2899   Y-Range: 54701.06707 to 59589.93774
2900   Z-Range: -0.119693311644 to 4.16498545386
2901
2902 LOWER SURFACE
2903   Level Surface defined by Z = 1
2904
2905 VOLUMES
2906   Approximated Volume by
2907   Trapezoidal Rule: 654726.454469

2908   Simpson's Rule: 654453.725642
2909   Simpson's 3/8 Rule: 653383.588418
2910
2911 CUT & FILL VOLUMES
2912   Positive Volume [Cut]: 775672.59286
2913   Negative Volume [Fill]: 120946.138391
2914   Cut minus Fill: 654726.454469
2915
2916 AREAS
2917   Positive Planar Area
2918   (Upper above Lower): 1197081.0468
2919   Negative Planar Area
2920   (Lower above Upper): 206498.032438
2921   Blanked Planar Area: 7094973.60557
2922   Total Planar Area: 8498552.68481
2923
2924   Positive Surface Area
2925   (Upper above Lower): 1197400.74145
2926   Negative Surface Area
2927   (Lower above Upper): 206554.30438
2928
2929 VOLUME COMPUTATIONS
2930
2931 UPPER SURFACE
2932   Grid File: C:\Users\Vaudrey\Dropbox\bathymetry\Niantic\NRE model
2933 2018\NRbathCCmean_out_LOWER_2018.grd
2934   Grid size as read: 100 cols by 285 rows
2935   Delta X: 17.5590585859
2936   Delta Y: 17.2143333451
2937   X-Range: 229335.0473 to 231073.3941
2938   Y-Range: 54701.06707 to 59589.93774
2939   Z-Range: -0.119693311644 to 4.16498545386
2940
2941 LOWER SURFACE
2942   Level Surface defined by Z = 1.5
2943
2944 VOLUMES
2945   Approximated Volume by
2946   Trapezoidal Rule: -83561.8842938
2947   Simpson's Rule: -84254.4290752
2948   Simpson's 3/8 Rule: -84845.7137261
2949
2950 CUT & FILL VOLUMES
2951   Positive Volume [Cut]: 322873.298372
2952   Negative Volume [Fill]: 406435.182666
2953   Cut minus Fill: -83561.8842938
2954

2955	AREAS
2956	Positive Planar Area
2957	(Upper above Lower):	538895.866977
2958	Negative Planar Area
2959	(Lower above Upper):	864683.212263
2960	Blanked Planar Area:	7094973.60557
2961	Total Planar Area:	8498552.68481
2962
2963	Positive Surface Area
2964	(Upper above Lower):	539153.501851
2965	Negative Surface Area
2966	(Lower above Upper):	864801.543979
2967
2968	VOLUME COMPUTATIONS
2969
2970	UPPER SURFACE
2971	Grid File:	C:\Users\Vaudrey\Dropbox\bathymetry\Niantic\NRE model
2972	2018\NRbathCCmean_out_LOWER_2018.grd
2973	Grid size as read:	100 cols by 285 rows
2974	Delta X: 17.5590585859
2975	Delta Y: 17.2143333451
2976	X-Range:	229335.0473 to 231073.3941
2977	Y-Range:	54701.06707 to 59589.93774
2978	Z-Range:	-0.119693311644 to 4.16498545386
2979
2980	LOWER SURFACE
2981	Level Surface defined by Z = 2
2982
2983	VOLUMES
2984	Approximated Volume by
2985	Trapezoidal Rule:	-821850.223056
2986	Simpson's Rule: -822962.583793
2987	Simpson's 3/8 Rule:	-823075.01587
2988
2989	CUT & FILL VOLUMES
2990	Positive Volume [Cut]:	150530.179633
2991	Negative Volume [Fill]:	972380.402689
2992	Cut minus Fill:	-821850.223056
2993
2994	AREAS
2995	Positive Planar Area
2996	(Upper above Lower):	225236.170104
2997	Negative Planar Area
2998	(Lower above Upper):	1178342.90914
2999	Blanked Planar Area:	7094973.60557
3000	Total Planar Area:	8498552.68481
3001

3002   Positive Surface Area
3003   (Upper above Lower):   225415.276274
3004   Negative Surface Area
3005   (Lower above Upper):   1178539.76956
3006
3007   VOLUME COMPUTATIONS
3008
3009   UPPER SURFACE
3010   Grid File: C:\Users\Vaudrey\Dropbox\bathymetry\Niantic\NRE model
3011   2018\NRbathCCmean_out_LOWER_2018.grd
3012   Grid size as read: 100 cols by 285 rows
3013   Delta X: 17.5590585859
3014   Delta Y: 17.2143333451
3015   X-Range: 229335.0473 to 231073.3941
3016   Y-Range: 54701.06707 to 59589.93774
3017   Z-Range: -0.119693311644 to 4.16498545386
3018
3019   LOWER SURFACE
3020   Level Surface defined by Z = 2.5
3021
3022   VOLUMES
3023   Approximated Volume by
3024   Trapezoidal Rule: -1560138.56182
3025   Simpson's Rule: -1561670.73851
3026   Simpson's 3/8 Rule: -1561304.31801
3027
3028   CUT & FILL VOLUMES
3029   Positive Volume [Cut]: 63017.5577738
3030   Negative Volume [Fill]: 1623156.11959
3031   Cut minus Fill: -1560138.56182
3032
3033   AREAS
3034   Positive Planar Area
3035   (Upper above Lower):   129104.01182
3036   Negative Planar Area
3037   (Lower above Upper):   1274475.06742
3038   Blanked Planar Area: 7094973.60557
3039   Total Planar Area: 8498552.68481
3040
3041   Positive Surface Area
3042   (Upper above Lower):   129212.895921
3043   Negative Surface Area
3044   (Lower above Upper):   1274742.14991
3045
3046   VOLUME COMPUTATIONS
3047
3048   UPPER SURFACE

3049   Grid File: C:\Users\Vaudrey\Dropbox\bathymetry\Niantic\NRE model
3050   2018\NRbathCCmean_out_LOWER_2018.grd
3051   Grid size as read: 100 cols by 285 rows
3052   Delta X: 17.5590585859
3053   Delta Y: 17.2143333451
3054   X-Range: 229335.0473 to 231073.3941
3055   Y-Range: 54701.06707 to 59589.93774
3056   Z-Range: -0.119693311644 to 4.16498545386
3057
3058   LOWER SURFACE
3059   Level Surface defined by Z = 3
3060
3061   VOLUMES
3062   Approximated Volume by
3063   Trapezoidal Rule: -2298426.90058
3064   Simpson's Rule: -2300378.89323
3065   Simpson's 3/8 Rule: -2299533.62016
3066
3067   CUT & FILL VOLUMES
3068   Positive Volume [Cut]:   16631.3595701
3069   Negative Volume [Fill]:   2315058.26015
3070   Cut minus Fill: -2298426.90058
3071
3072   AREAS
3073   Positive Planar Area
3074   (Upper above Lower):   55576.9763848
3075   Negative Planar Area
3076   (Lower above Upper):   1348002.10286
3077   Blanked Planar Area: 7094973.60557
3078   Total Planar Area: 8498552.68481
3079
3080   Positive Surface Area
3081   (Upper above Lower):   55627.0397632
3082   Negative Surface Area
3083   (Lower above Upper):   1348328.00607
3084
3085   VOLUME COMPUTATIONS
3086
3087   UPPER SURFACE
3088   Grid File: C:\Users\Vaudrey\Dropbox\bathymetry\Niantic\NRE model
3089   2018\NRbathCCmean_out_LOWER_2018.grd
3090   Grid size as read: 100 cols by 285 rows
3091   Delta X: 17.5590585859
3092   Delta Y: 17.2143333451
3093   X-Range: 229335.0473 to 231073.3941
3094   Y-Range: 54701.06707 to 59589.93774
3095   Z-Range: -0.119693311644 to 4.16498545386

3096
3097   LOWER SURFACE
3098   Level Surface defined by Z = 3.5
3099
3100   VOLUMES
3101   Approximated Volume by
3102   Trapezoidal Rule: -3036715.23934
3103   Simpson's Rule: -3039087.04795
3104   Simpson's 3/8 Rule: -3037762.9223
3105
3106   CUT & FILL VOLUMES
3107   Positive Volume [Cut]: 2112.75440496
3108   Negative Volume [Fill]: 3038827.99375
3109   Cut minus Fill: -3036715.23934
3110
3111   AREAS
3112   Positive Planar Area
3113   (Upper above Lower):   11020.2011188
3114   Negative Planar Area
3115   (Lower above Upper):   1392558.87812
3116   Blanked Planar Area: 7094973.60557
3117   Total Planar Area: 8498552.68481
3118
3119   Positive Surface Area
3120   (Upper above Lower):   11033.5436069
3121   Negative Surface Area
3122   (Lower above Upper):   1392921.50222
3123
3124   VOLUME COMPUTATIONS
3125
3126   UPPER SURFACE
3127   Grid File: C:\Users\Vaudrey\Dropbox\bathymetry\Niantic\NRE model
3128   2018\NRbathCCmean_out_LOWER_2018.grd
3129   Grid size as read: 100 cols by 285 rows
3130   Delta X: 17.5590585859
3131   Delta Y: 17.2143333451
3132   X-Range: 229335.0473 to 231073.3941
3133   Y-Range: 54701.06707 to 59589.93774
3134   Z-Range: -0.119693311644 to 4.16498545386
3135
3136   LOWER SURFACE
3137   Level Surface defined by Z = 4
3138
3139   VOLUMES
3140   Approximated Volume by
3141   Trapezoidal Rule: -3775003.57811
3142   Simpson's Rule: -3777795.20266

```
3143          Simpson's 3/8 Rule:      -3775992.22444
3144
3145   CUT & FILL VOLUMES
3146          Positive Volume [Cut]:   25.233158399
3147          Negative Volume [Fill]:  3775028.81126
3148          Cut minus Fill:   -3775003.57811
3149
3150   AREAS
3151          Positive Planar Area
3152          (Upper above Lower):   421.908081785
3153          Negative Planar Area
3154          (Lower above Upper):   1403157.17116
3155          Blanked Planar Area:    7094973.60557
3156          Total Planar Area:      8498552.68481
3157
3158          Positive Surface Area
3159          (Upper above Lower):   422.365678914
3160          Negative Surface Area
3161          (Lower above Upper):   1403532.68015
3162
```

check this equation –max specific growth rate seems high (0.8/d)

$$mu\text{-}max = 0.0183$$

(Duarte 1995; Short et al. 1993)

k for light

(mol m^{-2} d^{-1})

5

(Short et al. 1993)

1.4-2.7% Palacios, S.L., Zimmerman, R.C., 2007. Response of eelgrass Zostera marina to CO2 enrichment: Possible impacts of climate change and potential for remediation of coastal habitats. Marine Ecology Progress Series 344: 1-13. 10.3354/meps07084.

3-9% Ruesink, J.L., Yang, S., Trimble, A.C., 2015. Variability in Carbon Availability and Eelgrass (Zostera marina) Biometrics Along an Estuarine Gradient in Willapa Bay, WA, USA. Estuaries and Coasts 38(6): 1908-1917. 10.1007/s12237-014-9933-z.

1-3% Zimmerman, R.C., Kohrs, D.G., Alberte, R.S., 1996. Top-Down impact through a bottom-Up mechanism: The effect of limpet grazing on growth, productivity and carbon allocation of Zostera marina L. (eelgrass). Oecologia 107(4): 560-567. 10.1007/BF00333949.

Iizumi, H., Hattori, A., 1982. Growth and organic production of eelgrass (Zostera marina L.) in temperate waters of the Pacific coast of Japan. III. The kinetics of nitrogen uptake. Aquatic Botany 12(C): 245-256. 10.1016/0304-3770(82)90020-1.